

# POLITECNICO DI TORINO

Master's Degree in Mechatronic Engineering



Master's Degree Thesis

## Low cost solutions based on wearable devices to measure fatigue in workers

Supervisor

Prof. Massimo VIOLANTE

Co-Supervisor

Gea CARENA, M.Eng.

Candidate

Alessia SIMONETTI

11<sup>th</sup> April 2025



# Abstract

Every year, many workplace accidents occur due to workers' accumulated fatigue, especially in jobs that require a high level of physical exertion, resulting in stressful environments. This research fits into this contest, with the goal of monitoring physical fatigue: laying the groundwork for developing a device able to determine when a person is too fatigued to continue working safely.

To create a controlled environment that induces physical fatigue, each of the 30 volunteers underwent an incremental exercise protocol designed to induce cardio-respiratory fatigue. The protocol was performed on a Garmin bicycle (Tacx Neo Bike Plus) and monitored via a Polar Chest strap (Polar H10). At each stage of the exercise, participants were asked to complete the Rate of Perceived Exertion (RPE) scale to obtain a subjective evaluation of fatigue.

Regarding data analysis, an adaptive filter algorithm was applied to RR intervals to mitigate artifacts using a threshold range of 280-1200 ms (corresponding to 210-50 bpm). Artifacts were identified and replaced using an adaptive estimation of the mean and standard deviation, preserving physiological variability while minimizing nonphysiological distortions.

Subsequently, Detrended Fluctuation Analysis (DFA), a nonlinear method for analyzing fractal signals such as heart rate variability (HRV), was applied. Since HRV exhibits rapid fluctuations due to autonomic nervous system activity and slow oscillations influenced by circadian rhythms and other physiological adaptations, traditional linear analysis methods are limited in distinguishing these components. In contrast, DFA applies detrending at different scales, allowing HRV fluctuations to be more effectively analyzed.

By applying DFA to measure short-term correlation persistence (scales from 4 to 16

beats), the  $\alpha_1$  value ranged approximately from 1 to 1.4 for all subjects at rest. As the Rate of Perceived Exertion (RPE) increased,  $\alpha_1$  gradually decreased, reaching a minimum of around 0.5 at maximal fatigue, followed by a rapid increase during the recovery phase.

The results show an inverse relationship between perceived fatigue (RPE) and  $\alpha_1$ : as subjective fatigue perception increases,  $\alpha_1$  decreases. The findings suggest that DFA applied to HRV is a promising approach to detect acute physical fatigue.

This research represents a first step in the algorithm development of low-cost wearable devices aimed at monitoring and predicting worker fatigue, with potential applications for workplace safety.

Future studies could extend this methodology to other contexts, focusing particularly on fatigue in different industrial sectors.



# Table of Contents

List of Tables	VIII
List of Figures	X
Acronyms	XIII
<b>1 Introduction</b>	<b>1</b>
1.1 Background and Context . . . . .	1
1.1.1 Motivation . . . . .	2
1.2 Objective of the Study . . . . .	3
<b>2 Theoretical Insights</b>	<b>4</b>
2.1 Heart Rate Variability . . . . .	4
2.1.1 HRV and the Autonomic Nervous System: Mechanisms and Implications . . . . .	5
2.1.2 HRV analysis . . . . .	7
2.2 Fractal Time Series . . . . .	9
2.2.1 Fractal and Fractal Dimension definitions . . . . .	10
2.2.2 Long term memory and 1/f process . . . . .	11
2.2.3 HRV as a fractal time series . . . . .	15
2.3 DFA - Detrended Fluctuation Analysis . . . . .	16
2.3.1 DFA Algorithm . . . . .	16
2.3.2 Interpretation of the $\alpha$ Exponent . . . . .	18
2.3.3 DFA applied to HRV . . . . .	18
<b>3 State of Art</b>	<b>19</b>
3.1 Fatigue: definition and measurements . . . . .	19
3.2 RPE: Rate of Perceived Exertion . . . . .	21
3.3 HRV and Fatigue Detection: Literature Review . . . . .	22

3.3.1	HRV Analysis in Sports Field: The Role of DFA . . . . .	23
3.3.2	Assessing Work-Related Fatigue via HRV: The Role of DFA . . . . .	24
3.3.3	Rationale for Using DFA for Fatigue Detection . . . . .	24
<b>4</b>	<b>Methodology</b> . . . . .	<b>28</b>
4.1	Study Design . . . . .	28
4.2	Literature Review and Rationale for Protocol Design . . . . .	29
4.2.1	Analysis of Literature . . . . .	29
4.2.2	Protocol Design . . . . .	30
4.3	Instrumentation . . . . .	31
4.4	Data Collection . . . . .	32
<b>5</b>	<b>Data Analysis and Pre-Processing</b> . . . . .	<b>34</b>
5.1	RRi: Filtering and Artifact Removal . . . . .	34
5.2	Data Acquisition and Segmentation . . . . .	35
5.3	Application of DFA . . . . .	36
<b>6</b>	<b>Results</b> . . . . .	<b>37</b>
6.1	Introduction . . . . .	37
6.2	Filter Application . . . . .	38
6.3	DFA Algorithm Application . . . . .	45
6.3.1	DFA- $\alpha_1$ and RPE Analysis . . . . .	49
6.3.2	DFA- $\alpha_1$ Before and After Exercise . . . . .	57
<b>7</b>	<b>Discussion</b> . . . . .	<b>59</b>
7.1	Filter Application . . . . .	59
7.2	DFA Algorithm Application . . . . .	60
7.2.1	DFA- $\alpha_1$ and RPE: A Reliable Marker of Fatigue . . . . .	60
7.2.2	Radial Plots: Another Visualization . . . . .	61
7.2.3	RPE and DFA- $\alpha_1$ : General Remarks . . . . .	62
7.2.4	DFA- $\alpha_1$ Before and After Test . . . . .	65
<b>8</b>	<b>Conclusions</b> . . . . .	<b>67</b>
8.1	Summary of Results . . . . .	67
8.2	Limits of the Study and Purpose for the Future . . . . .	69
<b>A</b>	<b>Informed Consent Form</b> . . . . .	<b>71</b>
A.1	Informed Question: To signature . . . . .	75

B Sleep Questionnaire	77
C Physical Activity Questionnaire	80
D Perceived Stress Questionnaire	83
E Individual Subject Plots	85
Bibliography	91

# List of Tables

2.1	Summary Table of Noise Processes and Their Characteristics [19]	14
2.2	Scaling exponent interpretation	18
3.1	Various Definitions of Fatigue According to the Literature	20
3.2	RPE Scale (Borg 6-20) [46]	21
3.3	RPE Scale (CR10: 0-10) [47]	22
3.4	HRV Literature Review	26
3.6	HRV Literature Review	27
4.1	Summary of different incremental cycling test protocols from the literature.	29
4.2	Incremental test protocol for men.	32
4.3	Incremental test protocol for women.	32
6.1	Signal Statistics of Raw and Filtered Data	41
6.2	Percentage Distribution of RPE by DFA- $\alpha_1$ Ranges (7-Class Classification)	50
6.3	Percentage Distribution of RPE by DFA- $\alpha_1$ Ranges (4-Class Classification)	52
6.4	Correspondence Between DFA- $\alpha_1$ Ranges, RPE Values and Fatigue Classification	53
6.5	Accuracy of DFA- $\alpha_1$ Fatigue Classification Compared to RPE Labels (4-Class Scheme)	53
6.6	Last Stage and Cool Down: $\Delta_\alpha$ , RPE	55
6.7	DFA- $\alpha_1$ Values of candidates: Before Test, Cool Down, Recovery (min. 0-3), Recovery (min. 3-6), Recovery (min. 6-9)	58
7.1	Summary of DFA- $\alpha_1$ and RPE Ranges for Fatigue Classification with Corresponding Accuracy	63

D.1 Perceived Stress Questionnaire (Likert Scale 1-4) . . . . .	84
---	----

# List of Figures

2.1	Consecutive R-R distances [2]. . . . .	4
2.2	Electrophysiology of SA Node Pacemaker Cells[3]. . . . .	5
2.3	Sierpinsky triangle [15]. . . . .	11
2.4	Signals with different Hurst Exponents[23]. . . . .	13
2.5	White, Pink and Brown Noises, Power Spectra[26] . . . . .	14
2.6	Example of self-similar structure and a self-similar signal [28]. . . . .	15
2.7	Detrended Fluctuation Analysis: Schematic Resume [33] . . . . .	17
6.1	RR Intervals Raw vs Filtered . . . . .	38
6.2	RR Intervals Filtered . . . . .	39
6.3	RRi Filtered: Zoom-In1 . . . . .	40
6.4	RRi Filtered: Zoom-In2 . . . . .	40
6.5	Mean Raw Vs Mean Filtered . . . . .	42
6.6	Percentage of Artifacts for Each Subject . . . . .	43
6.7	Total Artifacts for Each Subject . . . . .	43
6.8	Heatmap About Artifacts Distribution . . . . .	44
6.9	ScatterPlot of Percentage of Artifacts . . . . .	44
6.10	DFA-alpha1 vs RPE and Power Stages . . . . .	45
6.11	Inverse of DFA-alpha1 vs RPE . . . . .	46
6.12	Radial Plot of All Subjects: DFA-alpha1, Heart Rate, and RPE Across Exercise Stages . . . . .	47
6.13	Radial Plot of All Subjects: DFA-alpha1, Heart Rate, and RPE Across Exercise Stages . . . . .	47
6.14	Radial Plot of All Subjects Together: DFA-alpha1, HR, and RPE . . . . .	48
6.15	DFA- $\alpha_1$ and RPE: Box Plot . . . . .	49
6.16	Percentage Distribution of RPE by DFA- $\alpha_1$ Ranges - 7 Class: Heatmap	51
6.17	Percentage Distribution of RPE by DFA- $\alpha_1$ Ranges - 4 Class: Heatmap	52
6.18	DFA- $\alpha_1$ values vs RPE and Fatigue Classification . . . . .	54

6.19	DFA- $\alpha_1$ values vs RPE During Cool-Down . . . . .	56
6.20	DFA- $\alpha_1$ values Before Test, Cool Down, Recovery (min. 0-3), Recovery (min. 3-6), Recovery (min. 6-9) . . . . .	57
E.1	DFA-alpha1 vs RPE and Power Stages: 1-15 . . . . .	86
E.2	DFA-alpha1 vs RPE and Power Stages: 16-30 . . . . .	87
E.3	DFA-alpha1 vs RPE and Fatigue Classification: 1-15 . . . . .	88
E.4	DFA-alpha1 vs RPE and Fatigue Classification: 16-30 . . . . .	89



# Acronyms

**ACF**

Auto Correlation Function

**ANS**

Autonomic Nervous System

**BPNN**

Back Propagation Neural Network

**CD**

Cool Down (fase di defaticamento)

**CFS**

Chronic Fatigue Syndrome

**CNS**

Central Nervous System

**DFA**

Detrended Fluctuation Analysis

**ECG**

Electrocardiogram

**EEG**

Electroencephalography

**fBm**

Fractional Brownian Motion

**fGn**

Fractional Gaussian Noise

**HF**

High-Frequency band

**HR**

Heart Rate

**HRV**

Heart Rate Variability

**LF**

Low-Frequency band

**lnRMSSD**

Natural Logarithm of RMSSD

**ME**

Myalgic Encephalomyelitis

**ML**

Machine Learning

**NN50**

Number of successive RR intervals differing by more than 50ms

**PNS**

Parasympathetic Nervous System

**PSD**

Power Spectral Density

**RMSSD**

Root Mean Square of Successive RR Interval Differences

**RR**

Time intervals between successive R peaks in the ECG signal

**RPE**

Rate of Perceived Exertion

**SampEn**

Sample Entropy

**SD**

Standard

**SDANN**

Standard Deviation of the average NN interval

**SDNN**

Standard Deviation of all NN intervals

**SNS**

Sympathetic Nervous System

**TINN**

Triangular Interpolation of NN interval histogram

**ULF**

Ultra Low-Frequency band

**VLF**

Very Low-Frequency band

**VT2**

Second Ventilatory Threshold

# Chapter 1

## Introduction

### 1.1 Background and Context

Fatigue is a complex and multifactorial phenomenon that affects humans daily in different areas, including sports and occupational health. Being able to identify fatigue objectively and in real-time is crucial to optimize athletic training, prevent injuries, and improve safety in high-risk work environments.

In the occupational field, fatigue is a growing area of research due to its detrimental effects on productivity, increased injury risks, and potential long-term health consequences [1]. The fatigue onset in workplace varies significantly among individuals, it is influenced by factors such as age, fitness level, psychological state, and lifestyle conditions (e.g. stress, anxiety, sleep deprivation). These variables fluctuate day-to-day and are difficult to quantify, making fatigue detection a hard task.

Since fatigue is multifactorial there is no universal threshold for identifying fatigue, current detection methods remain largely subjective.

A common approach leans on self-reported questionnaires, which have acquired plausibility but they represent inherently subjective information.

Recent advances in **wearable sensor technology** have opened new opportunities for real-time physiological monitoring, representing a data-driven and objective approach to fatigue detection. The ability to constantly monitor individuals, in a **non-invasive** and accurate way, unlocks new perspectives in fatigue detection studies.

Among the various physiological markers, **Heart Rate Variability (HRV)** has gained significant attention as a reliable indicator of **autonomic nervous system (ANS) balance**, making it a promising tool for fatigue assessment. HRV analysis provides insight into sympathetic and parasympathetic regulation, which are closely related to fatigue accumulation during exercise and prolonged workload. HRV can be analyzed through three main approaches:

- Time-domain analysis.
- Frequency-domain analysis.
- Nonlinear analysis.

Recently, **nonlinear methods**, which capture hidden internal patterns in HRV dynamics, have earned popularity in fatigue field. These approaches quantify the complexity of RR interval fluctuations.

In particular, **Detrended Fluctuation Analysis (DFA)** is a widely used nonlinear technique that describes HRV fractal behavior across different time scales.

Unlike conventional HRV metrics, DFA provides a dynamic, complexity-based analysis. Given its strong correlation with exercise intensity and metabolic stress, DFA emerges as a promising candidate for real-time fatigue detection.

The **integration of physiological data and subjective fatigue perception** represents a crucial step toward developing reliable fatigue detection models. Leveraging wearable devices and advanced data analysis, this study aims to provide an **objective, low-cost and noninvasive solution for fatigue monitoring** with direct application in sport, and a first step for potential future applications in occupational health for high-risk occupations.

### 1.1.1 Motivation

The motivation for this study derives from a critical issue: fatigue is a major contributing factor in workplace accidents, many of which result in severe injuries or fatalities.

Every year, a significant number of occupational incidents are directly or indirectly linked to fatigue-related disorders, such as reduced alertness and slower reaction times. Despite the growing awareness of the impact of fatigue, it remains one of the most underestimated risks in occupational safety management.

## 1.2 Objective of the Study

The main goal of this research is to detect the onset of physical fatigue using an **incremental cycling test** designed to push participants to exhaustion. By analyzing data collected during this incremental exercise, the study aims to establish a correlation between objective physiological measures of heart rate variability (HRV) and subjective perceptions of fatigue.

Specifically, this research focuses on the HRV analysis through Detrended Fluctuation Analysis and its relationship with the **Rating of Perceived Exertion (RPE)**, which represents a subjective fatigue perception metric.

This study seeks to investigate how DFA correlates with RPE across different exercise intensities and to **validate DFA as a reliable metric for fatigue detection**. In this way, this research lays the foundations for future studies about fatigue onset, with potential applications not only in sports performance but also in high-risk occupations where fatigue management is critical.

# Chapter 2

## Theoretical Insights

This chapter provides the essential information necessary to fully understand Detrended Fluctuation Analysis (DFA) in the context of fatigue detection. It starts with the fundamental concepts of Heart Rate Variability (HRV), followed by essential notions of fractal time series, and it concludes with a detailed description of the DFA algorithm.

### 2.1 Heart Rate Variability

Heart rate variability measures the **time variation between two consecutive heartbeats**. One of the most commonly used methods to obtain HRV is by measuring the distance between consecutive R-wave peaks using an electrocardiogram (ECG).



**Figure 2.1:** Consecutive R-R distances [2].

### 2.1.1 HRV and the Autonomic Nervous System: Mechanisms and Implications

The cardiac electrical impulse starts from the sinoatrial node (SA Node) which contains the so-called "Pacemaker Cells". From a chemical point of view, what happened is that, at rest, the concentration of the  $K^+$  (Potassium) inside the cell is much greater than outside, so the membrane exhibits a higher permeability to  $K^+$ . So, this favors the outward flow of  $K^+$  making the inside part of the cell more electronegative concerning the outside, resulting in a maintaining resting potential of approximately  $-65mV$ . When an electrical stimulus occurs, the membrane depolarizes caused by the opening of ion channels.

#### SA Node: Pacemaker Cells

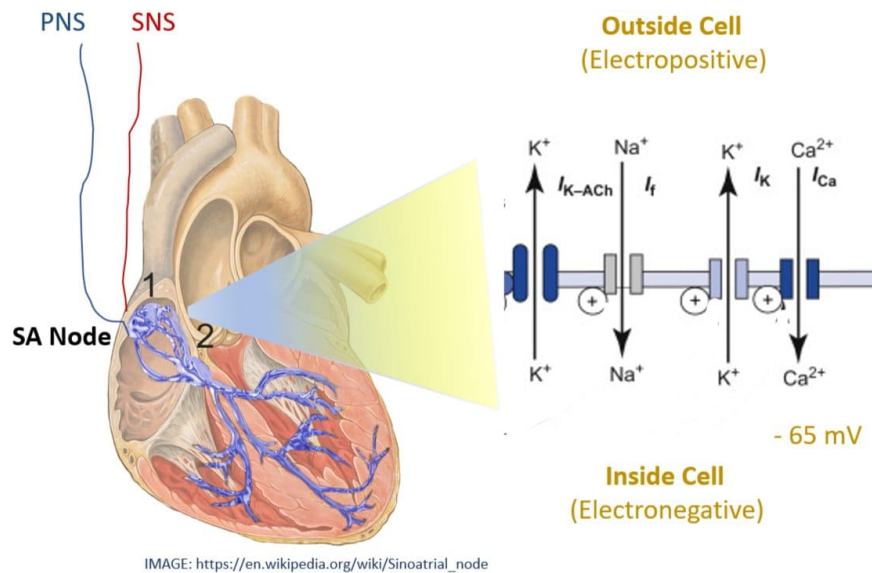


IMAGE: [https://en.wikipedia.org/wiki/Sinoatrial\\_node](https://en.wikipedia.org/wiki/Sinoatrial_node)



Feher J 2012 Quantitative Human Physiology p528-536.

**Figure 2.2:** Electrophysiology of SA Node Pacemaker Cells[3].

At some point, a potential threshold is reached and the sodium ( $Na^+$ ) and calcium ( $Ca^{2+}$ ) channels open, resulting in a rapid flux of positive ions inside the cell, the so-called depolarization part. In particular, thanks to the  $Ca^{2+}$  channel the potential inside the cell gets  $0mV$ . Then, once the potential reaches approximately  $+50mV$ ,  $Na^+$  channels close while the  $K^+$  channels open, allowing the outward

flow of  $K^+$  ions. This process restores the membrane's negative charge through repolarization. Before returning to its resting potential, the cell undergoes a phase called **hyperpolarization**, during which it becomes temporarily too negative. In this state, even if a new electrical stimulus arrives, the cell cannot respond, preventing premature activation.

The autonomic nervous system is composed of the **sympathetic nervous system (SNS)** and the **parasympathetic nervous system (PNS)**. The SNS primarily relies on noradrenaline as its neurotransmitter, which affects calcium ( $Ca^{2+}$ ) and potassium ( $K^+$ ) channels. **Noradrenaline** triggers the opening of L-type calcium channels, allowing more calcium to enter the cell. This speeds up depolarization, leading to an **increased heart rate**. At the same time, noradrenaline reduces the opening of potassium channels and slows down repolarization. As a result, the affected cells become more excitable and fire more frequently.

In contrast, the **parasympathetic nervous system (PNS)**, which uses **acetylcholine** as its neurotransmitter, has the opposite effect on ion channels. It reduces the opening of calcium ( $Ca^{2+}$ ) channels, slowing depolarization and thereby **decreasing the heart rate**. At the same time, it increases the opening of potassium ( $K^+$ ) channels, leading to faster repolarization and further reducing heart rate.

In a few words, the sympathetic nervous system (SNS) increases the heart rate while the parasympathetic nervous system (PNS) decreases the heart rate. For these reasons, it is possible to affirm that the **HRV represents an indirect measure of the ANS**. [3]

The autonomic nervous system (ANS) plays a key role in regulating human mood and activity. The **SNS is dominant during emergencies and physical exertion**, while the **PNS is more active during rest**.

Since heart rate variability (HRV) represents a reflection of ANS activity, it can be used to analyze different physiological and psychological states.

Moreover, HRV is influenced by respiration, body position, and individual characteristics such as age, gender, and physical condition [2]. Generally, younger individuals have higher HRV both at rest and during exercise[4]. Researches suggest that regular physical activity helps increase HRV[5].

A **high HRV** is typically associated with greater energy reserves, an adaptable physiological system, and well-functioning **autonomic control system**[6]. Conversely,

a **low HRV** is often linked to increased SNS activation, **ANS dysregulation**, chronic stress, reduced energy reserves, and overall autonomic imbalance[6].

### 2.1.2 HRV analysis

#### HRV analysis in time domain

HRV can be measured using short (5 to 10 min) or long (12 to 24 hours) periods.[7] The RR intervals without artifacts are called normal-to-normal intervals (NN).

The following methods analyze variations in successive NN intervals over time. They are divided into:

Main statistical measures:

- SDNN: Standard deviation of all NN intervals, the square root of variance. [8]
- SDANN: Standard deviation of the average NN interval computed over short periods, in general of 5 minutes. [8]
- RMSSD: Root mean square of successive RR interval differences. It reflects the vagal tone. [9]
- pNN50: the percentage of successive NN intervals longer than  $50ms$ . It reflects the vagal tone [9]

#### HRV analysis in frequency domain

In the frequency domain, the analysis requires filtering the signal into different bands:

- ULF: Ultra low-frequency band, below  $0.0033Hz$ . It reflects the circadian oscillations. It requires long period recordings, as 24 hours. [9]
- VLF: Very low-frequency band, between  $0.0033Hz$  and  $0.04Hz$ . It expresses long-term regulation mechanisms, thermoregulation, and hormonal mechanisms. [9]
- LF: Low-frequency band, between  $0.04Hz$  and  $0.15Hz$ . It represents a mix of sympathetic and vagal influences.[9]
- HF: High-frequency band, between  $0.15Hz$  and  $0.4Hz$ . It reflects the vagal tone, and, it is referred to as variations of HR related to the respiratory cycle, and it reflects the vagal tone (parasympathetic system).[9]

- LF/HF ratio: represents the sympathovaga balance, which means the balance between sympathetic and parasympathetic systems.[9]

### HRV with non linear methods

**HRV is connected to complexity science**, which analyses how systems behave as a whole rather than splitting them into little parts. In linear systems, the whole system's behavior can be explained by analyzing each component separately and then summing them. In contrast, in complex systems, the relationships between subsystems create properties that cannot be comprehended by examining each part individually. [7]

Physiological systems exhibit complexity due to the interplay between cardiovascular, endocrine, and autonomic functions, making them **inherently non-stationary**.

As a result, non-linear approaches can be particularly useful for HRV analysis when the assumption of stationarity is not met, providing insights that linear methods might miss. [10]

HRV is a fundamental feature for analyzing physiological complexity, drawing from dynamical systems theory, fractal and chaos theory[7]. Several non-linear methods are used to assess HRV, including:

- Poincare plot: scatter plot of HRV generated by plotting each RR interval as a function of the prior RR interval. Fitting an ellipse to the data series, it exploits three non-linear measures: [10]
  - S represents the total area and it is a measure of the total variability.
  - SD1, standard deviation related to fast HRV.
  - SD2, standard deviation, reflecting long-term variability.[10]
- Entropy: supplies a measure of the level of regularity and complexity within the time series. This method exploits the possibility that any given sequence of intervals will be replicated. The higher the probability to be repeated, the lower the computed entropy. [10]
- Detrended Fluctuation Analysis (DFA): a fractal-based method used to **assess the self-affinity of a signal**. It is defined by two exponents:
  - DFA- $\alpha_1$ , which evaluates RR intervals ranging from 4 to 16 beats.
  - DFA- $\alpha_2$ , which analyzes interbeat intervals between 16 and 64 beats.

This technique is particularly useful for **non-stationary data**. [7]

## 2.2 Fractal Time Series

When talking about fractals, it is important to take a step backward. Fractal is a concept highly correlated with **chaos theory, non-linearity, and complexity**. All these concepts together form the basis for properly analyzing biological systems. Biological systems are represented as a single unit, where each part is interconnected with others, and this single unit is in connection with the surrounding environment. So, because of the **interdependency of biological systems**, it is not possible to analyze parts as if they were 'stand-alone'.

### Chaos Theory

Chaos theory represents a way to describe complex phenomena since it provides a tool for looking at the entire structure instead of focusing on only a part.

Chaos theory can find order in systems that look completely random. Chaos refers to the behavior of dynamic systems that are highly sensitive to initial conditions, meaning that small changes can lead to divergence. It appears in **non-linear and interconnected systems** where patterns arise through repeated evolution. This process, often described as "fold and stretch," leads to self-similarity, making **chaos closely connected to fractals**. [11]

### Complex Systems

A complex system is characterized by a non-divisibility between the components of the system and the **system as a whole**. This means that the identity of the whole is shaped by its constituent parts, while at the same time, the identity of each part is influenced by the system's overall structure and interactions. Unlike simple systems, where components function independently, complex systems exhibit behaviors that result from the interrelated relationships among their elements. [12]

A fundamental property of complex systems is their **organization on multiple scales**. They can often be approximated or simplified as networks of smaller, interconnected elements, in which simpler and more complex structures exhibit similar patterns. This leads to **self-similarity** on different scales, a feature observed in fractals. However, despite these similarities, complex systems also exhibit emergent behavior, in which changes at different levels of observation—moving from finer to coarser scales—can reveal distinct dynamics that are not predictable from the properties of individual components. [11]

## 2.2.1 Fractal and Fractal Dimension definitions

Fractal can be intuitively defined as "a set that shows irregular but self-similar features on many or all scales"[13]. In this context, self-similarity means that different segments of the object or time series, despite their irregularity, exhibit structural resemblance to other parts. In other words, a fractal is a phenomenon that **has patterns repeated at different scales**. In nature, fractals are not exactly but almost the same at diverse scales.

The fractal dimension is a measure of the complexity of a self-similar system[11]. Fractal dimension was defined by the Hausdorff equation as mentioned in [14]:

$$d = \frac{\log(N(s))}{\log(1/s)} \quad (2.1)$$

where:

- d: Fractal dimension
- N(s): Number of self-similar copies into which the figure is divided at each iteration
- s: Scaling down factor at each iteration

To clarify this concept, let's consider the Sierpinski triangle and reconstruct how it is formed. As shown in Figure 2.3, starting with an equilateral triangle with side length  $l$ :

1. Draw a reverse triangle with vertices at mid-length of each side. It creates three equilateral triangles of side length  $l/2$ .
2. At each of these three triangle, draw a reverse triangle with vertices at the mid-length of each side. It generates other  $3^2$  equilateral triangles of side length  $2^{-2}l$ .

Iterating this, in iteration  $n$ , there will be  $3^n$  triangles of side length  $2^{-n}l$ . The fractal dimension of this object is:

$$d = \frac{\log(N(s))}{\log(1/s)} = \frac{\log(3)}{\log(2)} \approx 1.585 \quad (2.2)$$

It means that  $2^d = 3$



**Figure 2.3:** Sierpinsky triangle [15].

As the figure is iterated, it becomes more and more complex, but its basic element is a simple triangle. This is a distinctive feature of fractals: the **end result appears complex** and difficult to analyze, but if one understands the rule that governs its construction, it leads back to a simple, well-defined law.[16]

There exists different methods for the estimation of fractal dimension, but each of them follows the same principles[11]:

1. Define the characteristic of the signal or phenomenon and determine the scale of measurement.
2. Make measurements on multiple scales and analyze the limitations of any relationship.
3. Plot measured values against corresponding scales on a log-log graph.
4. Approximate the trend using a linear fit to the plotted data.
5. Determine the fractal dimension (FD) as the slope of the fitted line, which quantifies the complexity of the signal or event.

### 2.2.2 Long term memory and 1/f process

Fractal structures intrinsically exhibit **long-term memory**. This property manifests in both the time and frequency domains through different statistical manners. In the time domain, long-term memory is characterized by an **autocorrelation function (ACF)** that follows a power-law decay, meaning that correlations continue over long periods instead of decreasing exponentially as in short-memory processes [17]. In the frequency domain, this persistence is reflected in the spectral density function  $S(f)$ , which exhibits a power-law divergence around zero frequency, indicating that low-frequency components dominate the system's dynamics [18, 19]. Mandelbrot and Van Ness firmly established the in-depth **relationship between long-memory processes, scaling behavior, and fractal structures**. These properties underline the strong dependences within time series, where past events

continue to influence future outcomes over extended periods. Unlike short-term processes, where dependencies disappear quickly, **long-memory processes maintain correlations across multiple scales**[17].

An essential aspect of fractal structures is their ability to scale across different resolutions while maintaining characteristic statistical properties. As introduced before, this scaling behavior can be categorized into self-similarity and self-affinity. Self-similarity presents isotropic properties while self-affinity has anisotropic properties, which means that fractal's statistical properties scale in different ways along different dimensions.[21]. From a mathematical point of view, both, self-affine and self-similar processes, follows a **power-law distribution**. This relationship is fundamental in fractal analysis, as it allows for the estimation of the fractal dimension[22]. Specifically, if a phenomenon can be described by a single power-law function, it is called monofractal; otherwise, it is called multifractal. [11]

The following equation represents a power-law distribution[21]:

$$Y(Lt) \equiv L^H Y(t) \tag{2.3}$$

Where:

- Y: the process
- Y(t): value of the process at time window of length t
- Y(Lt): value of the process at time window Lt
- L: window length factor  $L > 0$
- H: Hurst parameter  $0 < H < 1$

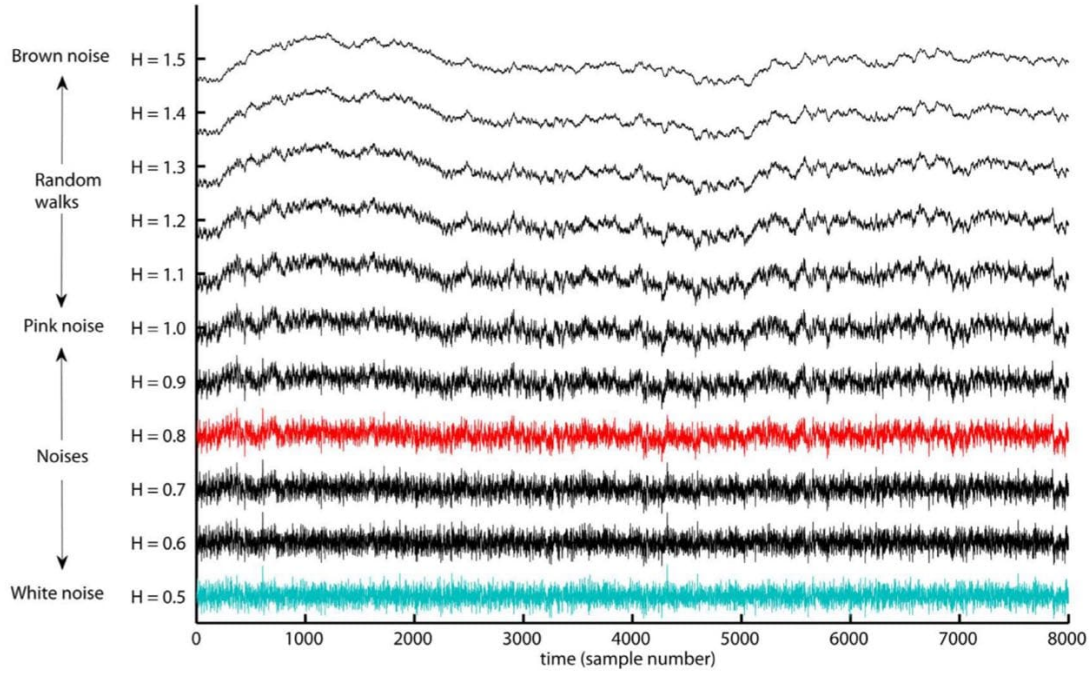


**Figure 2.4:** Signals with different Hurst Exponents[23].

The **Hurst exponent** is commonly referred to as the 'index of dependence' or '**index of long-range dependence**'[24]. The value of  $H$  provides insight into the nature of the process. Specifically:

- If  $0 < H < 0.5$ , the series is **anti-persistent**, meaning that increases are likely to be followed by decreases. It can be considered as a "stabilizer process".
- If  $H = 0.5$ , the series behaves like **white noise** (random process).
- If  $0.5 < H < 1$ , the series exhibits long-memory with increasing **persistence** as  $H$  approaches 1.

Then, applying the Fourier transform to the process  $Y(t)$  and computing the average power spectral density (PSD) as the mean of the distribution power, it results that the PSD follows a power-law function of the form:

$$S(f) \sim f^{-\beta} \quad (2.4)$$

Processes with PSD as mentioned above are called  $1/f$  processes[11].

Among these, an important example is the Fractional Gaussian Noise (fGn), where

the spectral exponent  $\beta$  is directly related to the Hurst parameter  $H$  by the following relationship:

$$\beta = 2H - 1 \quad (2.5)$$

Following this framework, Mandelbrot and Van Ness introduced a new family of Gaussian random functions, known as Fractional Brownian Motion (fBm), which extends the classical Brownian Motion model to incorporate long-term dependencies and self-similar properties.[25]

In this case,  $\beta$  is:

$$\beta = 2H + 1 \quad (2.6)$$

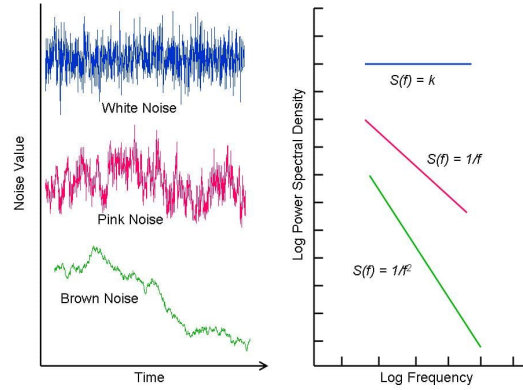


**Figure 2.5:** White, Pink and Brown Noises, Power Spectra[26]

The following table provides a concise summary of the  $\beta$  and  $H$  parameters for white, pink, and brown noise.

Process	Memory	Hurst exponent $H$	Power-law exponent $\beta$	Spectrum $S(f)$
White Noise	No Memory	$H = 0.5$	$\beta = 0$	Constant
Pink Noise ( $1/f$ noise)	Long Memory	$H = 1$	$\beta = 1$	$1/f$
Brown Noise (Brownian motion)	Infinite Memory	$H = 1.5$	$\beta = 2$	$1/f^2$

**Table 2.1:** Summary Table of Noise Processes and Their Characteristics [19]

## Random, Anti-correlation and Correlation Processes

As mentioned by Hardstone et al., it is important to do a differentiation between random walk and processes with memory.

- A random walk is a type of series that has a cumulative pattern but it does not present any trend. Thus, random walk is an example of an uncorrelated signal. In particular, each step is random and the signal is "memory-less", it means that it does not present a memory.
- An anti-correlated signal presents memory and has the tendency to "stabilize itself". In the sense that, for each increment it will be more likely a decrement. This leads to smaller fluctuations on longer time-scales.
- A correlated signal has memory and it tends to produce future values that correspond to past movements. This leads to large fluctuations.

### 2.2.3 HRV as a fractal time series

Heart rate variability (HRV) is **inherently nonstationary and scale-invariant**, so, it presents fractal properties.

Observing HRV data, it is possible to recognize **fast fluctuations** due to the autonomic nervous system (ANS), as well as **slower oscillations** influenced by circadian rhythms and physiological adaptations. These fluctuations are the result of continuous interactions between cardiovascular regulatory mechanisms and external factors, making HRV a complex system.[27]

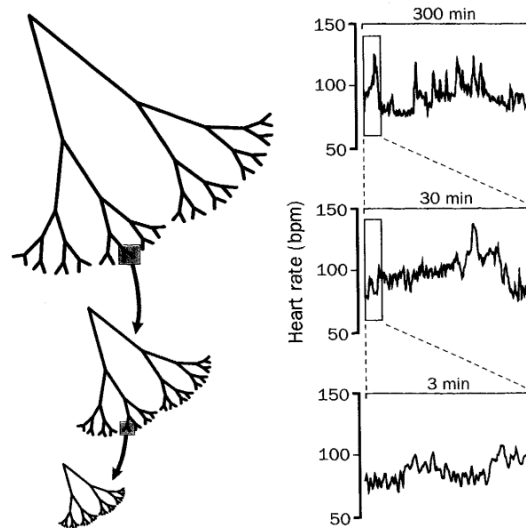


**Figure 2.6:** Example of self-similar structure and a self-similar signal [28].

Other studies have demonstrated that HRV fluctuations follow  $1/f$  noise processes, indicating the presence of long-term memory in cardiac regulation[29]. Moreover,

HRV is nonstationary, meaning its statistical proprieties vary in time. Traditional linear methods, such as time and frequency domain analysis, provide an understanding of the general magnitude of RR interval fluctuations but fail to capture the intrinsic nonlinearity and complexity of cardiac dynamics. [27, 30] Consequently, nonlinear analysis is crucial for extracting information that classical methods cannot find out.[27] Studies have underlined that HRV shows multifractal behaviours.

## 2.3 DFA - Detrended Fluctuation Analysis

Detrended Fluctuation Analysis (DFA) fits into this context. DFA represents a tool for **detecting trends** inside signals, fractal properties, and **long-term correlations** for **non-stationary** time series.[31]

The output of the DFA,  $\alpha$ , represents an estimation of the Hurst exponent.[32]

### 2.3.1 DFA Algorithm

As previously mentioned, scale-invariant processes can be modeled using either fractional Gaussian noise (fGn) for stationary signals, or fractional Brownian motion (fBm) for non-stationary signals.

An important relationship between these two is that the cumulative sum of an fGn process produces an fBm, while differentiating an fBm yields an fGn. This relationship is the basis of the first stage of detrended fluctuation analysis (DFA):

1. The signal of length  $N$  is transformed by computing its cumulative sum after subtracting the mean. This produces what is known as the **profile of the signal**:

$$y(k) = \sum_{i=1}^k (x(i) - \bar{x}) \quad (2.7)$$

$\bar{x}$  represents the mean of the signal. The subtraction of it allows the remotion of the global trend.

2. Split the profile into **non-overlapping windows**,  $w$ , of length called **scale**,  $s$ . For each scale, the total number of windows is defined as  $M$ :

$$M = \frac{N}{s} \quad (2.8)$$

3. Then, for each window of the time series compute the **local trend** by fitting a low-order polynomial using the least-squares method,  $p_{(s,w)}(k)$ .

4. For each window compute the *Squared Fluctuation Function*,  $F_{s,w}^2$ , as follow:

$$F_{s,w}^2 = \frac{1}{S} * \sum_{k \in w}^M (Y(k) - p_{s,w}(k))^2 \quad (2.9)$$

So, for each window of each chosen scale this function is performed.

5. Perform the average over the windows of the squared fluctuations, obtaining an unique *Fluctuation Function*,  $F_s$ , at each scale.

$$F_s = \sqrt{\frac{1}{M} * \sum_{k \in w} F_{s,w}^2} \quad (2.10)$$

The calculations for obtaining the *Fluctuation Function*,  $F_s$ , are repeated for different scales,  $s$ .

6. If the time series is fractal, it follows a power law of the following form:

$$F_s \propto s^\alpha \quad (2.11)$$

For this reason, plotting the  $\log(F_s)$  as function of the logarithm of the scale,  $\log(s)$ , it results a line. The slope of this line is the so-called *Scaling Exponent*,  $\alpha$ .

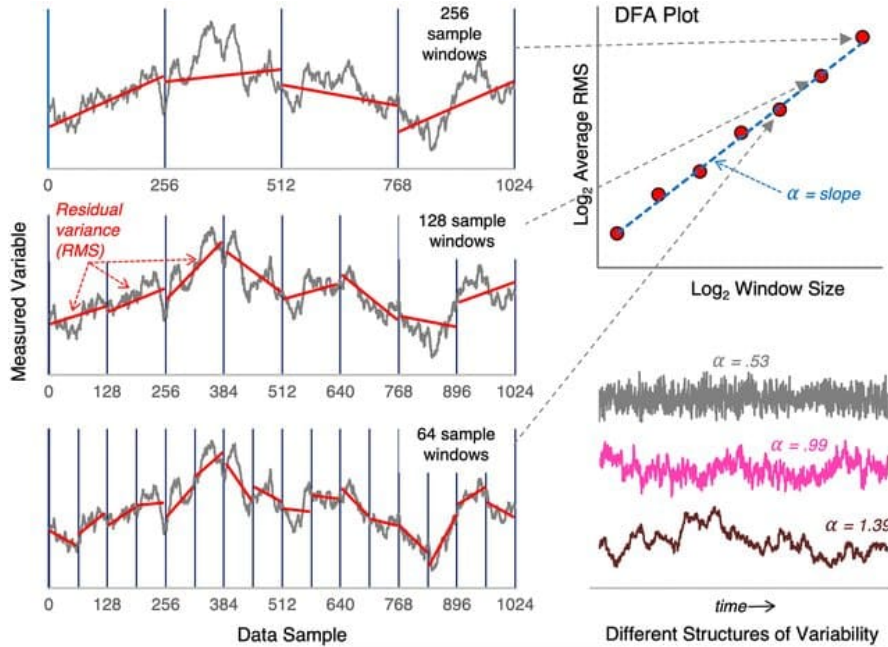


**Figure 2.7:** Detrended Fluctuation Analysis: Schematic Resume [33]

### 2.3.2 Interpretation of the $\alpha$ Exponent

The *Scaling Exponent*,  $\alpha$ , represents an estimation of the *Hurst Exponent*. In particular:

- For  $0 < \alpha < 1$ ,  $\alpha = H$
- For  $\alpha > 1$ ,  $\alpha = H + 1$

As mentioned by Peng et al., the interpretation of the *Scaling Exponent*,  $\alpha$  can be resumed by the following table.

Comparison with H	Scaling exponent	Interpretation	Stationarity
$\alpha = H$	$0 < \alpha < 1/2$	anti-correlated	stationary
$\alpha = H$	$\alpha = 1/2$	white noise	stationary
$\alpha = H$	$1/2 < \alpha < 1$	correlated	stationary
$\alpha = H$	$\alpha = 1$	$1/f$ (pink) noise	stationary
$\alpha = H + 1$	$1 < \alpha < 3/2$	anti-correlated increments	nonstationary
$\alpha = H + 1$	$\alpha = 3/2$	Brownian noise	stationary
$\alpha = H + 1$	$3/2 < \alpha < 2$	correlated increments	nonstationary

**Table 2.2:** Scaling exponent interpretation

### 2.3.3 DFA applied to HRV

Applying DFA to HRV signals, the *Scaling Exponent*,  $\alpha$ , is commonly calculated over two ranges of scales [35],[36]:

- $4 < s < 16$ :  $\alpha_1$ : *Short-Term Exponent*
- $16 < s < 64$ :  $\alpha_2$ : *Long-Term Exponent*

# Chapter 3

## State of Art

### 3.1 Fatigue: definition and measurements

Fatigue is a complex and multifaceted phenomenon that has been studied extensively, but it still remains difficult to define with precision. As highlighted in the review by Phillips, the concept of fatigue **lacks a unified definition across the literature**, due to its multidimensional nature and the diversity of contributing factors. Fatigue can refer to a subjective sensation, a physiological condition, or a measurable decline in performance, and these interpretations vary significantly across research fields.

In general terms, fatigue is defined as a **temporary reduction in physical and cognitive performance** caused by multiple factors, such as prolonged exertion, insufficient recovery, and external stressors [1]. It is influenced by a combination of physiological, psychological, and environmental variables, and it represents a significant challenge in terms of safety, productivity, and overall health [1].

To better illustrate the conceptual multiplicity of fatigue, Table 3.1 presents a synthesis of key definitions across different domains. Adapted from Phillips, this table underlines the diverse ways fatigue has been conceptualized, emphasizing different dimensions such as subjective experience, physiological mechanisms, and performance consequences.

A physiological distinction that is frequently discussed in the literature is between central fatigue and peripheral fatigue. **Central fatigue** originates in the central nervous system (CNS) and is associated with a reduced neural drive from the CNS to the muscles, resulting in decreased motor output. It is often aggravated

**Table 3.1:** Various Definitions of Fatigue According to the Literature

Category	Definition
Dictionary and Common Use	Fatigue is described as extreme tiredness resulting from physical or mental effort [38].
Subjective Experience	Fatigue is perceived as a sense of exhaustion, sleepiness, or reduced motivation to continue a task [39].
Physiological Condition	A state of imbalance in the body's physiological resources, caused by prolonged physical or mental effort, with consequences on metabolism and neural functioning [40].
Performance Decline	Fatigue leads to measurable decreases in performance, affecting attention, reaction time, and decision-making abilities [39].
Multidimensional Model	Fatigue is a complex phenomenon involving physiological, cognitive, and emotional aspects, resulting from a dynamic interaction between tasks, environment, and the individual's condition [41].

*Note.* Table adapted from Phillips.

by lack of sleep, mental fatigue, and stress, all of them influence brain activation and the perception of exertion [42].

On the other hand, **peripheral fatigue** is localized at the muscular level and is primarily caused by metabolic products and alterations in muscle contractility [43]. While central and peripheral fatigue are conceptually distinct, they are closely **interconnected**: mental exertion can influence muscle activation, and peripheral fatigue can impact motivation and cognitive performance. Therefore, both components should be considered in any comprehensive understanding or assessment of fatigue.

Another important distinction for this thesis concerns **muscular** and **cardio-respiratory** fatigue during physical exercise.

**Muscular fatigue** refers to an exercise-induced decline in the muscle's ability to generate force or power, regardless of task completion. Although often broadly used, most researchers define it more precisely as a reduction in contractile function or measurable performance[44].

**Cardio-respiratory fatigue** arises mainly during prolonged or high-intensity efforts, involving limitations in respiratory and cardiovascular systems. It is driven by factors such as arterial oxygen desaturation and respiratory muscle fatigue, which

can trigger a metaboreflex, causing sympathetic vasoconstriction and reducing limb blood flow, thus worsening muscular fatigue[45].

This suggests that cardio-respiratory fatigue may precede and amplify peripheral muscle fatigue in endurance activities.

### 3.2 RPE: Rate of Perceived Exertion

The RPE (Rate of Perceived Exertion), developed by Borg, represents a valid instrument for the evaluation of the personal fatigue exertion. The RPE scale, traditionally is represented by a scale from 6 to 20[46]. In particular, it follows the following division:

RPE	Exertion Meaning
6	Zero Exertion - Rest
7	
7.5	Extremely Light
8	
9	Very Light Exertion
10	
11	Light
12	
13	Something Hard
14	
15	Hard (Heavy)
16	
17	Very Hard
18	
19	Extremely Hard
20	Maximal Exertion

**Table 3.2:** RPE Scale (Borg 6-20) [46]

The RPE presents a correlation with the physiological parameters, as the heart rate, in particular, during aerobic training. So, it acquires importance not just on

the perceived exertion, but in the intensity of the exercise too.

There exist other conversion scales derived from the Borg-20, in particular the **Borg CR10 scale**[47], represented in Tabel 3.3, which was **used in this study in a modified version**, excluding the addition of 0.5.

RPE Value	Meaning
0	No exertion at all
0.5	Very, very slight
1	Very slight
2	Slight
3	Moderate
4	Somewhat severe
5	Severe
6	
7	Very severe
8	
9	Very, very severe (almost maximal)
10	Maximal Exertion

**Table 3.3:** RPE Scale (CR10: 0-10) [47]

Furthermore, it is important to highlight some limitations of this method. In particular, RPE can be influenced by external factors such as personal motivation and environmental conditions, which is an inherent drawback of using subjective metrics. Nevertheless, several studies **confirm its validity and usefulness**; together with the Karolinska Scale, it remains among the most used methods for assessing subjective exertion.

### 3.3 HRV and Fatigue Detection: Literature Review

The use of Detrended Fluctuation Analysis (DFA) for HRV analysis has arisen as a powerful tool for assessing fatigue across different domains, from sports performance to occupational health. Given that **HRV reflects autonomic nervous system (ANS) adaptations** in response to external stimuli, various studies have explored its potential in detecting fatigue [48],[49]. This review synthesizes key findings

from the literature, emphasizing why DFA stands out as a crucial method in this research.

### 3.3.1 HRV Analysis in Sports Field: The Role of DFA

Fatigue monitoring is particularly relevant in sport and endurance training fields, where physiological adaptations directly impact performance.

Traditional HRV metrics, such as time-domain measures (RMSSD, SDNN) and frequency-domain ones (LF, HF, LF/HF ratio), have long been used to assess stress. The 2018 review [50] confirmed that stress conditions lead to a decrease in HF and an increase in LF.

In contrast, DFA- $\alpha 1$  provides a nonlinear measure of HRV that reflects organismic demands during exercise. The study [51] showed that **DFA-alpha1 changes dynamically with exercise intensity**. In particular, during moderate intensities, it reaches 0.75, aligning with the **aerobic threshold**, then, as intensity increases, it drops below 0.5, indicating a transition to **uncorrelated fluctuations**.

This makes DFA- $\alpha 1$  particularly advantageous in the fitness domain since other traditional metrics are unable to differentiate these two phases, as they have already reached their minimum at the anaerobic threshold.

The literature even describes DFA as an indicator of **total "organismic demand"** rather than a subsystem-specific measure like HR or respiration rate [52].

Notably, during recovery phases, DFA-alpha1 exhibits a rapid increase, making it a promising marker for monitoring fatigue onset and recovery dynamics.

Additional validation of DFA's utility comes from [53], which confirms that DFA-alpha1 is reliable for estimating exercise intensity thresholds in incremental cycling tests.

Moreover, [54] combines DFA with time-domain, frequency-domain, and entropy-based methods in a machine learning model for fatigue detection. This supports the idea that combining DFA with other HRV features enhances its predictive power.

While time-domain HRV measures, such as RMSSD and SDNN, are widely used in sports science, their limited sensitivity in detecting fatigue transitions makes DFA a more suitable option. Studies such as [55], show that while RMSSD and its logarithmic transformation (lnRMSSD) are valid, they **cannot distinguish between different fatigue states**.

### 3.3.2 Assessing Work-Related Fatigue via HRV: The Role of DFA

HRV-based fatigue assessment has been extensively studied in construction workers, miners, and industrial laborers, where the ability to monitor fatigue in real-time could **prevent accidents** and improve worker safety.

One of the most compelling studies in this domain is [56], which used a machine learning approach to classify fatigue levels using HRV features. The study defined fatigue states based on the **Borg scale**, showing that time-domain HRV measures (SDNN, RMSSD) were the most accurate predictors. However, unsurprisingly, DFA- $\alpha_1$  and  $\alpha_2$  increased instead of decreasing, showing no clear correlation with fatigue.

Although this specific result differs from what has been observed in sports, it underscores the complexity of fatigue dynamics in different populations and working conditions.

In extreme and high-altitude environments, HRV-based fatigue monitoring is gaining popularity. The study [57] analyzed miners' HRV using time-domain, frequency-domain, and nonlinear methods (Poincaré plot, entropy measures). It found that LF/HF and SDNN increased with fatigue, while SD1, SD2, and sample entropy decreased, indicating heightened autonomic stress. This supports the notion that nonlinear HRV parameters are essential in differentiating fatigue states in demanding work conditions.

A broader perspective is offered by [58], which highlights HRV as a valuable fatigue assessment tool alongside body movement and skin conductivity. This reinforces the idea that HRV alone may not always be sufficient and that integrating DFA with other physiological markers could enhance fatigue detection accuracy.

### 3.3.3 Rationale for Using DFA for Fatigue Detection

The collective findings from sports and occupational fatigue research highlight the strengths and limitations of different HRV analysis methods. Traditional linear and frequency-domain metrics provide valuable insights, but they often **fail to capture the complexity** of fatigue-induced HRV changes.

DFA, in contrast, offers a **dynamic, fractal-based perspective on HRV**

**fluctuations.** Unlike measures such as SDNN and LF/HF, which may plateau or become unreliable at high levels of exertion, **DFA- $\alpha 1$  maintains sensitivity across different fatigue thresholds.** This is particularly evident in sports studies, where DFA provides a more nuanced reflection of exercise intensity and recovery, as well as in occupational settings, where nonlinear HRV features like DFA help to distinguish between fatigue and non-fatigue states in extreme conditions.

Additionally, machine learning models integrating DFA with time and frequency domain HRV features, as seen in [54] demonstrate that DFA enhances fatigue detection when combined with other metrics.

Finally, the previously mentioned capability of DFA to discern fractal properties, makes it an excellent tool for analyzing fatigue through HRV, providing a more precise and reliable metric compared to traditional HRV indices. Its ability to detect subtle variations in autonomic regulation further reinforces its value. Moreover, studies such as [48], where nonlinear metrics proved to be reliable despite the absence of DFA, highlight its unexploited potential.

Table 3.4: HRV Literature Review

Article	Summary (Goal)	Results	Methodology	Study Context
[50]	Review of 37 articles highlighting that under stress, HF decreases while LF increases.	Frequency and linear analysis for stress determination have been widely studied, focusing on RMSSD, SDNN, LF, and HF.	Frequency domain (LF, HF), Time-domain (RMSSD, SDNN)	
[59]	Using ML to identify 11 promising features for fatigue assessment, comparing them with RPE.	Confirmed that HRV analysis is a useful tool for physical fatigue assessment.	Time-domain (meanHR, NN50, SDANN, HRV/Ti, TINN), Frequency-domain (aVLF), Non-linear (sample, SD2, SD1/SD2, $\alpha_1$ )	
[48]	HRV analysis among agricultural workers using time, frequency, and some non-linear methods to assess fatigue and non-fatigue states.	Nine parameters correlated with fatigue; dispersion patterns were evident in non-linear metrics.	Time-domain (SDNN, SDDSD), Frequency-domain (VLF%, HFnorm, LF/HF), Non-linear (SD1, SD2, Sample Entropy)	Agricultural workers
[53]	Evaluation of DFA $\alpha_1$ in monitoring autonomic balance during incremental running tests.	DFA $\alpha_1$ is a reliable method for the estimation of the intensity thresholds.	Non-linear (DFA $\alpha_1$ )	SPORT
[54]	BPNN-based HRV analysis for detecting physical fatigue.	MeanHR, meanRR, and VLF were the most effective indicators of physical fatigue.	Time-domain (meanHR, meanRR), Frequency-domain (VLF), Non-linear (DFA, entropy)	SPORT
[55]	Use of RMSSD and its logarithm for fatigue assessment in elite athletes.	lnRMSSD is a significant marker for fatigue analysis.	Time-domain (RMSSD, lnRMSSD)	SPORT

Table 3.6: HRV Literature Review

Article	Summary (Goal)	Results	Methodology	Study Context
[52]	DFA $\alpha_1$ as a global marker for monitoring exercise intensity.	DFA $\alpha_1$ is a potential biomarker for intensity thresholds in physical exercise.	Non-linear (DFA $\alpha_1$ )	SPORT
[60]	Validation of DFA $\alpha_1$ as a method for estimating training load and intensity thresholds.	DFA $\alpha_1$ is a good method for estimating physical exercise load.	Non-linear (DFA $\alpha_1$ )	SPORT
[56]	HRV analysis as a promising method for fatigue assessment in construction workers. HRV in comparison with the Borg Scale to assess fatigue using a mix of metrics of time-domain, frequency-domain and non-linear methods through ML algorithms.	Time-domain features were most accurate in ML algorithms; DFA $\alpha_1$ and $\alpha_2$ did not correlate with fatigue.	Time-domain (various), Non-linear (DFA $\alpha_1, \alpha_2$ )	WORKERS
[61]	HRV analysis in chronic fatigue syndrome patients using complex methods.	New method for studying fractal behavior of HRV.	Fractal analysis	Clinical

# Chapter 4

## Methodology

### 4.1 Study Design

The main goal of the experiment is to be able to clearly determine the correlation between changes in behavior of physiological parameters, such as heart rate and heart rate variability, and the onset of fatigue. Specifically, this research focuses on monitoring physiological signals during an incremental cycling test until exhaustion. Therefore, **designing a protocol** that effectively induces **cardio-respiratory fatigue** is essential.

As discussed in previous chapters, physical fatigue can be primarily classified into two types:

- Muscular fatigue
- Cardio-respiratory fatigue

Although these two forms of fatigue are interrelated, this study aims to ensure that participants reach their limit primarily due to cardio-respiratory exhaustion rather than muscular fatigue.

During the incremental test, two types of data were collected:

- HRV (Heart Rate Variability), measured using a Polar H10 chest strap
- RPE (Rating of Perceived Exertion), recorded at each stage of the test

This dual approach allowed for the collection of both objective (HRV) and subjective (RPE) data, providing a comprehensive assessment of perceived fatigue.

The data-set counts 31 participants, 26 males and 5 females.

## 4.2 Literature Review and Rationale for Protocol Design

This section outlines the development of the protocol design, which was formulated based on a comprehensive review of the literature.

### 4.2.1 Analysis of Literature

The design of the testing protocol was developed based on a in-depth review of existing literature on incremental cycling tests and their impact on physiological parameters, particularly in relation to heart rate variability (HRV) and perceived fatigue.

Citation	Test Type	N. Participants	Participant Category
[62]	Stepwise (50W start, 50W/4min)	40	Healthy men (29-69 years)
[63]	Incremental (100W start, +20W/3min)	16	Trained cyclists (8h/week for 6 months)
[64]	Incremental (30W/4min) after warm-up	13	Elite cyclists
[65]	Incremental (25W men, 15W women / 2min)	40	General participants
[66]	Incremental (+14.6W/min after a rest of 3 min) until exhaustion	20	General participants
[67]	4 min at 20W, 6 min at 60W/80W, then 4 min at 20W followed by 15W, 30W, or 45W/min until exhaustion	21	General participants
[68]	Incremental (100W (Woman) and 160W (Men) start, 30W/2min) until exhaustion	56 (18W,38M)	Sub-elite Cyclists
[69]	Incremental (4-6 min rest, 5 min at 30W (W) and 40W (M) warm-up, 5W/20s) until exhaustion	26	16 ME/CFS patients and 10 healthy controls
[60]	Ramp protocol (3 min at 50W warm-up, +1W/3.6s) until cadence < 60rpm	31	General participants - only females

**Table 4.1:** Summary of different incremental cycling test protocols from the literature.

The analysis of the literature revealed a variety of approaches to incremental cycling tests, differing in intensity progression, duration, and termination criteria. The

studies examined (Table 4.1) highlight key methodological elements that influence physiological responses, particularly in relation to heart rate variability (HRV) and perceived fatigue.

From this review, several important considerations emerged:

- The majority of studies employed an **incremental protocol** to ensure progressive fatigue induction.
- **Termination criteria** varied, with some studies defining exhaustion based on cadence drop [60], while others relied on volitional fatigue [66].
- Studies using stepwise increments with specific time intervals [62] provided insights into the optimal workload increase to elicit fatigue without premature muscular failure.
- Participant populations were diverse, with different studies targeting trained cyclists, general participants, and clinical populations, indicating the need for a **protocol adaptable to different fitness levels**.

Taking these findings into account, a **customized protocol was developed** to induce cardio-respiratory fatigue while maintaining control over workload increments, ensuring comparability with previous research while addressing gaps identified in the literature. The following section outlines the final protocol design.

### 4.2.2 Protocol Design

Before starting the study, participants were required to sign an informed consent form, which detailed the study’s objectives, procedures, and their rights as participants. The full document can be found in **Appendix A**.

The protocol is divided into three stages:

- **Qualitative phase:** Participants begin by completing three questionnaires to assess their baseline conditions:
  - Stress Level (**Appendix D**)
  - Quality and quantity of sleep (**Appendix B**)
  - Physical Condition (**Appendix C**)

These assessments provide a comprehensive understanding of each participant’s **initial state** before performing the physical tests.

- **Physical test:** At each stage of the test, participants are asked to report their Rate of Perceived Exertion (RPE) to provide direct feedback on their exertion levels. Heart Rate Variability (HRV) and heart rate (HR) are collected.
- **Recovery Phase:** The final stage lasts 10 minutes, during which participants remain seated while physiological parameters continue to be monitored. At the end of this period, they are also required to report their final RPE to assess their post-exercise condition.

## Physical Test

After remaining **stationary on the bike for 5 minutes**, the test begins with a **5-minute warm-up**, followed by an **incremental phase** where power increases by 15 Watts every 3 minutes for women and 20 Watts every 3 minutes for men, continuing **until exhaustion** ( $RPE = 10$ , corresponding to volitional exhaustion). Upon completing the test, participants undergo a **3-minute cool-down**. Since the test continues until the participant reaches their limit, its duration is not predetermined but varies based on individual endurance.

The stages of test are described in Table 4.2 for men and Table 4.3 for women.

## 4.3 Instrumentation

To ensure accurate and reliable data collection throughout the experiment, a combination of wearable and environmental monitoring devices was employed. The following instruments were used:

- *Polar H10*  
The Polar H10 was used as the primary sensor for monitoring heart rate (HR) and heart rate variability (HRV). Known for its high accuracy and reliability, this chest strap sensor records RR intervals with a sampling rate of 1000 Hz, making it ideal for analyzing autonomic nervous system (ANS) activity during exertion and recovery phases.
- *Tacx NEO Bike Plus Trainer*  
The physical test was conducted using the Tacx NEO Bike Plus Trainer, a high-precision stationary cycling ergometer. This device allows for precise control of resistance and power output, ensuring a standardized and replicable testing protocol across all participants. Additionally, it provides real-time

MEN TEST			
Stage	Duration	Power(W)	Minute
Warm up	00:05:00	60 to 70	00:05:00
Stage 1	00:03:00	90	00:08:00
Stage 2	00:03:00	110	00:11:00
Stage 3	00:03:00	130	00:14:00
Stage 4	00:03:00	150	00:17:00
Stage 5	00:03:00	170	00:20:00
Stage 6	00:03:00	190	00:23:00
Stage 7	00:03:00	210	00:26:00
Stage 8	00:03:00	230	00:29:00
Stage 9	00:03:00	250	00:32:00
Stage 10	00:03:00	270	00:35:00
Stage 11	00:03:00	290	00:38:00
Stage 12	00:03:00	310	00:41:00
Stage 13	00:03:00	330	00:44:00
Stage 14	00:03:00	350	00:47:00
Stage 15	00:03:00	370	00:50:00
Stage 16	00:03:00	390	00:53:00
Stage 17	00:03:00	410	00:56:00
Stage 18	00:03:00	430	00:59:00
Stage 19	00:03:00	450	01:02:00
Stage 20	00:03:00	470	01:05:00

**Table 4.2:** Incremental test protocol for men.

WOMEN TEST			
Stage	Duration	Power(W)	Minute
Warm up	00:05:00	40 to 50	00:05:00
Stage 1	00:03:00	65	00:08:00
Stage 2	00:03:00	80	00:11:00
Stage 3	00:03:00	95	00:14:00
Stage 4	00:03:00	110	00:17:00
Stage 5	00:03:00	125	00:20:00
Stage 6	00:03:00	140	00:23:00
Stage 7	00:03:00	155	00:26:00
Stage 8	00:03:00	170	00:29:00
Stage 9	00:03:00	185	00:32:00
Stage 10	00:03:00	200	00:35:00
Stage 11	00:03:00	215	00:38:00
Stage 12	00:03:00	230	00:41:00
Stage 13	00:03:00	245	00:44:00
Stage 14	00:03:00	260	00:47:00
Stage 15	00:03:00	275	00:50:00
Stage 16	00:03:00	290	00:53:00
Stage 17	00:03:00	305	00:56:00
Stage 18	00:03:00	320	00:59:00
Stage 19	00:03:00	335	01:02:00
Stage 20	00:03:00	350	01:05:00

**Table 4.3:** Incremental test protocol for women.

feedback on power and cadence, contributing to a comprehensive analysis of exertion levels.

- *Room thermometer*

A room thermometer was used to measure the ambient temperature at both the beginning and the end of each participant’s test session. Monitoring environmental conditions ensures that external factors, such as temperature variations, do not influence the physiological responses recorded during the experiment. The temperature data were recorded systematically to assess potential correlations with performance and fatigue levels.

## 4.4 Data Collection

During the test, an Excel table was compiled for each participant to systematically record key time points and environmental conditions. The information collected in

this phase included:

- **Room Temperature Before the Test**
- **Exact Start Time**
- **Exact Sitting Time** (performing the qualitative phase)
- **End of the Qualitative Phase Time**
- **Sitting on the Bicycle Time**
- **Start of the Physical Test Time** (at least 5 minutes after resting on the bicycle)
- **Time at the End of the Final Stage of the Physical Test** ( $\equiv$  Start of Cool Down Phase)
- **Cool Down Stop Time** (after a minimum of 3 minutes of cool down)
- **Recovery Start Time**
- **Recovery Stop Time** (after a minimum of 10 minutes of recovery)
- **Final Room Temperature**

This table was particularly useful for data analysis, as it provides a clear reference for determining the exact phase of the test each participant was in at any given time.

## Chapter 5

# Data Analysis and Pre-Processing

The data analysis process was conducted in **MATLAB** and involved multiple steps to ensure accurate feature extraction while minimizing noise interference.

The process began with acquiring the previously mentioned time table, followed by loading the RPE data for each subject along with their RR and HR data. Once the RR data were imported, the initial step focused on filtering to enhance signal quality and eliminate potential artifacts. This was followed by the segmentation of the data, which will be explained in the subsequent section.

### 5.1 R<sub>Ri</sub>: Filtering and Artifact Removal

To ensure high signal quality and artifact correction, an **adaptive filter** was applied to the R<sub>Ri</sub>. The filter used in this study is a modified version of the method proposed by Wessel et al. The applied filter involves the following steps:

- Initial Artifact Removal: R<sub>Ri</sub> values outside the range of  $(280 - 1500)ms$  (corresponding to  $(214 - 40)$  bpm) were considered artifacts and removed.
- Artifact Percent Filter: A dynamic correction was applied based on the relative percentage change between consecutive RR intervals. If the variation exceeded 30%, the suspect value was replaced with the mean of the previous valid intervals. This was integrated with an adaptive smoothing process using a moving average (window of 7 samples), with a recursive estimation of mean

( $\mu$ ), variance ( $\lambda$ ), and standard deviation ( $\sigma$ ). Sudden deviations exceeding both a relative threshold ( $\rho = 15\%$ ) and a sigma-scaled threshold ( $c_x = 3\sigma$ ) were identified as artifacts and replaced with a random value within the physiological range considering 7 values before.

- **Adaptive Control Filter:** A final pass was conducted using local adaptive statistics (moving mean and standard deviation) to detect outliers. Intervals deviating more than  $3\sigma$  plus a fixed bias ( $\sigma_b = 0.02$ ) from the local mean were corrected to reduce residual fluctuations.
- **Adaptive Mean and Variance Update:** The adaptive mean  $\mu(n)$  and variance  $\lambda(n)$  were updated iteratively using a forgetting factor  $c$ , ensuring dynamic adjustment to the signal trend. The standard deviation  $\sigma(n)$  was then computed to characterize RRi variability.
- **Final Storage of Filtered Data:** The corrected RR intervals were stored for further analysis.

This approach ensures that RRi artifacts are effectively removed while preserving physiological variability, making the filtered signal more reliable for HRV analysis.

## 5.2 Data Acquisition and Segmentation

Filtered RRi data was segmented according to each subject's time table, following these phases:

- 3 minutes seated during the qualitative assessment phase.
- 3 minutes **resting on the bicycle**.
- 5 minutes after the test initiation, corresponding to the **warm-up** phase.
- 3 minutes for **each exercise stage**.
- 3 minutes during the **cool-down** phase.
- 3 minutes in the **recovery** phase.

This segmentation results fundamental for the application of the described DFA algorithm.

## 5.3 Application of DFA

To analyze fluctuations in the heart rate signal, the **Detrended Fluctuation Analysis (DFA)** method was applied to each segment.

DFA was previously described in 2.3.1, and its implementation followed these key steps:

- Step 1: Importing each segmented data.
- Step 2: Set the parameters as:
  - Scales: 4 – 16
  - Polynomial Order,  $m = 1$ : Linear Detrending
  - Generalized Fluctuation Exponent,  $q = 2$ : Standard DFA
- Step 3: Extract the Fluctuation Function  $F_s$  from the *DFA function*.
- Step 4: Extract the Scaling Exponent,  $\alpha_1$ .

# Chapter 6

## Results

### 6.1 Introduction

This chapter presents the results obtained from the application of the filter, described in Chapter 5, on RR intervals and the subsequent analysis based on Fluctuation Analysis Detrended (DFA), described in the previous chapters.

The analysis is divided into two main steps:

- Application of the filter on the raw RR data to remove artifacts and outliers, with comparison between the original and filtered signals.
- Analysis of heart rate variability (HRV) by DFA, applied to the filtered signals to obtain DFA- $\alpha_1$  and correlate it with fatigue level.

To ensure the reliability of the analysis, a comparative statistical analysis is also conducted on the data before and after filtering. In particular, the following parameters are evaluated:

- The mean of total raw signal and mean of the filtered signal.
- The standard deviation of the raw and the filtered signal.
- The number of total corrected artifacts by applying filter, and the percentage of them.
- The CV ( $CV = \frac{std}{mean}$ ) of raw and filtered signal.

From this analysis, subjects with a high percentage of artifacts, will be excluded from further analysis.

The results obtained are displayed through comparative graphs and statistical metrics, thus providing a detailed picture of the effectiveness of filtering and the impact on the subsequent analysis of cardiac variability.

## 6.2 Filter Application

Figure 6.1 shows a **comparison** between raw data and filtered ones of the RRi of each subject.

The raw data, represented in blue, show a lot of artifacts and sudden variations, which may result from movement, detection errors, or problems in the quality of the acquired signal.

Filtered data (green signal) significantly reduces these abnormalities while conserving the expected physiological pattern of RR variability.

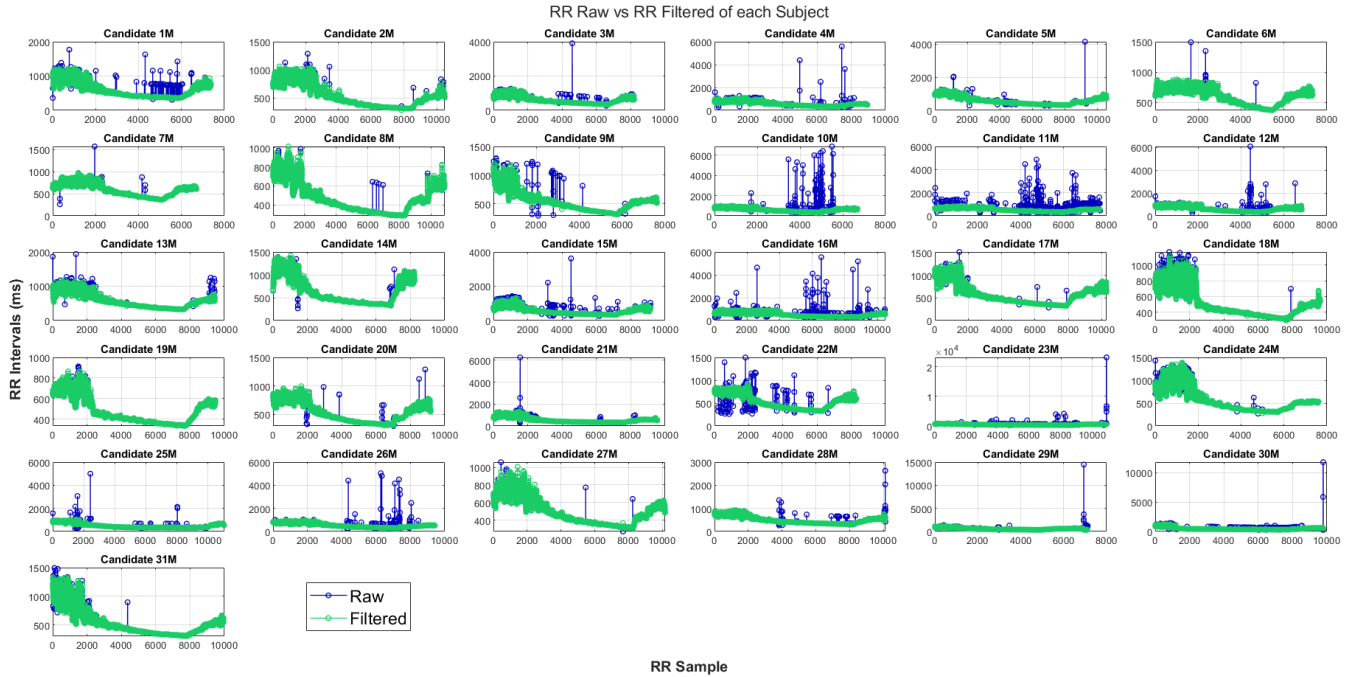


**Figure 6.1:** RR Intervals Raw vs Filtered

Figure 6.2 shows the filtered RR signals for each candidate.

It can be seen that the filter removed most of the outliers, returning a **smoother** and more interpretable signal.

The overall trend indicates a **common pattern** among the subjects, with a gradual

decrease in RR intervals during the power increase throughout the test, followed by an increase in the cooling phase and a peak in the recovery phase.

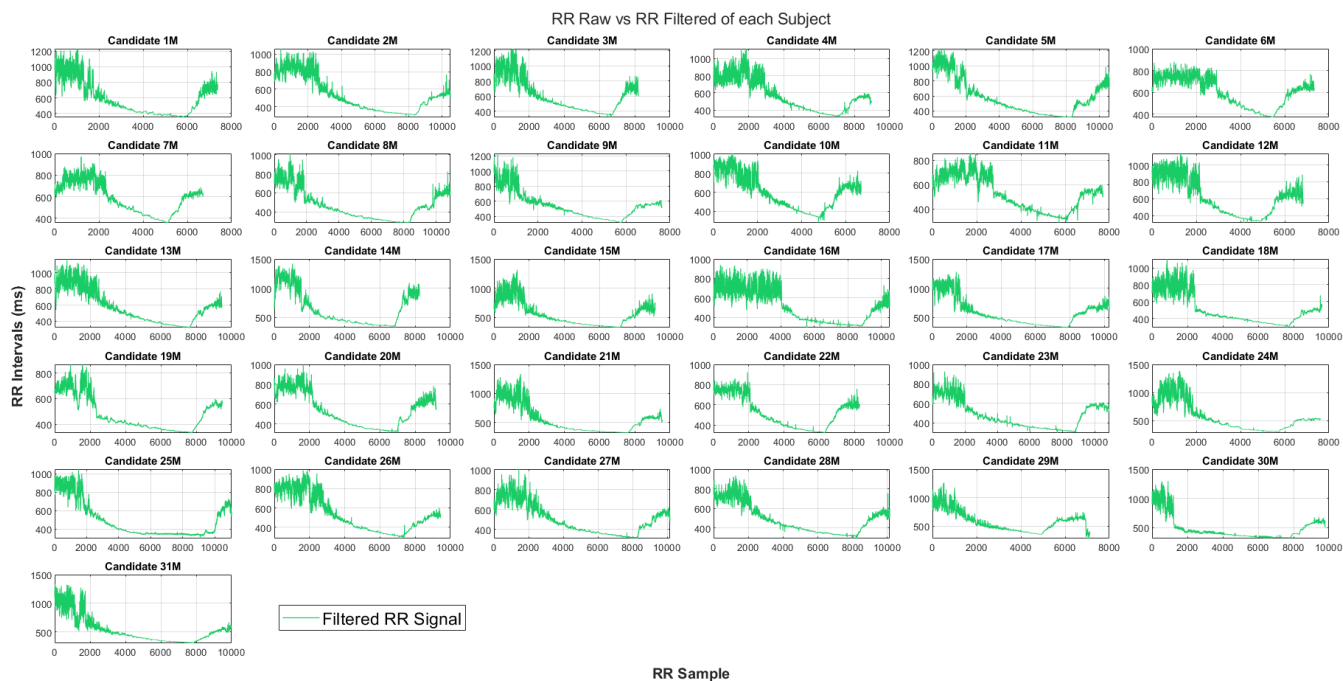
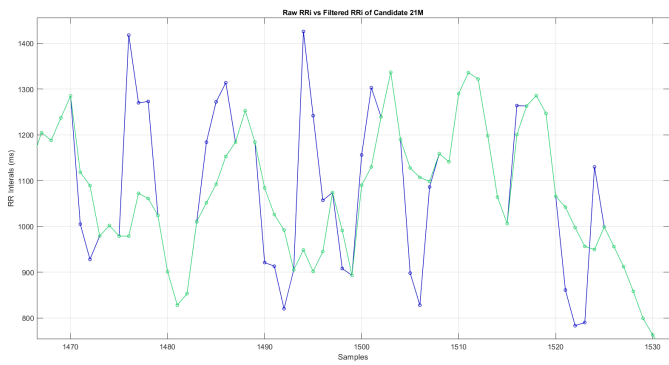
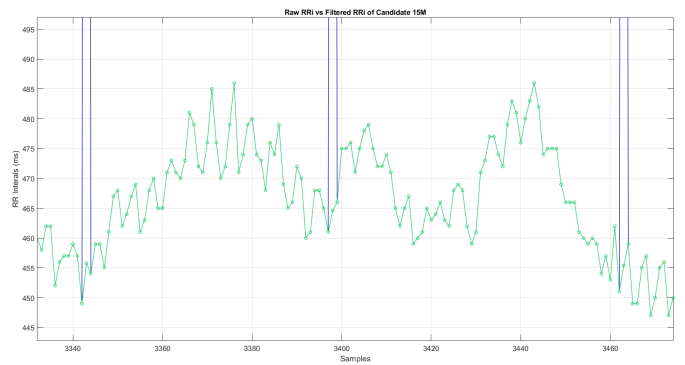


Figure 6.2: RR Intervals Filtered

Figures 6.3 and 6.4 show a **zoomed-in portion of the RRi** before and after the application of the filter. In Figure 6.3, the raw signal exhibits continuous noise and irregularities. While, Figure 6.4 reveals a more stable raw signal, but with some evident artifacts approximately every 60 samples. In both of them it is evident the filter performs: signals are corrected but the **physiological variability is maintained**.



**Figure 6.3:** RRI Filtered: Zoom-In1



**Figure 6.4:** RRI Filtered: Zoom-In2

Table 6.1 presents the statistical analysis of raw and filtered signals for different candidates. The columns 'Mean Raw' and 'Std Raw' represent the mean and standard deviation of the raw signal, while 'Mean Filt.' and 'Std. Filt.' correspond to the same metrics applied to the filtered signal. The 'Tot. Art' column indicates the total number of detected artifacts substituted during the preprocessing analysis, while '%Art.' shows the proportion of data points substituted due to artifacts.

This table illustrates how the total signal of each candidate is affected by the application of the previously described filter. Candidates exceeding a 2.5% artifact rate will be excluded from further analysis to ensure data quality and reliability.

**Table 6.1:** Signal Statistics of Raw and Filtered Data

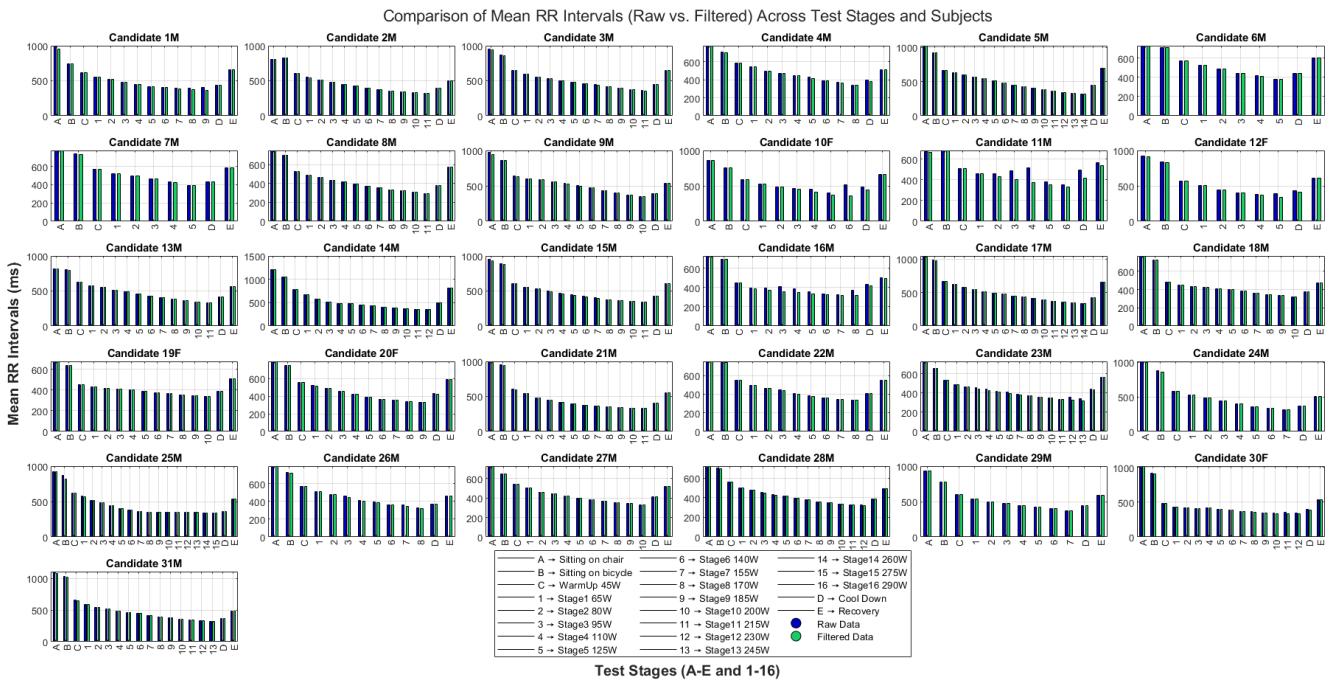
Subject	Mean Raw	Std Raw	Mean Filt.	Std Filt.	Tot Art.	%Art.	CV Raw	CV Filt.
Candidate 1M	596.22	221.78	587.66	216.44	151	2.0472	0.3720	0.3683
Candidate 2M	532.18	194.88	531.65	194.06	8	0.0763	0.3662	0.3650
Candidate 3M	602.42	217.32	599.50	211.62	42	0.5119	0.3607	0.3530
Candidate 4M	568.90	199.21	564.53	179.04	59	0.6586	0.3502	0.3171
Candidate 5M	577.39	231.69	576.55	227.81	19	0.1795	0.4013	0.3951
Candidate 6M	599.36	132.80	598.87	131.83	9	0.1228	0.2216	0.2201
Candidate 7M	586.06	143.25	585.86	142.61	7	0.1044	0.2444	0.2434
Candidate 8M	464.81	152.43	464.56	152.14	5	0.0460	0.3279	0.3275
Candidate 9M	540.21	172.53	537.07	166.19	62	0.8131	0.3194	0.3094
Candidate 10F	620.45	317.17	595.79	178.34	124	1.8499	0.5112	0.2993
Candidate 11M	555.73	225.24	524.45	140.56	416	5.3977	0.4053	0.2680
Candidate 12F	620.94	240.14	612.86	216.55	80	1.1708	0.3867	0.3533
Candidate 13M	574.07	205.77	571.55	201.02	45	0.4757	0.3584	0.3517
Candidate 14M	640.61	291.44	640.45	291.37	12	0.1456	0.4549	0.4549
Candidate 15M	556.12	215.87	550.20	203.46	116	1.2675	0.3882	0.3698
Candidate 16M	524.20	212.42	511.06	164.06	258	2.4597	0.4052	0.3210
Candidate 17M	576.38	226.56	575.33	224.65	22	0.2137	0.3931	0.3905
Candidate 18M	503.95	178.83	501.75	174.18	42	0.4368	0.3549	0.3471
Candidate 19F	475.85	126.11	475.68	125.71	3	0.0317	0.2650	0.2643
Candidate 20F	532.19	168.60	531.91	168.21	16	0.1742	0.3168	0.3162
Candidate 21M	545.00	242.16	542.15	230.50	59	0.6170	0.4443	0.4252
Candidate 22M	525.79	156.12	525.56	153.88	89	1.0724	0.2969	0.2928
Candidate 23M	485.23	282.58	476.33	135.83	126	1.1572	0.5824	0.2852
Candidate 24M	561.55	258.60	557.67	251.78	70	0.9191	0.4605	0.4515
Candidate 25M	493.15	204.93	490.63	193.54	70	0.6332	0.4156	0.3945
Candidate 26M	538.60	216.10	531.65	186.26	102	1.0809	0.4012	0.3503
Candidate 27M	497.19	148.31	496.97	147.93	6	0.0590	0.2983	0.2977
Candidate 28M	486.41	148.64	484.91	145.01	35	0.3455	0.3056	0.2990
Candidate 29M	582.47	252.39	574.42	180.66	120	1.6847	0.4333	0.3145
Candidate 30F	487.13	239.85	479.44	196.65	167	1.7069	0.4924	0.4102
Candidate 31M	534.92	236.17	531.50	229.11	83	0.8322	0.4415	0.4311

Figure 6.5 visually compares the mean RR intervals before and after filtering across all test stages and candidates. Each subplot represents a specific candidate, where the blue bars correspond to raw mean RR intervals and the green bars represent the filtered values.

The x-axis denotes the different test stages, including rest phases (A, B, C), increasing workload levels (1–16), the cool-down phase (D) and the recovery one (E). The y-axis displays the mean RR interval in milliseconds (ms).

As expected, the results show a consistent decrease in RR intervals with increasing workload, reflecting the expected cardiovascular response to exercise.

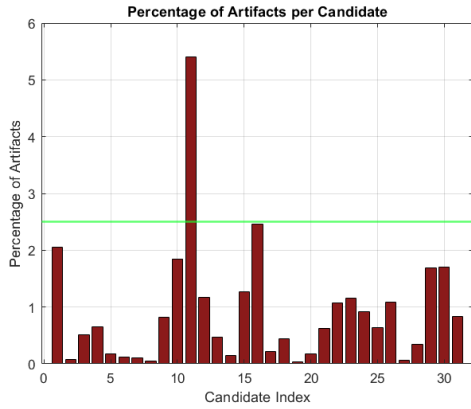
The close alignment between raw and filtered data suggests that the applied filtering method effectively **preserves the essential signal characteristics** while removing artifacts.



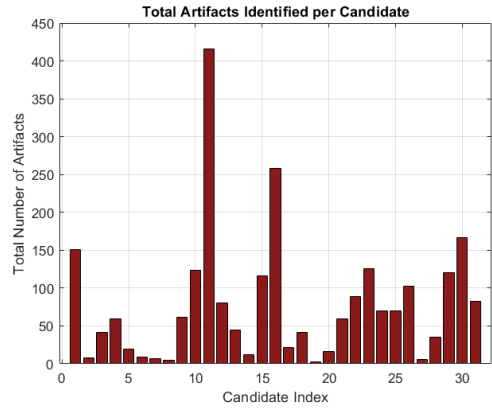
**Figure 6.5:** Mean Raw Vs Mean Filtered

Figure 6.6 illustrates the total percentage of **detected artifacts** for each candidate. The x-axis represents the candidate index, while the y-axis quantifies the percentage of artifacts present in the signal. The horizontal green line marks the predefined exclusion threshold of 2.5%. Candidates exceeding this threshold are excluded from further analysis. As observed, Candidate 11 exceeds this limit, while Candidate 16 is just below the threshold.

While figure 6.7 shows the total number of artifacts for each subject.



**Figure 6.6:** Percentage of Artifacts for Each Subject



**Figure 6.7:** Total Artifacts for Each Subject

Figure 6.8 illustrates the **distribution of artifact percentages** relative to the segment length for each subject across all stages of the test. Each cell in the heatmap represents a specific subject-stage combination, where the color intensity encodes the artifact percentage. Dark blue shades correspond to low artifact presence, indicating high signal quality during that stage, while warmer colors (ranging from yellow to red) highlight stages with higher percentages of artifacts, suggesting lower data quality. This visual representation allows for a rapid and intuitive identification of both isolated artifact peaks and subjects who consistently exhibit high artifact rates across multiple stages.

Figure 6.9 presents a scatter plot illustrating the percentage of artifacts for each test stage, calculated relative to the total number of RR intervals for each subject; each color represents a different Candidate. The data, aggregated across all participants, show that artifact percentages remain consistently low across stages, with a maximum of approximately 0.9%, excluding Candidate11M, who exhibited the highest artifact levels in stages 2, 3, 4, 5, as well as Cool-Down and Recovery (depicted in burgundy).

## Results

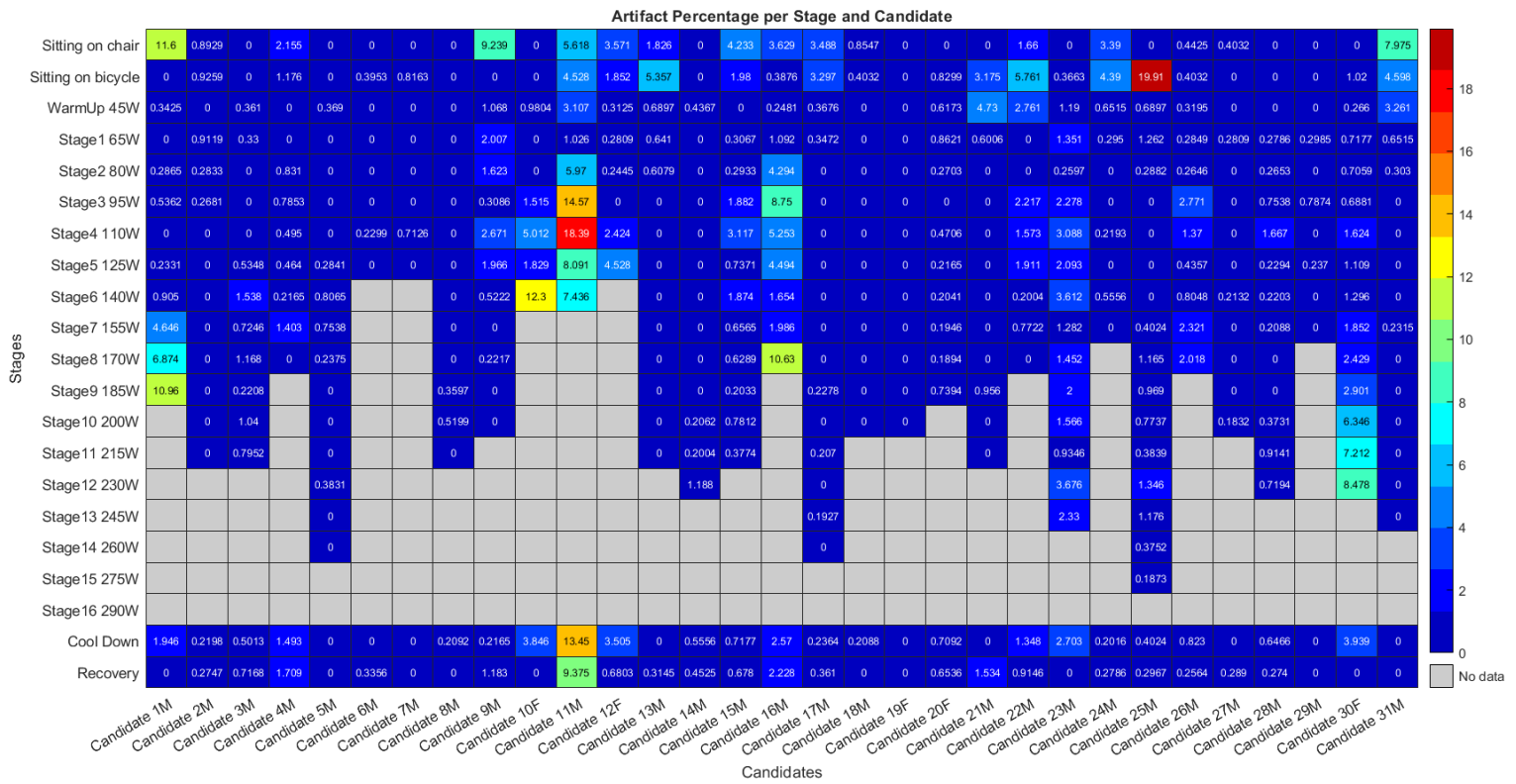


Figure 6.8: Heatmap About Artifacts Distribution

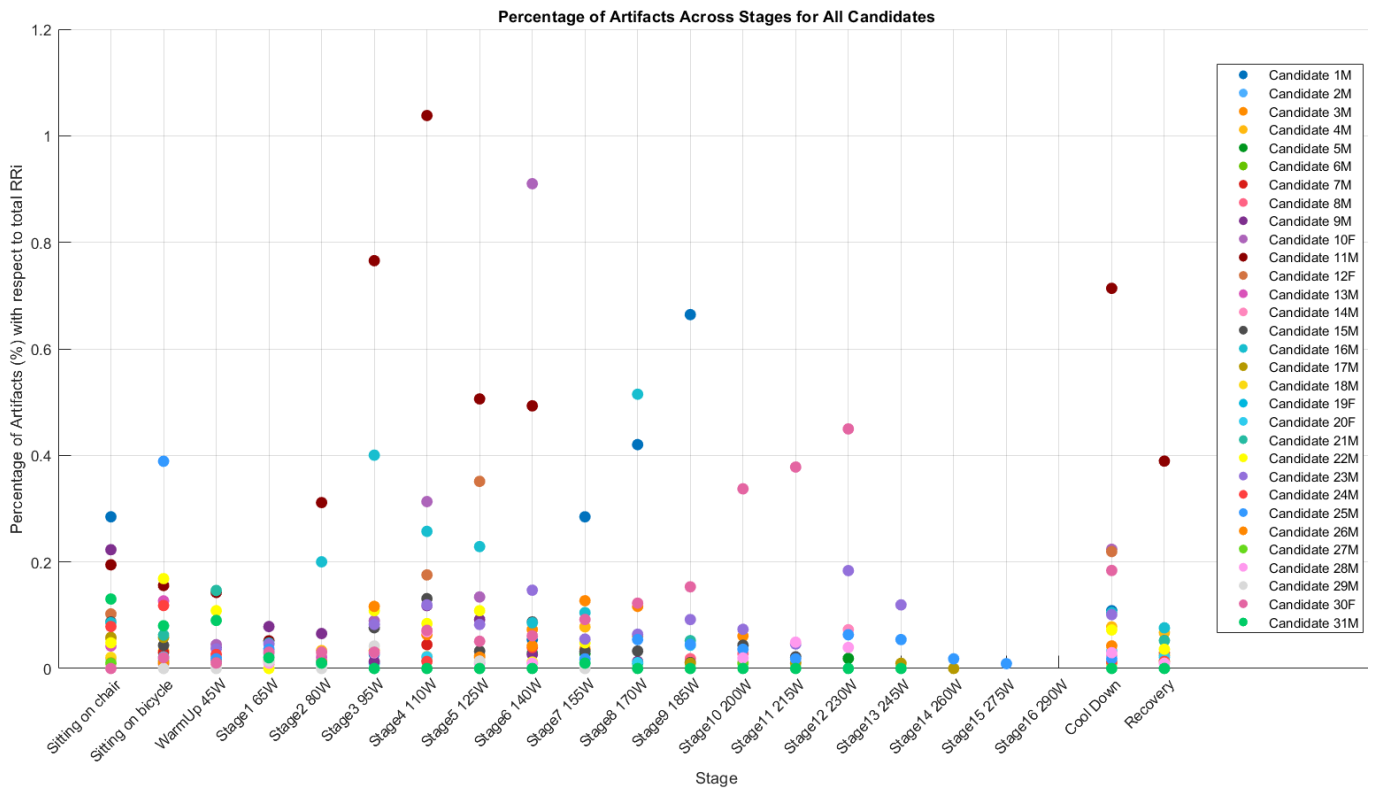


Figure 6.9: ScatterPlot of Percentage of Artifacts

### 6.3 DFA Algorithm Application

This figure 6.10 shows the trend of DFA- $\alpha_1$  of HRV with respect to RPE during the incremental test. Colours represent the bicycle power during the exercise, while the blue line and the red one, correspond respectively to the DFA- $\alpha_1$  and the RPE values. Appendix E, shows a better visualization of the following subplots.

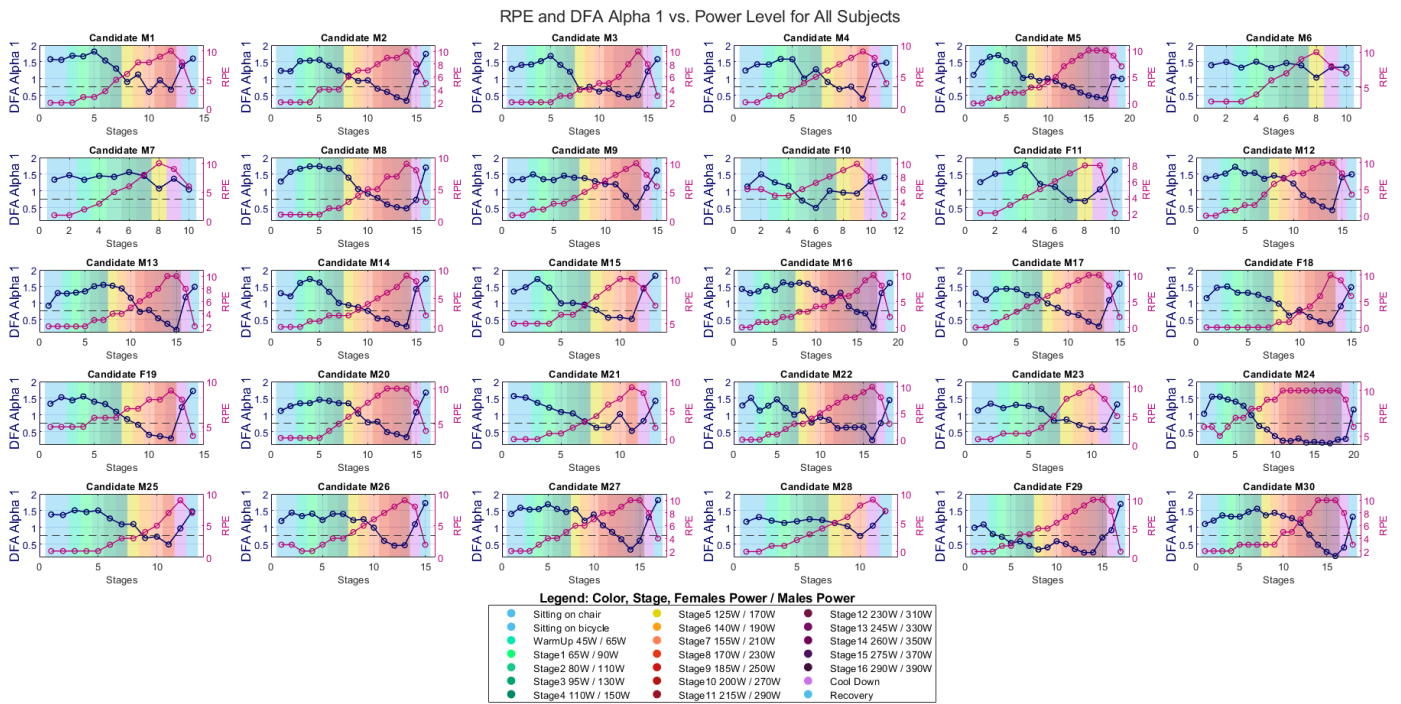


Figure 6.10: DFA-alpha1 vs RPE and Power Stages

The following figure 6.11 is similar to the previous one, but it represents the inverse of DFA- $\alpha_1$  of HRV with respect to RPE. This representation emphasizes that, for the majority of subjects, as the exercise power increases, the inverse of DFA- $\alpha_1$  increases as the RPE does.

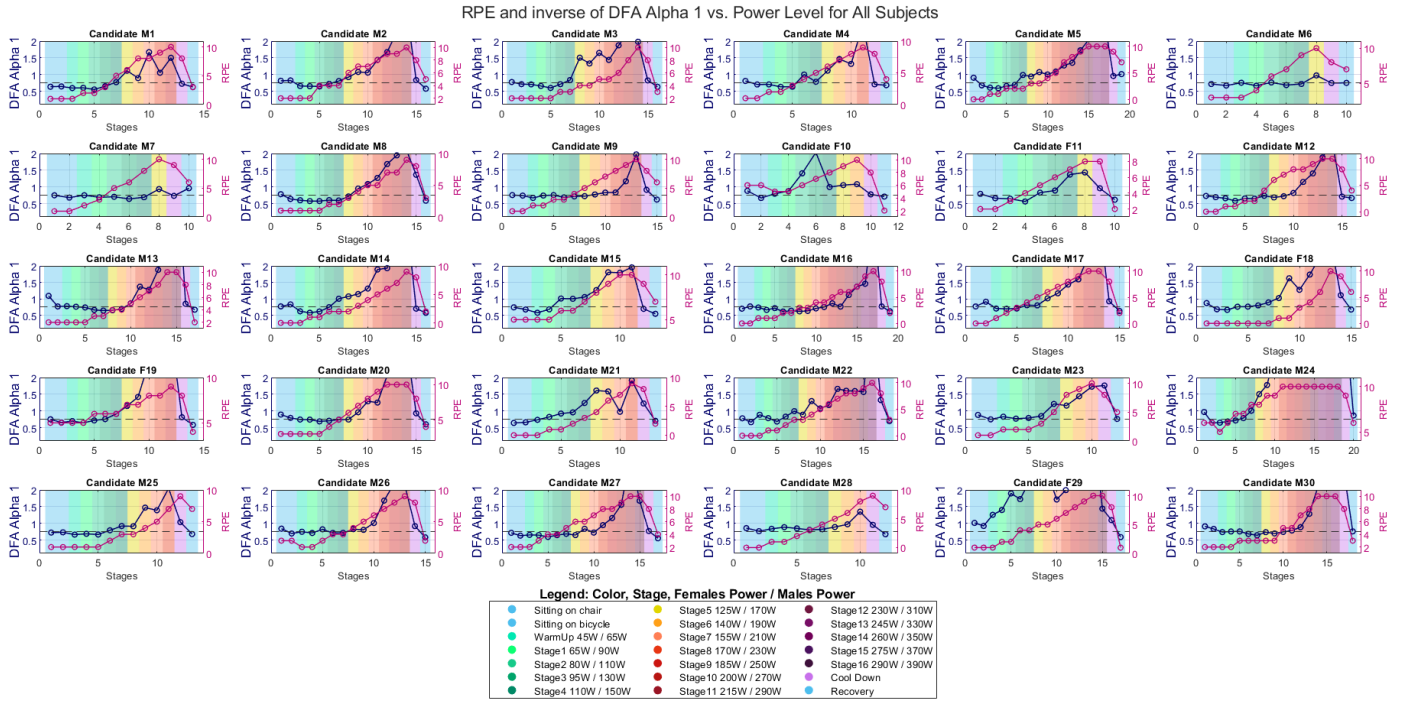


Figure 6.11: Inverse of DFA-alpha1 vs RPE

The following figures, 6.12 and 6.13, represent the  $DFA-\alpha_1$  values as radius, the RPE as dimension of markers and HR as the colors, for each subject. Each part of the circle represents a step of the exercise, starting from the resting one to the maximum effort, without taking into account the recovery phase. It can be observed:

- Rest part: little markers representing lower RPE values, low HR values and higher  $DFA-\alpha_1$  values.
- Increment of test: HR and RPE increases and  $DFA-\alpha_1$  decreases.

Majority of subjects shows a **spiral pattern**, with the marker becoming bigger (higher values of RPE), color becoming red (HR to higher values) and the radius becoming shorter ( $DFA-\alpha_1$  decrement).

This results, in a clear way demonstrates that as the effort increases, HR increases and  $DFA-\alpha_1$  decreases as the subjective perception of effort is increasing.

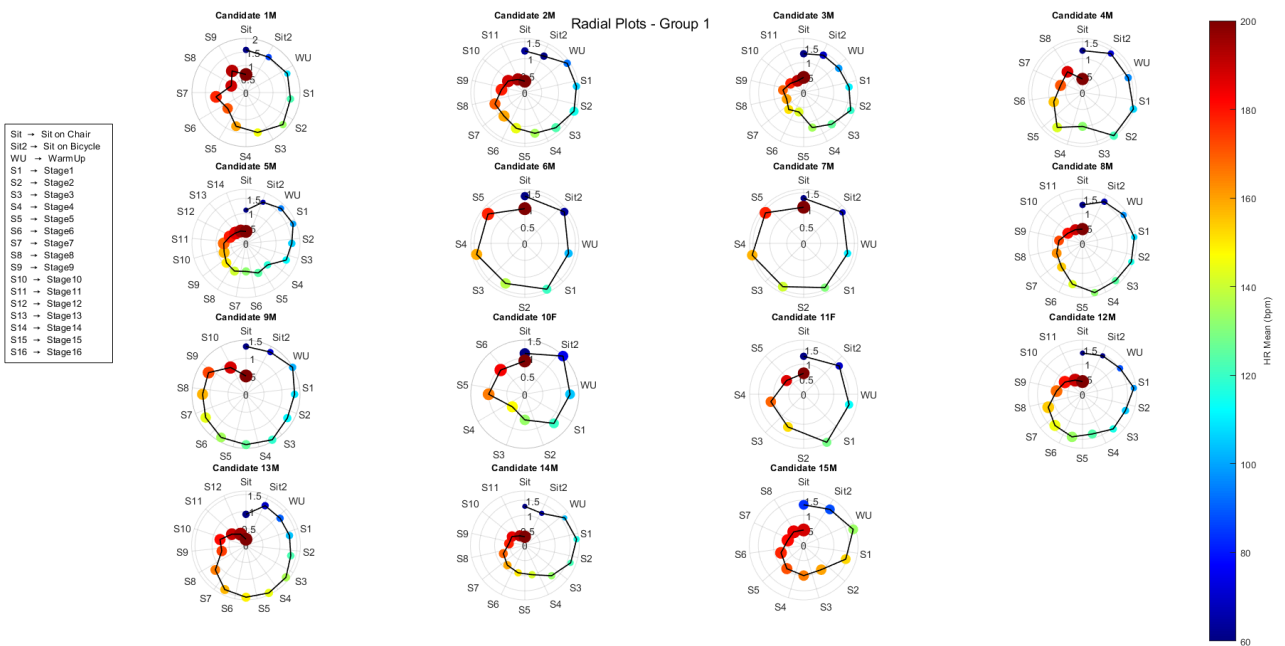


Figure 6.12: Radial Plot of All Subjects: DFA-alpha1, Heart Rate, and RPE Across Exercise Stages

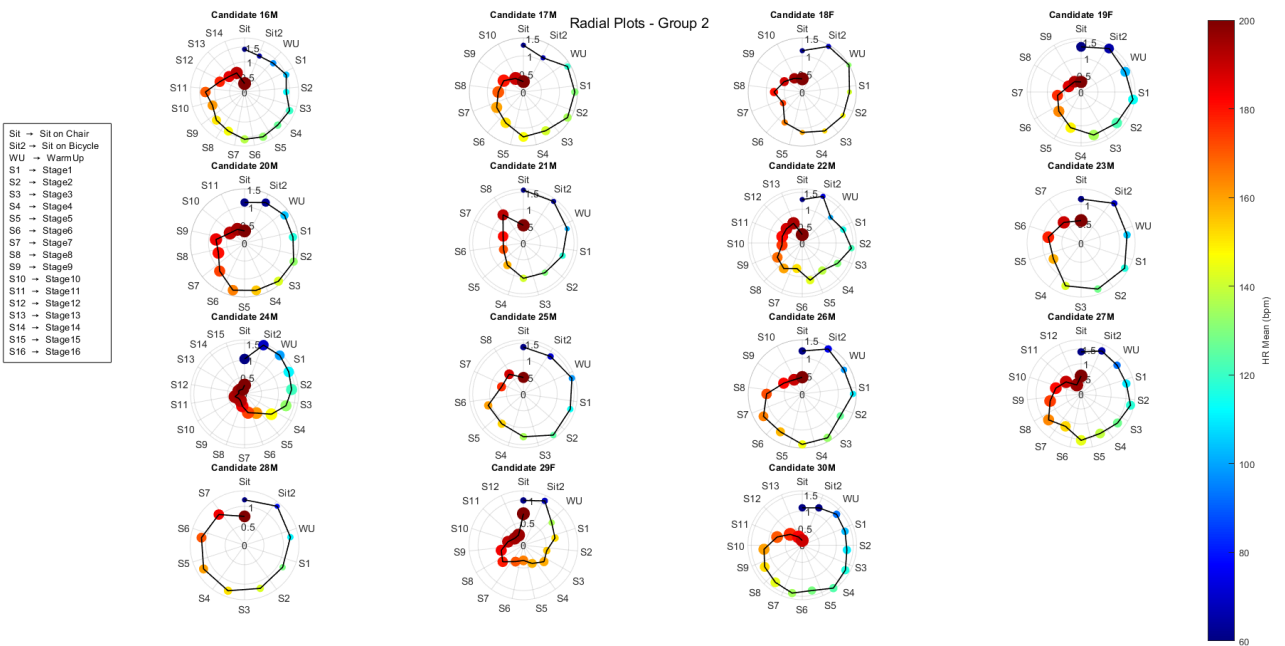
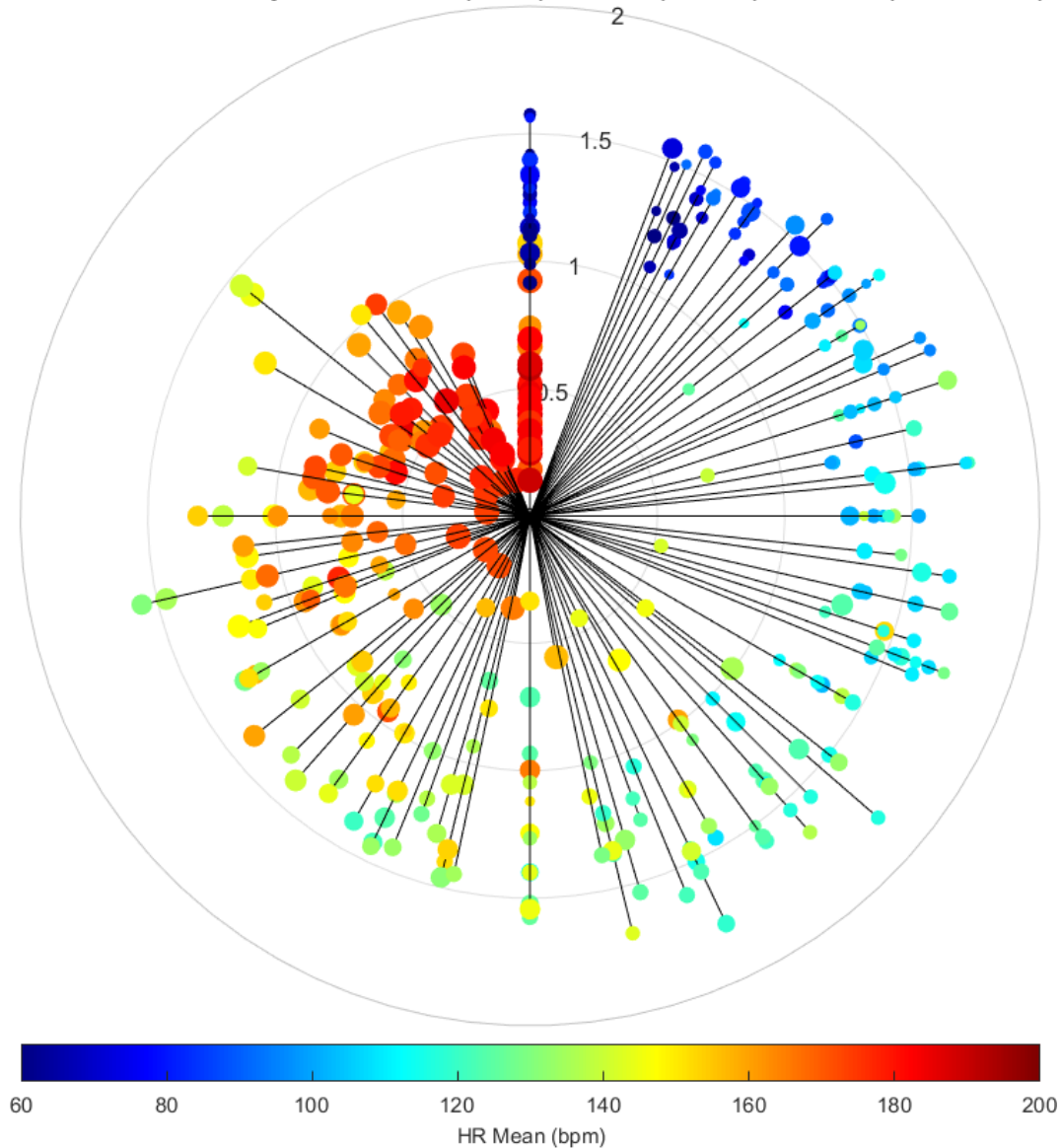


Figure 6.13: Radial Plot of All Subjects: DFA-alpha1, Heart Rate, and RPE Across Exercise Stages

The following plot, 6.14, shows all subjects together. Again the radius represents

DFA- $\alpha_1$ , HR is represented by the color of markers and RPE values are represented by the markers' size. This plot also displays the progression from resting phase to maximal effort, excluding cool-down and recovery stages. This visualization results useful to observe that **the pattern is common for the majority of subjects**, so, at the resting phase the values of DFA- $\alpha_1$  are more dispersive, then, they become more concentrate and lower as the fatigue increases.

**Radial Plot of All Subjects: HR Mean (Color), DFA  $\alpha_1$  (Radius), and RPE (Marker Size)**



**Figure 6.14:** Radial Plot of All Subjects Together: DFA-alpha1, HR, and RPE

### 6.3.1 DFA- $\alpha_1$ and RPE Analysis

The first figure 6.15, represents a box plot of DFA- $\alpha_1$  with respect to RPE values:

- $X$  – Axis  $\rightarrow$  RPE Values [0 – 10].
- $Y$  – Axis  $\rightarrow$  DFA- $\alpha_1$  values.
- Blue Box  $\rightarrow$  contains the 50% of total data.
- Red Line  $\rightarrow$  data median for the correspondent RPE level
- Black Lines  $\rightarrow$  data dispersion, without taking into account outliers.
- Blue Circles  $\rightarrow$  outliers, values out of normal range.

In general, it can be observed a decrease in DFA- $\alpha_1$  corresponding to an increase of RPE. This representation clearly illustrates that the pattern of decrease in DFA- $\alpha_1$  is common for all the subjects.

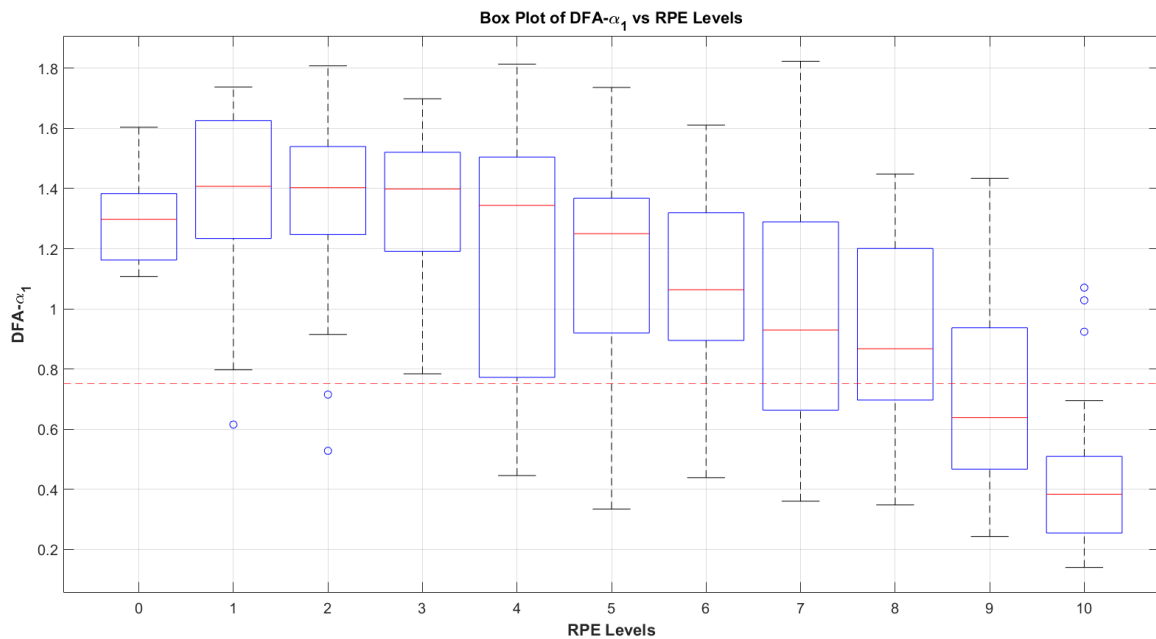


**Figure 6.15:** DFA- $\alpha_1$  and RPE: Box Plot

Table 6.2 presents the percentage distribution of DFA- $\alpha_1$  ranges for each RPE (Rating of Perceived Exertion) level. Each column corresponds to a specific RPE value, and the percentages within that column indicate how the DFA- $\alpha_1$  values are distributed. To better illustrate, the cell in position (1,1), which reports a value of 17.647%, indicates that among all the observations with  $RPE = 0$ , 17.647% fall within the range  $\alpha_1 > 1.45$ . So, the values in each column sum to 100%, reflecting the relative occurrence of each DFA- $\alpha_1$  range within that specific level of perceived exertion.

**Table 6.2:** Percentage Distribution of RPE by DFA- $\alpha_1$  Ranges (7-Class Classification)

DFA- $\alpha_1$ Range	0	1	2	3	4	5	6	7	8	9	10
$\alpha_1 > 1.45$	17.647	45.946	39.286	36.364	32.353	16.667	16.667	12.121	0.000	0.000	0.000
$1.2 < \alpha_1 \leq 1.45$	52.941	32.432	42.857	38.636	32.353	41.667	16.667	18.182	25.000	9.677	0.000
$1.0 < \alpha_1 \leq 1.2$	29.412	10.811	8.929	15.909	5.882	11.111	25.000	9.091	19.231	6.452	5.000
$0.75 < \alpha_1 \leq 1.0$	0.000	8.108	5.357	9.091	11.765	13.889	22.222	24.242	21.154	19.355	2.500
$0.5 < \alpha_1 \leq 0.75$	0.000	2.703	3.571	0.000	14.706	11.111	16.667	27.273	23.077	35.484	22.500
$0.25 < \alpha_1 \leq 0.5$	0.000	0.000	0.000	0.000	2.941	5.556	2.778	9.091	11.538	25.806	45.000
$\alpha_1 \leq 0.25$	0.000	0.000	0.000	0.000	0.000	0.000	0.000	0.000	0.000	3.226	25.000

While Figure 6.16 represents a heatmap of the previous table, providing a more intuitive and immediate visualization of the distribution of RPE values across different ranges of DFA- $\alpha_1$ . Each color indicates a range of RPE percentage occurring. Specifically, colors indicate:

- $0\% < \textit{blue} < 10.5\%$
- $10.5\% < \textit{cyan} < 21\%$
- $21\% < \textit{green} < 31.5\%$
- $31.5\% < \textit{yellow} < 42\%$
- $42\% < \textit{orange} < 52.5\%$

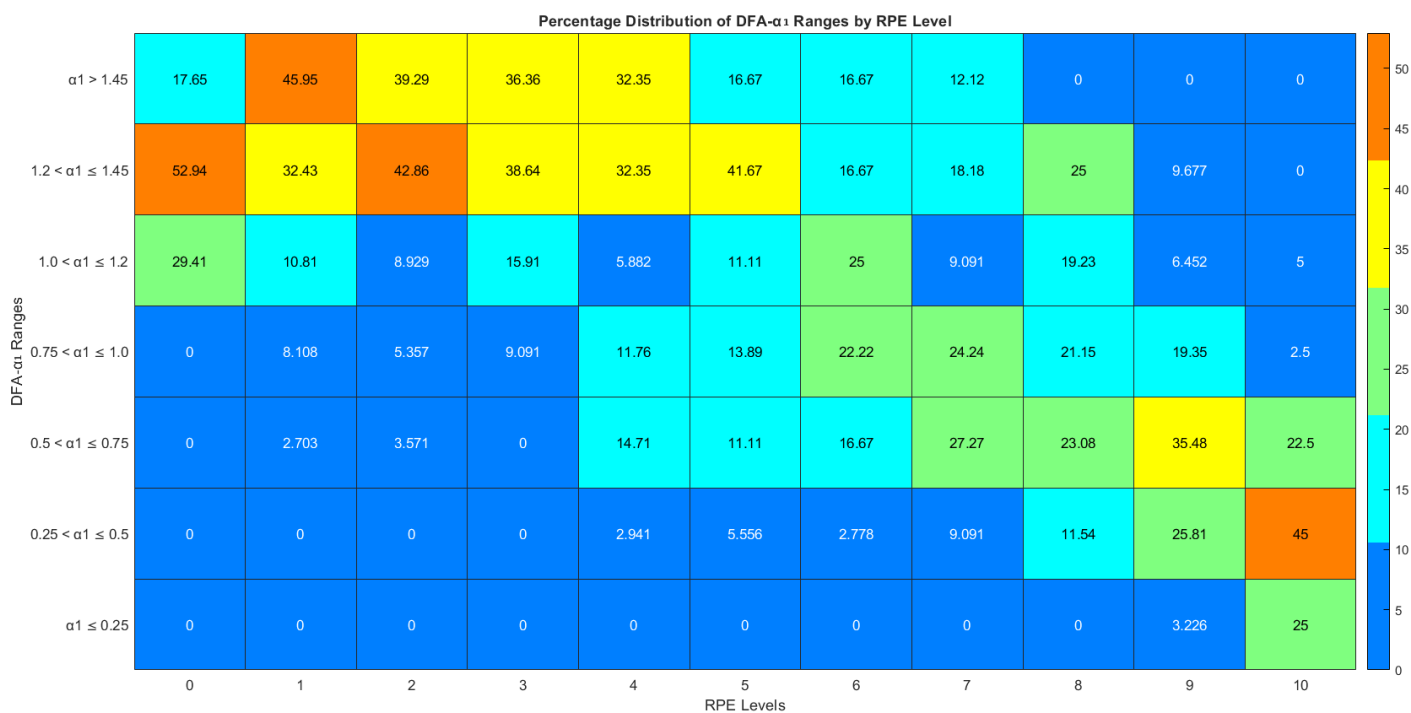


**Figure 6.16:** Percentage Distribution of RPE by DFA- $\alpha_1$  Ranges - 7 Class: Heatmap

Table 6.3 is directly derived from Table 6.2, through a simplified categorization of DFA- $\alpha_1$  values into four wider ranges. This summarization aims to enhance interpretability while preserving the physiological meaning of each range. The ranges are defined as:

- $\alpha_1 > 1.15$
- $0.85 < \alpha_1 \leq 1.15$
- $0.59 < \alpha_1 \leq 0.85$
- $0.0 < \alpha_1 \leq 0.59$

In particular, the table, together with the corresponding Figure 6.17, illustrates the percentage distribution of RPE values across these four DFA- $\alpha_1$  intervals, offering a clear visual representation of how perceived exertion relates to the progressive loss of fractal complexity in physiological dynamics.

**Table 6.3:** Percentage Distribution of RPE by DFA- $\alpha_1$  Ranges (4-Class Classification)

DFA- $\alpha_1$ Range	0	1	2	3	4	5	6	7	8	9	10
$\alpha_1 > 1.15$	76.471	81.081	85.714	77.273	64.706	63.889	38.889	30.303	10.345	4.167	0.000
$0.85 < \alpha_1 \leq 1.15$	23.529	13.514	10.714	18.182	8.824	13.889	41.667	27.273	24.138	12.500	7.500
$0.59 < \alpha_1 \leq 0.85$	0.000	5.405	1.786	4.545	17.647	13.889	8.333	27.273	44.828	33.333	7.500
$0.0 < \alpha_1 \leq 0.59$	0.000	0.000	1.786	0.000	8.824	8.333	11.111	15.152	20.690	50.000	85.000

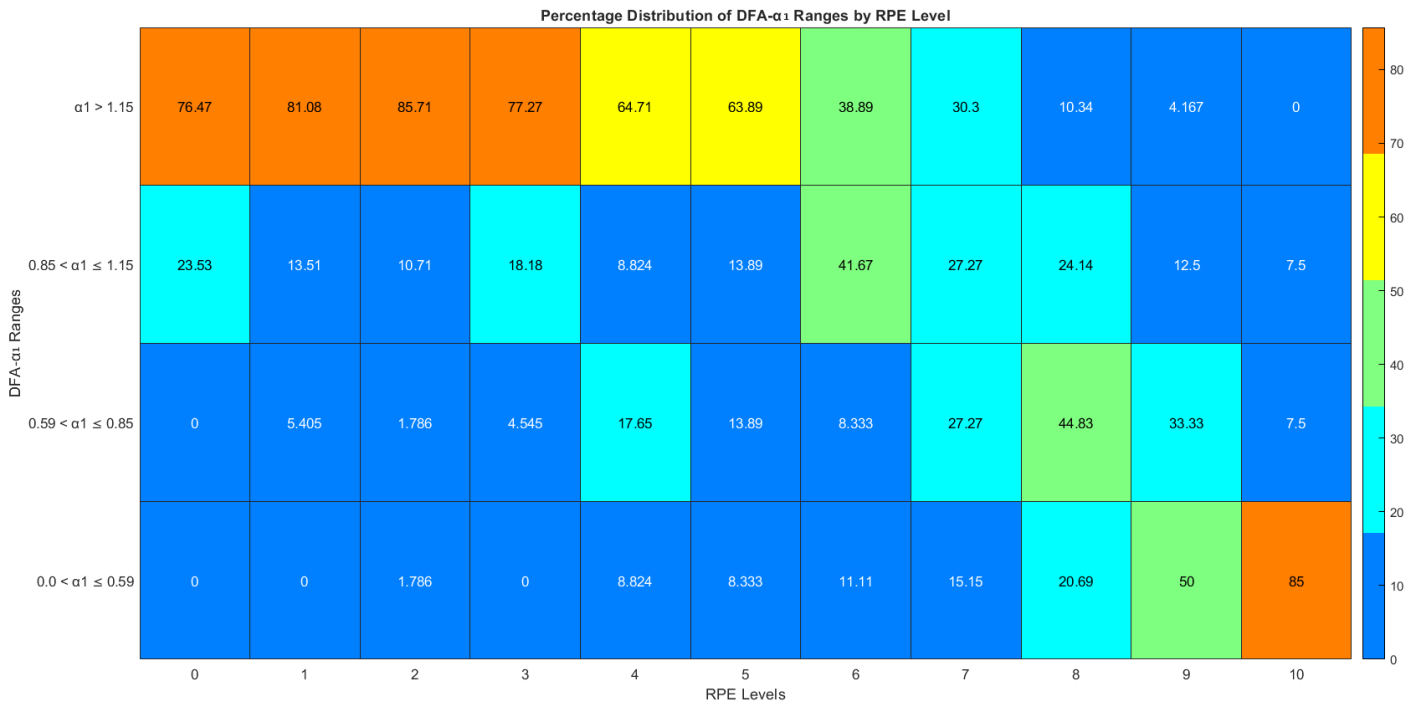


**Figure 6.17:** Percentage Distribution of RPE by DFA- $\alpha_1$  Ranges - 4 Class: Heatmap

Based on these results, a **fatigue classification** is proposed, achieving an **overall accuracy of 61.78%**.

The classification scheme, which combines DFA- $\alpha_1$  thresholds and corresponding RPE values, is presented in Table 6.4.

The classification performance, including the per-class accuracy, is reported in Table 6.5.

**Table 6.4:** Correspondence Between DFA- $\alpha_1$  Ranges, RPE Values and Fatigue Classification

DFA- $\alpha_1$ Range	RPE Values	Fatigue Classification
$\alpha_1 > 1.15$	0, 1, 2, 3, 4, 5	Low fatigue
$0.85 < \alpha_1 \leq 1.15$	6, 7	Moderate fatigue
$0.59 < \alpha_1 \leq 0.85$	8	High fatigue
$\alpha_1 \leq 0.59$	9, 10	Critical fatigue

**Table 6.5:** Accuracy of DFA- $\alpha_1$  Fatigue Classification Compared to RPE Labels (4-Class Scheme)

Class	N.Total	N.Correct	Accuracy (%)
Low fatigue	224	170	75.893
Moderate fatigue	36	15	41.667
High fatigue	85	25	29.412
Critical fatigue	71	47	66.197

Figure 7.1 represents the obtained values of DFA- $\alpha_1$  and RPE at each stage with the displayed color based on the classification proposed with respect to DFA- $\alpha_1$  ranges. Specifically:

- Green: Low Fatigue
- Yellow: Moderate Fatigue
- Orange High Fatigue
- Red Critical Fatigue

A better representation is illustrated in E.

Table 6.6 summarizes, for each subject, the number of the last completed stage, the corresponding DFA- $\alpha_1$  value, the DFA- $\alpha_1$  during the cool-down phase, the resulting  $\Delta_{\alpha_1}$ , the respective RPE values (at the end of the test and during cool-down), and the self-reported fitness level obtained from the questionnaire. The data in this table show that the cool-down (CD) phase results in a  $\approx 87\%$  error rate.

Highlighted  $\alpha_{CD}$  values represent cases in which the cool-down DFA- $\alpha_1$  lies outside the expected range for RPE values of 8 or 9 (the only values reported by the subjects).

Highlighted **StageNum** cells indicate high performance levels, using 8 as the threshold ( $>8$ ).

Highlighted  $\Delta\alpha_1$  values represent cases where the difference exceeds 0.5, suggesting a rapid autonomic recovery following intense exercise, a potential indicator of good fitness.

Highlighted **Fitness** cells indicate subjects who self-reported a fitness level  $> 8$ .

Figure 6.19 provides a graphical representation of the corresponding table. Notably, it highlights that the majority of subjects (27 out of 30) exhibit DFA- $\alpha_1$  values outside the expected range during the cool-down phase.

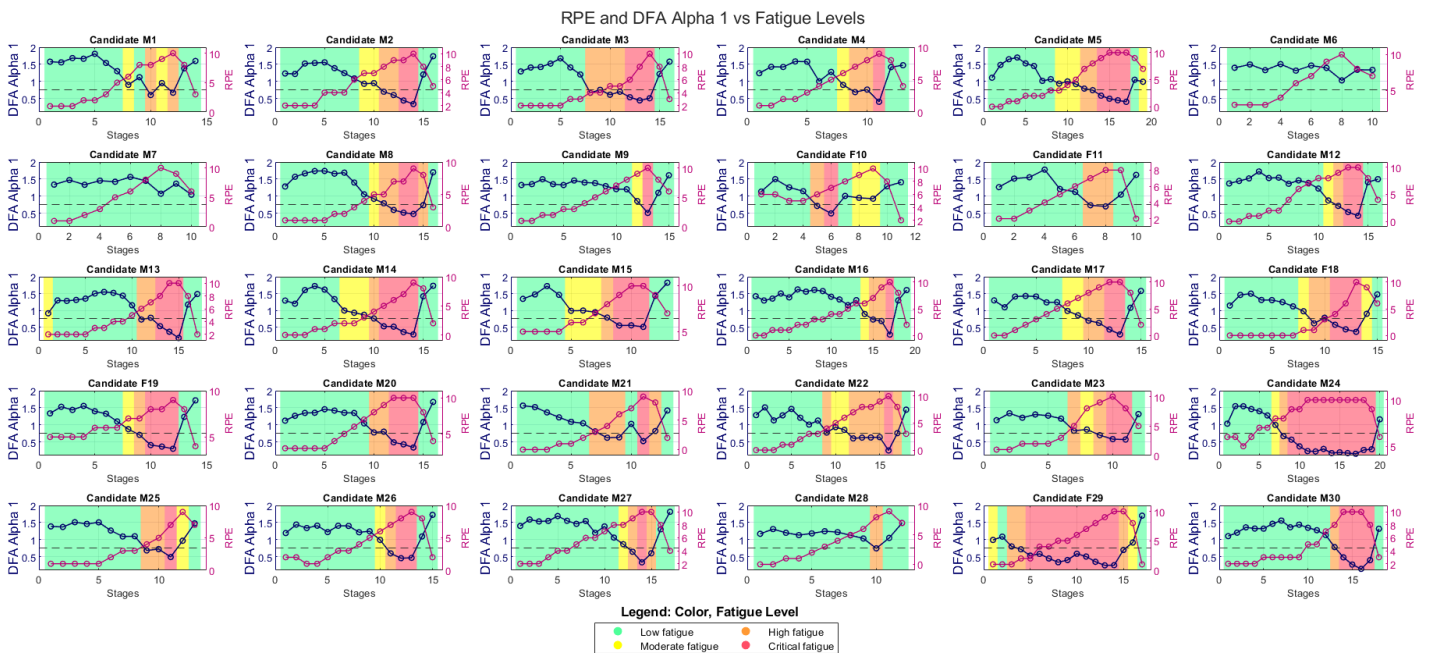


Figure 6.18: DFA- $\alpha_1$  values vs RPE and Fatigue Classification

Table 6.6: Last Stage and Cool Down: $\Delta_\alpha$ , RPE

Subject	StageNum	$\alpha_{last}$	$\alpha_{CD}$	$\Delta\alpha$	$RPE_{Last}$	$RPE_{Cool}$	Fitness
Candidate 1	9	0.666533768	1.3806251	0.714091333	10	8	8
Candidate 2	11	0.334891278	1.201579809	0.866688531	10	8	6
Candidate 3	11	0.504759432	1.2146616	0.709902168	10	8	8
Candidate 4	8	0.400748689	1.417679957	1.016931268	9	8	7
Candidate 5	14	0.398720231	1.046700696	0.647980464	10	9	8
Candidate 6	5	1.028254854	1.339334491	0.311079637	10	8	6
Candidate 7	5	1.070367408	1.365071873	0.294704465	10	9	6
Candidate 8	11	0.47641187	0.733594819	0.257182949	9	8	8
Candidate 9	10	0.506922572	1.095095467	0.588172895	10	8	8
Candidate 10	6	0.923950578	1.288608245	0.364657667	10	8	9
Candidate 11	5	0.697389517	1.043324339	0.345934821	8	8	6
Candidate 12	11	0.422909736	1.40897502	0.986065283	10	8	6
Candidate 13	12	0.182699128	1.174863121	0.992163993	10	8	8
Candidate 14	11	0.287809984	1.420887308	1.133077324	9	8	10
Candidate 15	8	0.511328079	1.43358863	0.922260551	10	9	7
Candidate 16	14	0.282542765	1.296825603	1.014282838	10	8	8
Candidate 17	10	0.288382058	1.079204476	0.790822419	10	8	8
Candidate 18	10	0.365381858	0.90001991	0.534638051	10	9	10
Candidate 19	9	0.298049461	1.232454737	0.934405276	9	8	7
Candidate 20	11	0.33398518	1.078155815	0.744170634	10	8	7
Candidate 21	8	0.522597339	0.817794888	0.295197549	9	8	7
Candidate 22	13	0.247225902	0.754502112	0.50727621	10	8	7
Candidate 23	7	0.579513922	0.56764964	-0.011864283	10	8	7
Candidate 24	15	0.261492118	0.282855324	0.021363207	10	9	7
Candidate 25	8	0.488275345	0.96560533	0.477329986	7	9	8
Candidate 26	10	0.463737367	1.091058489	0.627321122	9	8	7
Candidate 27	12	0.596992557	1.299303502	0.702310945	10	8	7
Candidate 28	7	0.741749849	1.047996386	0.306246537	8	9	7
Candidate 29	12	0.694460598	0.912788221	0.218327622	10	8	8
Candidate 30	13	0.139949575	0.395684693	0.255735119	10	8	6

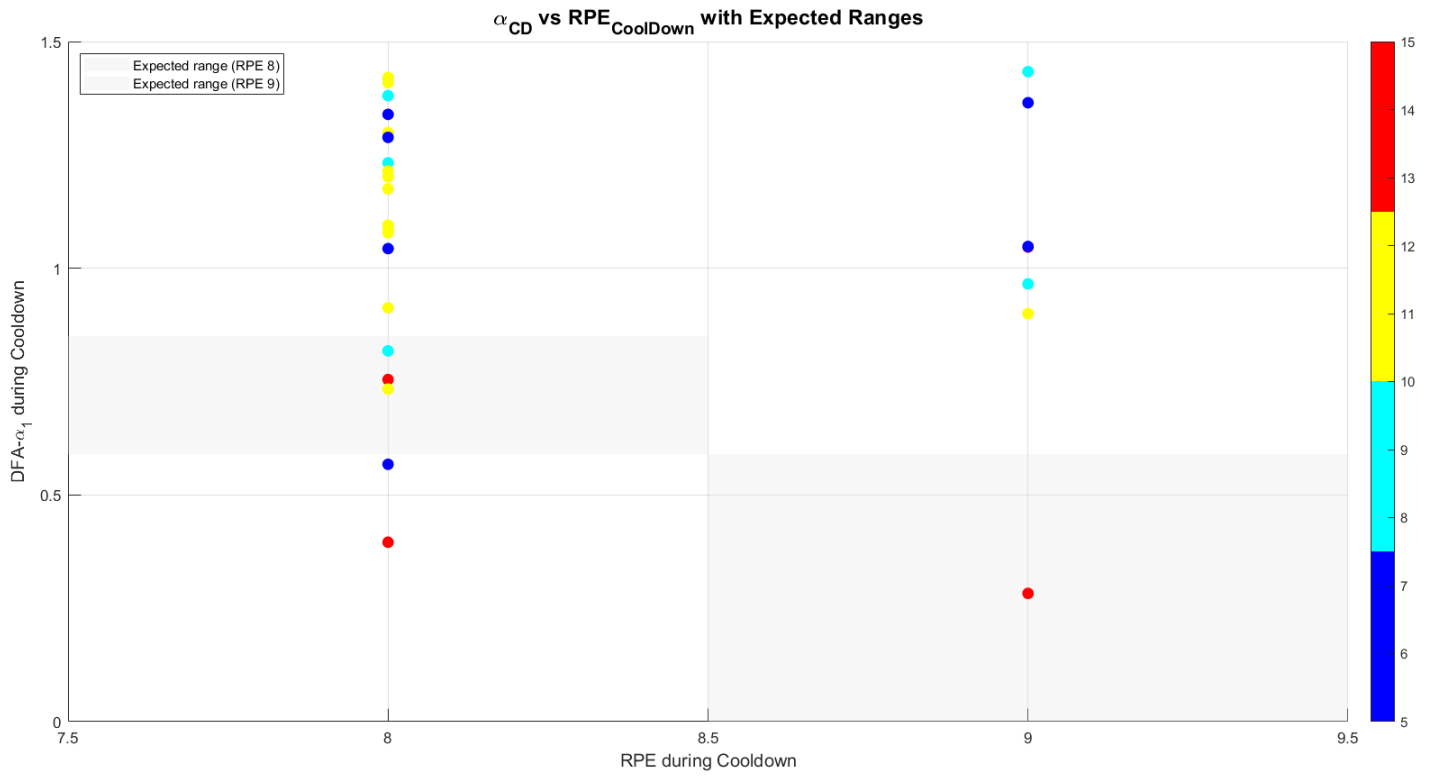
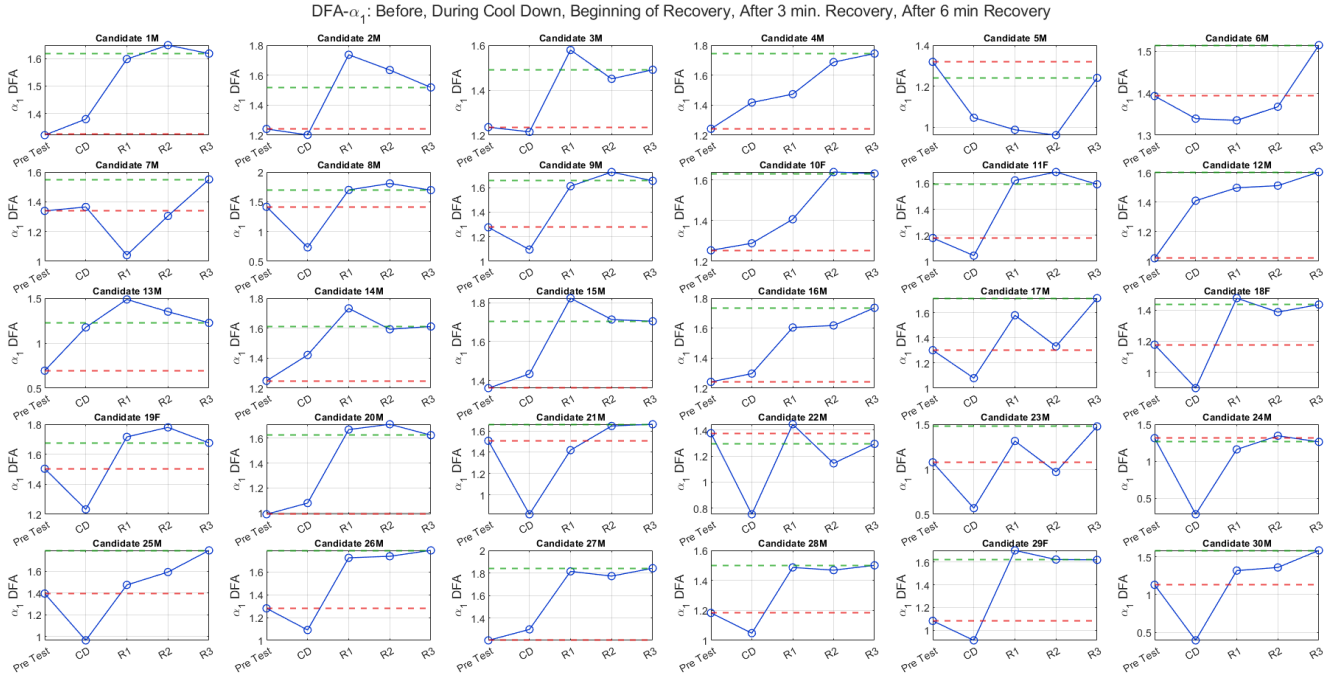


Figure 6.19: DFA- $\alpha_1$  values vs RPE During Cool-Down

### 6.3.2 DFA- $\alpha_1$ Before and After Exercise

The following table 6.7 and figure 6.20, show DFA- $\alpha_1$  values before the test, during the cool down phase, at the very beginning recovery phase (minute 0 to 3), successive recovery part (minut 3 to 6) and the end of the recovery (minute 6 to 9).

It can be notice that for almost all the candidates the DFA- $\alpha_1$  at the end of the last recovery phase rises with respect to DFA- $\alpha_1$  before test.



**Figure 6.20:** DFA- $\alpha_1$  values Before Test, Cool Down, Recovery (min. 0-3), Recovery (min. 3-6), Recovery (min. 6-9)

**Table 6.7:** DFA- $\alpha_1$  Values of candidates: Before Test, Cool Down, Recovery (min. 0-3), Recovery (min. 3-6), Recovery (min. 6-9)

Candidate	Pre Test	CD	Recovery	Recovery2	Recovery3
Candidate 1M	1.323	1.381	1.598	1.648	1.618
Candidate 2M	1.241	1.202	1.736	1.634	1.518
Candidate 3M	1.235	1.215	1.578	1.450	1.491
Candidate 4M	1.242	1.418	1.473	1.687	1.744
Candidate 5M	1.319	1.047	0.988	0.962	1.241
Candidate 6M	1.393	1.339	1.335	1.368	1.515
Candidate 7M	1.339	1.365	1.041	1.305	1.550
Candidate 8M	1.415	0.734	1.699	1.808	1.695
Candidate 9M	1.276	1.095	1.611	1.726	1.654
Candidate 10F	1.254	1.289	1.407	1.639	1.632
Candidate 11F	1.179	1.043	1.622	1.687	1.592
Candidate 12M	1.020	1.409	1.496	1.511	1.603
Candidate 13M	0.694	1.175	1.486	1.350	1.225
Candidate 14M	1.249	1.421	1.732	1.593	1.611
Candidate 15M	1.361	1.434	1.823	1.713	1.705
Candidate 16M	1.242	1.297	1.605	1.618	1.736
Candidate 17M	1.301	1.079	1.578	1.331	1.714
Candidate 18F	1.178	0.900	1.476	1.387	1.435
Candidate 19F	1.504	1.232	1.716	1.779	1.676
Candidate 20M	0.988	1.078	1.670	1.713	1.625
Candidate 21M	1.508	0.818	1.419	1.646	1.662
Candidate 22M	1.375	0.754	1.443	1.144	1.293
Candidate 23M	1.077	0.568	1.314	0.970	1.476
Candidate 24M	1.312	0.283	1.160	1.344	1.262
Candidate 25M	1.396	0.966	1.475	1.594	1.793
Candidate 26M	1.281	1.091	1.725	1.739	1.790
Candidate 27M	1.202	1.299	1.814	1.772	1.842
Candidate 28M	1.183	1.048	1.486	1.468	1.500
Candidate 29F	1.083	0.913	1.700	1.620	1.617
Candidate 30M	1.129	0.396	1.317	1.358	1.583

# Chapter 7

## Discussion

### 7.1 Filter Application

As illustrated in Figure 6.1, the raw RR intervals (RRi) exhibit various artifacts and instabilities caused by motion, detection errors, or sensor inaccuracies. These disturbances can affect HRV analysis, making artifact correction a crucial pre-processing step. To address this issue, the previously described filtering method was applied to the data, aiming to remove artifacts while preserving physiological variability.

The necessity of filtering is evident and further emphasized in the zoomed-in views shown in Figures 6.3 and 6.4. These figures clearly illustrate how the filter effectively **identifies and corrects artifacts by substituting them with plausible values**, ensuring that the natural variability of the signal remains intact.

Figure 6.2 reveals a **common trend among all subjects**: a progressive decrease in RRi during the exercise phase, followed by an increase during the cool-down stage and a peak during the recovery phase. The consistency of this pattern across different subjects suggests that the filtering process successfully eliminates artifacts while preserving the physiological characteristics of the signal.

Also, Table 6.1 presents statistical measures, including the Standard Deviation (Std), Mean, Coefficient of Variation (CV), total number of artifacts, and percentage of artifacts for the entire RR signal. The standard deviation, which quantifies data dispersion around the mean, **systematically decreases** for all subjects after filtering. This decline highlights how raw data, which contains sudden changes and wide artifacts, exhibited higher standard deviation. By removing these extreme

instabilities, the filtering process produces a more stable signal, characterized by lower standard deviation values. A similar interpretation applies to the Mean RRi and CV, both of which decrease in the filtered signals. This systematic decline confirms that **artifacts have been effectively detected and corrected** with plausible values, reinforcing the reliability of the processed data for further HRV analysis.

Figure 6.6 shows the total percentage of artifacts detected for each subject. Candidates **exceeding the 2.5% artifact rate** were considered outliers and excluded from further analysis. This threshold was chosen **based on the heatmap** shown in Figure 6.8, which highlights the distribution of artifacts across stages. Notably, Candidate 11M exhibited artifact rates above 7% in six out of eleven stages, suggesting a signal quality issue likely due to an improper fit of the heart rate monitor, possibly related to a very lean body type. In contrast, Candidate 16M, despite a total artifact rate close to 2.5%, was retained because the artifacts were limited to only two out of thirteen stages.

The heatmap thus proves essential not only for quantifying artifact presence but also for evaluating their distribution, **supporting the 2.5% threshold** as a robust criterion for data quality control.

The scatter plot in Figure 6.9 shows that, excluding Candidate11M (represented in burgundy), all data points exhibit an artifact percentage with respect to the total RR intervals below  $\approx 0.9\%$ , confirming the **general high quality** of the collected RRi. Moreover, the plot reveals a general trend of slightly higher artifact percentages during the “Sitting on Chair” and “Cool Down” stages, suggesting these phases may be more prone to signal disturbances.

## 7.2 DFA Algorithm Application

### 7.2.1 DFA- $\alpha_1$ and RPE: A Reliable Marker of Fatigue

The results in Figure 6.10 prove an **inverse relationship between DFA- $\alpha_1$  and RPE**. As the exercise intensity increases, DFA- $\alpha_1$  gradually decreases, while the subjective perception of effort (RPE) rises. This outcome confirms previous research, showing that DFA- $\alpha_1$  can be used as an objective physiological indicator of physical fatigue during exercise [71, 52].

In the initial phase of the incremental exercise, DFA- $\alpha_1$  **temporarily stabilizes or slightly increases**, due to the autonomic nervous system (ANS) adaptation to an increasing metabolic demand. So, the rise at the very beginning stage is explained by the **well-balanced autonomic regulation**.

After this phase, as exercise intensity rises, the sympathetic nervous system (SNS) becomes progressively dominant, while PNS declines. This change is visible through a **gradual reduction in DFA- $\alpha_1$** , describing a **loss of self-similarity** in RRi. During high-intensity exercise, DFA- $\alpha_1$  drops below 0.75-0.5, showing an important reduction of the HRV complexity. This phase aligns with the anaerobic threshold (VT2), where the metabolic stress and fatigue become more evident [71, 35].

The evident inverse relationship between RPE and DFA- $\alpha_1$ , suggests and supports the idea that DFA- $\alpha_1$  can be used as a **non-invasive marker of fatigue**.

The inverse of DFA- $\alpha_1$ , presented in figure 6.11, offers a different visualization that emphasizes the correlation between DFA- $\alpha_1$  and RPE.

### 7.2.2 Radial Plots: Another Visualization

The radial plots in Figures 6.12 and 6.13 illustrate the strong correlation between **RPE, DFA- $\alpha_1$ , and HR** during the incremental exercise. An invariant pattern emerges across all subjects, showing that as exercise intensity increases, HR and RPE rise, while DFA- $\alpha_1$  progressively declines.

The **spiral pattern** is even more evident in Figure 6.14, where all subjects are represented together. The previously mentioned, **ANS adaptation** phase is reflected by higher and **more scattered** DFA- $\alpha_1$  values, accompanied by **low HR and RPE**. This variability is evident in the first half of the radial plot, highlighting subject-specific autonomic responses.

As the exercise progresses and power increases, HR rises and RPE grows, signaling a higher perceived effort. Consequently, DFA- $\alpha_1$  starts decreasing, reflecting a progressive loss of complexity in heart rate variability (HRV) due to the increasing dominance of the sympathetic nervous system (SNS). This shift is visible in the second half of the radial plot, where data points become more concentrated and DFA- $\alpha_1$  values tend to cluster at lower levels. This outcome reinforces the previously discussed **ANS adaptation** hypothesis:

- Initially, the body adapts efficiently to the increased workload, maintaining a stable DFA- $\alpha_1$  with low HR.
- Later, as exercise intensity rises, DFA- $\alpha_1$  declines, becoming progressively more concentrated as subjects approach higher effort levels.

Moreover, this spiral pattern further confirms that DFA- $\alpha_1$  is a reliable parameter for fatigue detection, **as it does not suddenly collapse**, but, its **gradual decline** throughout the exercise reflects the progressive accumulation of fatigue.[51, 53]

### 7.2.3 RPE and DFA- $\alpha_1$ : General Remarks

The box plot of DFA- $\alpha_1$  and RPE (Figure 6.15) reinforces the trends previously discussed, highlighting the **gradually decline** in DFA- $\alpha_1$  as RPE increases.

The red line at 0.75, recognized as aerobic threshold, corresponds predominantly to RPE values greater than 8.

Interestingly, in the **mid-range of RPE**, particularly 4,7,8, DFA- $\alpha_1$  exhibits a **broader distribution**. This variability can be attributed to two key factors:

- **Inter-individual differences in fitness levels:** Subjects with varying levels of aerobic capacity may perceive exertion differently, leading to a wider dispersion of DFA- $\alpha_1$  values.
- **Uncertainty in RPE estimation:** While at the extremes of effort (very low and very high RPE values), individuals can more accurately assess their perceived exertion, mid-range RPE values may be more challenging to self-evaluate, contributing to the observed variability.

These two factors together suggest that RPE assessment in the middle stages of the test is **more subjective** and less reliable.

Conversely, at the very beginning and towards the end of the test (RPE = 0,1,2,3 and 9,10), the range of DFA- $\alpha_1$  values appears more constrained, further supporting its role as an objective, non-invasive marker for monitoring perceived fatigue.

In general, Figure 6.15 clearly highlights a progressive decline in DFA- $\alpha_1$  values as RPE increases, suggesting that a **fatigue classification** can be meaningfully derived from this result. To deepen this analysis, the distribution of RPE across seven ranges of DFA- $\alpha_1$  was computed. As shown in Figure 6.16, values of DFA- $\alpha_1$  **greater than 1.2** are predominantly associated with **low levels** of perceived exertion (RPE 0 to 4).

The mid-range of  $DFA-\alpha_1$  appears more ambiguous or transitional, which is consistent with the previous explanation. Still, a clear lowered trend in  $DFA-\alpha_1$  emerges, as RPE increases. Most notably, the **highest RPE scores** (9 and 10) are almost exclusively associated with the **lowest range of  $DFA-\alpha_1$**  ( $< 0.5$ ).

These results prompted the development of Figure 6.17, which shows the percentage distribution of RPE levels across four broader  $DFA-\alpha_1$  ranges, allowing a practical interpretation of fatigue states. Based on the Borg Scale of perceived exertion [47], the following categories are proposed:

- **Slight exertion:**  $0 \leq RPE \leq 5$  corresponding to low fatigue level.
- **Moderate exertion:**  $6 \leq RPE \leq 7$  corresponding to moderate fatigue level.
- **Severe exertion:**  $RPE = 8$  corresponding to high fatigue level.
- **Maximal exertion:**  $9 \leq RPE \leq 10$  corresponding to critical fatigue level.

Based on the explained results, a **classification that correlates  $DFA-\alpha_1$ , fatigue level and RPE** values is proposed.

**Table 7.1:** Summary of  $DFA-\alpha_1$  and RPE Ranges for Fatigue Classification with Corresponding Accuracy

<b><math>DFA-\alpha_1</math> Range</b>	<b>RPE Values</b>	<b>Fatigue Classification</b>	<b>Accuracy (%)</b>
$\alpha_1 > 1.15$	0, 1, 2, 3, 4, 5	Low fatigue	75.893
$0.85 < \alpha_1 \leq 1.15$	6, 7	Moderate fatigue	41.667
$0.59 < \alpha_1 \leq 0.85$	8	High fatigue	29.412
$\alpha_1 \leq 0.59$	9, 10	Critical fatigue	66.197

The classification boundary between moderate and high exertion is notably **borderline**, reflecting the previously discussed difficulty in accurately selecting the appropriate RPE value.

This observation is also reflected in the computed accuracy. The proposed classification achieves an **overall accuracy** of **61.78%**.

As shown in Table 7.1, the classifier performs well in identifying low and critical fatigue levels (with accuracies of 75.893% and 66.197%, respectively), but shows lower precision for the intermediate categories: moderate and high fatigue (with accuracies of 41.667% and 29.412%, respectively). The **lowest performance** is

observed for the **high fatigue category** ( $RPE = 8$ ). Although this category is based on a single RPE score, so it is more restricted, it is possible to draw additional insights from the analysis in Table 6.6:

- 20 out of 23 DFA- $\alpha_1$  values associated with  $RPE_{CD} = 8$  fall **outside the range** defined by the proposed classification.
- Considering RPE=8,9, the values out of the classification rise to 26/30.
- Subjects with higher self-reported fitness levels exhibit  $\Delta_{\alpha_1}$  values greater than 0.5 between the last stage and the cool-down phase.

These observations suggest that the **CD phase negatively impacts the accuracy** of the suggested classification.

In particular, subjects with higher fitness levels tend to experience a **rapid increase in DFA- $\alpha_1$**  within just 3 minutes post-exercise, with differences ranging from 0.5 to 1.13 between the last active stage and the cool-down. This points to a **fast autonomic recovery following intense effort**.

While DFA- $\alpha_1$  increases significantly, RPE values remain elevated, highlighting a **disconnect between subjective perception and physiological recovery**, especially in well-trained individuals.

This emphasizes the limitations of RPE as a reliable fatigue indicator during the cool-down phase.

When **excluding the CD phase** from the classification and recomputing the accuracy, the **overall performance improves to 65.54%**

Moreover, it is important to highlight a notable discrepancy between the official Borg scale classification proposed by Jakobsen et al. and the experimental classification introduced in this study. Specifically, while **RPE = 5** is categorized as "**severe**" exertion in the original scale, it is considered part of the **low fatigue** range in the proposed model.

This divergence can be attributed to the previously discussed **adaptive behavior of the ANS**. Although subjects may begin to perceive increased effort at this stage, the ANS appears to be adapting without a substantial decline in complexity. These findings further underscore the importance of incorporating an objective physiological marker, such as DFA- $\alpha_1$ , to enhance the accuracy and robustness of fatigue assessment.

For the sake of completeness, Figure 6.18 illustrates both the **strengths and limitations** of the classification model.

Subjects M6 and M7, are always classified within the low fatigue zone, with **no transitions to higher** fatigue levels. This could be attributed to their relatively low training status, suggesting that the classifier may not be fully accurate for individuals with lower fitness levels.

Conversely, subject F30 presents unusually low DFA- $\alpha_1$  values during the entire test. Starting from the warm-up phase, all DFA- $\alpha_1$  values remain below 1.15, not allowing a distinguishable classification for this subject.

Overall, the figure reveals that for many participants, an RPE of 5 appears to mark a transitional point between low/moderate or low/high fatigue. As the incremental protocol progresses, most subjects finally **reach the critical fatigue level** by the end of the test.

The presented classification agrees with findings in the existing literature, where high DFA- $\alpha_1$  values are typically associated with resting or non-exertional states, while the threshold around 0.75 has been linked to the aerobic threshold and 0.5 indicates a transition to uncorrelated fluctuations, indicating high efforts.[35, 51].

#### 7.2.4 DFA- $\alpha_1$ Before and After Test

Figure 6.20 shows values of DFA- $\alpha_1$  before test, during cool down, and after respectively 3,6,9 minutes of recovery.

In **recovery** phase, an important increment is shown leading to **higher values with respect to rest**.

This result is confirmed by previous research, [72], where was studied the ANS during the recovery phase after single and multiple Wingate tests. Millar et al., obtained higher DFA- $\alpha_1$  values immediately after exercise.

A similar result was obtained by Casties et al., whose studied different HRV indicators, including DFA- $\alpha_1$ , during and after an incremental exercise. The recovery phase takes into account up to 60 minutes after the end of the exercise. In particular, during the **firstly 10 minutes** of recovery, it is highlighted an important

**rise** in DFA- $\alpha_1$ , higher than the value at rest. After 60 minutes, DFA- $\alpha_1$  value returns closely to the rest one. The author explains that, in the first 10 minutes of recovery, the heart and autonomic nervous system go through a readjustment phase after intense exercise, which can temporarily disrupt normal heart rate variability.

The same outcome is shown in another study of Gronwald et al., explaining that after intense exercise, the body may over-activate the parasympathetic system, the so-called **supercompensation**, to compensate for the autonomic stress experienced and stimulate recovery.

These studies clearly explain why some subjects show higher DFA- $\alpha_1$  post-exercise compared to pre-exercise.

# Chapter 8

## Conclusions

### 8.1 Summary of Results

The results obtained from applying Detrended Fluctuation Analysis (DFA) to Heart Rate Variability (HRV) during the designed incremental test demonstrate that DFA- $\alpha_1$  **progressively decreases as exercise intensity increases**. This reduction correlates with a rise in subjective fatigue, as measured by the Rating of Perceived Exertion (RPE). At the heart of this physiological response is the dominance of the sympathetic nervous system (SNS) during exercise, leading to a **loss of auto-correlation of the HRV**, with the subsequent DFA- $\alpha_1$  decrease supporting results of previous studies [71],[35],[51]. Additionally, at the onset of exercise, many subjects exhibited a temporary **increase in DFA- $\alpha_1$** , likely due to the autonomic nervous system (**ANS**) **adaptation**, before the above-mentioned, shift towards sympathetic activation.

During the recovery phase, it was observed a **super-compensation phenomenon**. This phenomenon is characterized by the excessive parasympathetic nervous system (PNS) activation, which is reflected with a **momentaneous peak in DFA- $\alpha_1$** . This effect was already discussed in previous studies [72],[73],[71], and it highlights the interplay between autonomic nervous system dynamics and exercise-induced stress.

Such results confirm DFA- $\alpha_1$  as a **reliable marker of autonomic recovery and organismic demand**, in line with previous research [52]. They also support its utility in assessing exercise-induced fatigue, as demonstrated in recent studies [63, 52, 53, 54].

A **classification model** was proposed by relating DFA- $\alpha_1$  ranges with RPE values, specifically adapted to physical exertion in sports. **Four fatigue levels** were identified (low, moderate, high, and critical) each corresponding to specific ranges of both DFA- $\alpha_1$  and RPE. The model achieved an **overall accuracy** of **61.8%**, with particularly strong performance in detecting low (75.9%) and critical (66.2%) fatigue. In contrast, classification accuracy for moderate and high fatigue (the mid-range), was lower, at 41.7% and 29.4% respectively.

The reduced performance in the mid-range of exertion may reflect **inter-individual variability in fitness** and the **inherent subjectivity of RPE scoring**. In these zones, autonomic responses and perceived effort can diverge, highlighting the importance of **incorporating other objective markers**.

An important observation was the **role of the cool-down** phase. When included in the classification, this phase introduced **mismatches** between DFA- $\alpha_1$  and RPE, especially in trained individuals who exhibited rapid autonomic recovery. The analysis shows that during this phase, only two RPE values are reported: 8 and 9. Among the 30 subjects, 26 present DFA- $\alpha_1$  values outside the proposed classification range, resulting in an **error rate** of  $\approx 87\%$  for this phase. Excluding the CD phase led to an improvement in model accuracy, increasing it to 65.5%.

Moreover, some inconsistencies emerged when comparing the proposed model to the original Borg scale. In particular, RPE = 5, typically considered "severe" in literature, was classified as low fatigue in this model, an outcome explained by the **adaptive behavior of the autonomic nervous system**. In particular, outcomes highlight that for this experiment, for the majority of subjects, RPE=5 indicates a **transitional** point between low fatigue and moderate/high fatigue.

Finally, **individual fitness level** played a key role: subjects with higher fitness tended to show faster recovery and greater  $\Delta_{\alpha_1}$  between the final exercise stage and the CD phase. This supports the potential of DFA- $\alpha_1$  not only as a marker of acute fatigue, but also as an indicator of **recovery capacity and overall fitness level**.

An essential aspect of this analysis is the **pre-processing analysis**. By the application of the filter on the RRi, was guaranteed integrity and reliability in

HRV analysis. Although artifact presence was slightly higher during low-intensity phases such as "Sitting on Chair" and "Cool Down", the **overall signal quality remained high across all stages**. However, due to sensitivity of DFA to signal fluctuations, employing a filter capable of preserving physiological variability was crucial to maintain the validity and accuracy of the analysis.

Moreover, the results demonstrate that the **designed exercise protocol was effective**, generating outcomes that align with the study's initial hypothesis. Specifically, the protocol successfully induced cardiorespiratory exhaustion, as originally intended and confirmed by the observed data.

## 8.2 Limits of the Study and Purpose for the Future

Although DFA- $\alpha_1$  has been validated as a reliable method for fatigue detection, the results of the proposed classification model, while acceptable, especially considering that it relies exclusively on DFA- $\alpha_1$  and the inherently subjective RPE scale, still reveal some important limitations that should be handled in future research.

Indeed, one limitation concerns the use of RPE. While it is a **valuable tool** for assessing subjective fatigue, it remains an inherently self-reported metric, introducing inevitable limitations. Participants may have **overestimated or underestimated** their fatigue levels, as shown in the middle stages of the test. In particular, to enhance the accuracy of the proposed classification in the transitional zone, it is recommended to **merge additional objective markers**, such as lactate thresholds or muscle oxygenation levels. Combining these physiological indicators with the subjective RPE and other techniques such as machine learning, would allow for a more precise and reliable classification of exertion, especially in the intermediate intensity range.

Another limitation concerns the **recovery** period. As shown in the results, a clear peak in DFA- $\alpha_1$  was observed during this phase, likely due to the previously discussed **supercompensation** effect. For future studies, it would be advantageous to **extend post-exercise monitoring** to determine how long it takes for DFA- $\alpha_1$  to return to baseline values. This would provide valuable insights into recovery dynamics and help refine strategies for fatigue management.

Then, sports domain was chosen as the testing field, as it allows for a **controlled induction of fatigue**. However, **real-world workplace** conditions differ, as they involve **lower-intensity** but prolonged physical demands and additional environmental stressors. Future studies should further **explore occupational settings**, where fatigue accumulates gradually over extended periods rather than occurring acutely, as in high-intensity exercise scenarios. So, from a methodological point of view, for future studies in occupational settings, it may be beneficial to **incorporate DFA- $\alpha_2$**  analysis, which accounts for longer-range correlations, offering a more comprehensive understanding of autonomic fluctuations over extended durations. Furthermore, **expanding HRV analysis metrics** could further improve the accuracy and reliability of fatigue detection.

Lastly, a significant limitation of this study was the underrepresentation of female participants, mainly due to recruitment challenges. Future research would benefit from a more heterogeneous dataset.

In summary, while this study represents an important initial step in exploring non-linear HRV analysis for fatigue assessment, further research is needed to **validate these findings in occupational settings**. The integration of advanced analytical techniques and a more diverse participant pool will be important in advancing this field and useful for developing even more reliable and personalized monitoring systems with possible applications in both sports and workplace safety fields.

# Appendix A

## Informed Consent Form

Informed consent for the study on the monitoring of physiological signals during an incremental physical fatigue test on a stationary bike

### STUDY

The aim of this study is to monitor physiological signals, such as electrocardiogram (ECG) and photoplethysmography (PPG), to gather information on parameters such as heart rate, respiratory rate, and other indicators of fatigue. The goal is to collect data to develop and improve an advanced algorithm capable of detecting levels of physical fatigue across individuals of different ages, genders, and fitness levels. To achieve this, the acquired data will be correlated with the information provided voluntarily by participants through three pre-test questionnaires: a sleep quality and quantity questionnaire, a stress level questionnaire, and a physical activity level questionnaire.

This combination of objective measurements and self-reported data will facilitate the development of an algorithmic model capable of accurately detecting varying levels of physical fatigue in different contexts.

### METHOD

The physiological signals from participants will be recorded using three devices: a commercial smartwatch worn on the wrist (Garmin Venu), a chest strap for ECG measurement (Polar H10), and an armband for PPG measurement (Polar OH1+). Additionally, the test will be conducted using a stationary bike (Tacx Neo Bike Plus) that allows for incremental power adjustments.

Participants are required to follow certain guidelines prior to the test:

- Avoid caffeine intake in the 12 hours preceding the test. If consumed, participants must specify the time of consumption.
- Refrain from eating in the hour prior to the test and report any food intake within the past three hours.
- Indicate whether they are smokers and if they have smoked or consumed alcohol within the last 24 hours.

If the test is conducted around lunchtime, participants will be provided with a glass of water and sugar before the test begins to prevent hypoglycemia.

Upon arrival at the study site, participants will be required to wear the previously mentioned monitoring devices. At this point, data collection will begin, and participants will be asked to complete the three aforementioned questionnaires (sleep quality, stress level, and physical activity level) and to perform the Psychomotor Vigilance Task (PVT), a 5-minute test to assess attention and reaction time.

This preliminary phase, including the questionnaires and the PVT, lasts approximately 20 minutes.

Following this, participants will sit on the stationary bike for a 5-minute adaptation period before commencing the main test.

The test consists of an initial warm-up phase of 5 minutes, followed by a gradual increase in power every 3 minutes, continuing until the participant reaches their fatigue limit or decides to stop due to discomfort or fatigue.

It is emphasized that participants may choose to stop the incremental test at any time due to fatigue or any other discomfort.

After completing the incremental test, a 3-minute cool-down phase at a low intensity follows.

During each incremental stage, participants will assess their perceived fatigue using a subjective scale from 0 to 10, known as the Rating of Perceived Exertion (RPE) scale.

After the cool-down phase, participants will engage in a recovery phase lasting approximately 10 minutes. During this time, once their normal breathing has resumed, they will perform the PVT again and provide a final assessment of their perceived exertion using the RPE scale.

## **RISKS**

As with any physical exercise, there are potential risks associated with this test. These may include abnormal blood pressure, fainting, irregular heart rhythm (either accelerated or slowed), and in rare cases, heart attack, stroke, or death. Every effort will be made to minimize these risks by evaluating the participant's preliminary health and fitness information and carefully observing them during the test.

Under normal conditions, participants may experience temporary discomfort in breathing and/or muscle soreness (especially in the quadriceps), similar to what one might feel during or after intense physical activity such as running, gym workouts, or other strenuous exercise.

Please note that no medical personnel will be present during the test.

Based on the information provided regarding your health status and risk level, the laboratory reserves the right to cancel the exercise test if it is deemed unsafe.

## **RESPONSIBILITIES OF THE PARTICIPANT**

The information you have regarding your health or any previous experiences of exercise-related or cardiac symptoms (such as shortness of breath during low-effort activities, pain, pressure, tightness, or heaviness in the chest, neck, jaw, back, and/or arms) may impact the safety of your test. It is crucial that you communicate these details.

Promptly reporting any unusual symptoms or sensations during the test is of great importance. Any symptoms considered abnormal must be reported immediately. You are responsible for disclosing your medical history and any symptoms that may arise during the test.

Additionally, you are required to report all medications taken recently, particularly those taken on the day of the test.

## **POTENTIAL BENEFITS FOR THE PARTICIPANT**

Participating in this study will offer you the opportunity to receive a detailed analysis of your physical condition, with particular emphasis on aerobic capacity. During the test, key physiological parameters such as heart rate, respiratory rate, and other fatigue indicators will be monitored. This data will provide a thorough evaluation of your response to exercise, allowing you to gain valuable insights for optimizing your training regimen or monitoring your general health status.

Furthermore, direct involvement in this research may enhance your awareness of

your physical capabilities. This heightened awareness could translate into increased motivation to improve your athletic performance, leading to positive impacts on overall quality of life and promoting a healthier, more active lifestyle.

## **POTENTIAL BENEFITS FOR SOCIETY**

By participating in this research, you contribute significantly to scientific progress in the field of physical fatigue detection. The data collected and results obtained may help in the development of advanced algorithms for the early detection of fatigue. In the future, such algorithms could have a significant impact on various sectors of society, aiding in the prevention of accidents and enhancing safety in high-risk work environments. Specifically, this technology could be used to monitor fatigue in professions that require high levels of attention and physical endurance, where an error due to fatigue could have serious consequences for the worker and those nearby. Examples include truck drivers, operators of heavy machinery, and other critical occupations. Integrating fatigue detection systems in these settings could help reduce the risk of accidents caused by fatigue and improve working conditions, with benefits potentially extending to the entire community.

Your involvement, therefore, not only enriches scientific research but also promotes the development of innovative solutions with positive effects on safety and quality of life.

## **QUESTIONS FROM THE PARTICIPANT**

You are encouraged to ask any questions regarding the test procedures or test results.

## **USE OF DATA**

All information collected for this test will be treated as confidential and safeguarded. However, the data may be used for statistical analysis or scientific purposes and subsequently published in an anonymous form, ensuring your right to privacy is maintained.

## INCIDENTAL FINDINGS

Data analysis may occasionally reveal anomalies in the parameters measured during the study.

If you are interested, you may choose to be informed of such findings.

### A.1 Informed Question: To signature

I, the undersigned principal investigator, \_\_\_\_\_, hereby declare that I have clearly and comprehensively informed the volunteer, \_\_\_\_\_, about the objectives, methods, potential consequences, and possible risks associated with this study. Furthermore, I confirm my availability to provide the participant with any additional clarification or information needed.

Turin, \_\_\_\_\_.

Signature of the principal investigator \_\_\_\_\_.

## VOLUNTARY CONSENT

I, the undersigned volunteer, \_\_\_\_\_, born on \_\_\_\_\_ in \_\_\_\_\_ residing at \_\_\_\_\_ hereby declare:

- I am fully aware and capable of making autonomous decisions.
- I have carefully read and understood this document, including the test procedures, potential risks, and associated discomforts.
- I have received clear and satisfactory answers to all additional questions posed to the study coordinator.
- I am participating in this study voluntarily and without any coercion.
- I am aware of my right to withdraw from the test at any time, without needing to provide an explanation and without any negative consequences.
- I will disclose any pre-existing medical conditions, including chronic illnesses or diseases, of which I am aware prior to the test.
- I will inform the study coordinator of any medications, supplements, or substances recently taken. I commit to promptly reporting to the staff any unusual symptoms or discomforts experienced during the test.

- I acknowledge that there will be no supervising physician present on-site during the test.
- I confirm that all information has been provided clearly and comprehensively, and that I have had sufficient time to consider my participation.

Therefore, I voluntarily consent to participate in the study:

Yes

No

I consent to the collection, storage, reuse and publication of my data (anonymously and while safeguarding your privacy):

Yes

No

If anomalies are found in my physiological parameters during data analysis, I wish to be informed:  Yes

No

In accordance with Legislative Decree N°196/03 (Articles 7 and 13) concerning the protection of personal data, you are informed that your personal data will be collected and stored appropriately and will be used exclusively for scientific research purposes. Storage and data processing procedures will be followed to prevent individuals outside our research group from associating your name with the data.

Turin, \_\_\_\_\_

Signature of the volunteer \_\_\_\_\_

Signature of the principal investigator \_\_\_\_\_

# Appendix B

## Sleep Questionnaire

### Personal Information

1. ID (Name and Surname or Nickname):  
\_\_\_\_\_
2. Age: \_\_\_\_\_
3. Sex:  M  F  Other
4. Weight (kg): \_\_\_\_\_
5. Height (cm): \_\_\_\_\_

### Medication and Health Conditions

6. Do you take medications for hypertension?  
 Yes  No  
If yes, which ones? \_\_\_\_\_
7. Do you take medications for other heart problems (e.g., antiarrhythmics, digoxin)?  
 Yes  No  
If yes, which ones? \_\_\_\_\_
8. Do you take medications for insomnia and anxiety (e.g., tranquilizers, hypnotics, anxiolytics)?  
 Yes  No  
If yes, which ones? \_\_\_\_\_

9. Are you currently taking allergy medications (e.g., antihistamines)?  
 Yes  No  
If yes, which ones? \_\_\_\_\_

10. Do you have a pacemaker?  
 Yes  No

11. Do you take other medications regularly?  
 Yes  No  
If yes, which ones? \_\_\_\_\_

### Timing and Characteristics of Sleep

12. Do you use a CPAP (Continuous Positive Airway Pressure) device?  
 Yes  No  
If yes, what pressure is set?  
\_\_\_\_\_
13. How much coffee do you drink per day?  
\_\_\_\_\_
14. How much alcohol do you drink per day (or per week)? \_\_\_\_\_
15. What time do you go to bed on weekdays?  
\_\_\_\_\_

16. What time do you usually go to bed at the weekend? \_\_\_\_\_
17. How long does it take for you to fall asleep once you go to bed?
- Less than 10 minutes
  - Between 10 and 30 minutes
  - More than 30 minutes
18. What time do you usually wake up on working days? \_\_\_\_\_
19. What time do you usually wake up at the weekend? \_\_\_\_\_
20. Do you wake up during the night?
- No, never or almost never
  - Yes, every night at least once
  - Yes, every night at least twice
21. When you sleep next to another person, do they report that you snore?
- Yes, every night
  - Yes, but only under certain circumstances
  - No, never
  - I don't know
22. If you snore only under certain circumstances, specify: \_\_\_\_\_
23. When you sleep next to another person, do they report that you have sleep apnea?
- Yes, every night
  - Yes, occasionally
  - No, never
  - I don't know
24. When you sleep next to another person, do they report that you move a lot?
- Yes, often
25. How often do you feel tired or fatigued after sleeping?
- Yes, occasionally
  - No, never
  - I don't know
  - Almost every day
  - 2-3 times per week
  - Never or almost never
  - I don't know

**Epworth Sleepiness Scale (ESS)** *Rate your tendency to fall asleep in the following situations (0-3 scale): 0 = Never, 1 = Slight chance, 2 = Moderate chance, 3 = High chance*

26. Sitting and reading  
 0  1  2  3
27. Watching TV  
 0  1  2  3
28. Sitting, inactive, in a public place (e.g., in a meeting, theater, or conference)  
 0  1  2  3
29. As a passenger in a car for an hour or more without stopping for a break  
 0  1  2  3
30. Lying down to rest when circumstances permit  
 0  1  2  3
31. Sitting and talking to someone  
 0  1  2  3
32. Sitting quietly after a meal without alcohol  
 0  1  2  3
33. In a car, while stopped for a few minutes in traffic or at a light  
 0  1  2  3

# Appendix C

## Physical Activity Questionnaire

### Personal Information

1. ID (Name and Surname or Nickname):

\_\_\_\_\_

2. Age: \_\_\_\_\_

3. Sex:  M  F  Other

### Physical Activity Level

4. How many years have you been practicing physical activity regularly?

- Less than 1 year
- 1-2 years
- 3-5 years
- More than 5 years
- I am not practicing regularly

5. How many days a week do you practice physical activity (on average)?

- 0 days
- 1-2 days
- 3-4 days
- 5 or more days

6. What kind of physical activity do you do regularly? (Select all that apply)

- Cycling
- Running
- Gym (weight training, strength training)
- Swimming
- Football
- Tennis
- Something else: \_\_\_\_\_

7. What is the average length of your workouts?

- Less than 30 minutes
- 30-60 minutes
- 60-90 minutes
- More than 90 minutes

8. What intensity do you usually train with?

- Light (e.g., light walking, stretching)
- Moderate (e.g., jogging, moderate cycling)
- High (e.g., intense cycling, fast running, intense strength training)
- Very high (e.g., competitive level, competitions and competitive training)

**Work Activity and Sedentary Behavior**

- 9. Does your work require significant physical exertion?  
 Yes, my job is physically demanding (e.g., laborer, manual worker)  
 Moderately, sometimes I do physical activity (e.g., teacher, salesperson)  
 No, my work is mainly sedentary (e.g., office, computer work)
- 10. How many hours do you spend sitting on average each day (work and leisure)?  
 Less than 2 hours  
 2-4 hours  
 4-6 hours  
 More than 6 hours

**Current Physical Condition and Recovery**

- 11. Do you use active transportation (walking or cycling) to get around during the day?  
 Yes    No
- 12. Have you consumed alcohol in the last 24 hours?  
 Yes    No  
If yes, how many hours ago?  
\_\_\_\_\_
- 13. Have you eaten in the last 3 hours?  
 Yes    No  
If yes, specify if it was a full meal or a snack: \_\_\_\_\_
- 14. Do you smoke?  
 Yes    No
- 15. Did you smoke in the last 24 hours? If yes, when? \_\_\_\_\_

- 16. Did you drink coffee today?  
 Yes    No  
If yes, how many hours ago?  
\_\_\_\_\_

**Physical Fatigue and Perceived Effort**

- 17. Did you do intense training yesterday or in the previous days?  
 Yes, yesterday I carried out intense training  
 Yes, yesterday I did a workout, but not particularly intense  
 No, I didn't train in the previous days
- 18. How are you feeling physically today?  
 Physically tired  
 Slightly physically tired  
 Rested  
 Energetic
- 19. Do you have muscle or joint pain right now?  
 Yes, significant  
 Yes, slight  
 No, I feel good
- 20. How long does it take you to fully recover following intense training?  
 Less than 12 hours  
 12-24 hours  
 More than 24 hours
- 21. During usual physical activities (such as walking or taking the stairs), how often do you feel fatigue?  
 Never, I can do more than 5-10 floors without feeling fatigue  
 Rarely  
 Often, after 2 floors of stairs I feel the

fatigue  
 Always

1    2    3    4    5    6    7    8  
 9    10

**Perceived Effort Scale (0-10)**

22. How much effort do you perceive in your usual physical activities?

0    1    2    3    4    5    6    7  
 8    9    10

**Personal Sports Data (if known)**

23. How do you rate your ability to withstand physical fatigue during intense activities?

1    2    3    4    5

24. How do you rate your overall fitness level on a scale of 1 to 10?

25. Do you know your FTP (Functional Threshold Power)? If yes, what is it?

\_\_\_\_\_

26. Have you ever done tests to measure your VO2 max and Anaerobic/Aerobic Threshold? If yes, when? What were the results?

\_\_\_\_\_

27. Do you know your maximum heart rate (HRmax)? If yes, what is it?

\_\_\_\_\_

## Appendix D

# Perceived Stress Questionnaire

*Perceived Stress Questionnaire*

#	Question	Never	Rarely	Sometimes	Always
1	You feel rested	<input type="checkbox"/>	<input type="checkbox"/>	<input type="checkbox"/>	<input type="checkbox"/>
2	You feel calm	<input type="checkbox"/>	<input type="checkbox"/>	<input type="checkbox"/>	<input type="checkbox"/>
3	You are doing things you like	<input type="checkbox"/>	<input type="checkbox"/>	<input type="checkbox"/>	<input type="checkbox"/>
4	You are full of energy	<input type="checkbox"/>	<input type="checkbox"/>	<input type="checkbox"/>	<input type="checkbox"/>
5	You feel safe and protected	<input type="checkbox"/>	<input type="checkbox"/>	<input type="checkbox"/>	<input type="checkbox"/>
6	You enjoy yourself	<input type="checkbox"/>	<input type="checkbox"/>	<input type="checkbox"/>	<input type="checkbox"/>
7	You are lighthearted	<input type="checkbox"/>	<input type="checkbox"/>	<input type="checkbox"/>	<input type="checkbox"/>
8	You have enough time for yourself	<input type="checkbox"/>	<input type="checkbox"/>	<input type="checkbox"/>	<input type="checkbox"/>
9	Too many demands are being made on you	<input type="checkbox"/>	<input type="checkbox"/>	<input type="checkbox"/>	<input type="checkbox"/>
10	You are irritable or grouchy	<input type="checkbox"/>	<input type="checkbox"/>	<input type="checkbox"/>	<input type="checkbox"/>
11	You have too many things to do	<input type="checkbox"/>	<input type="checkbox"/>	<input type="checkbox"/>	<input type="checkbox"/>
12	You feel lonely or isolated	<input type="checkbox"/>	<input type="checkbox"/>	<input type="checkbox"/>	<input type="checkbox"/>
13	You find yourself in situations of conflict	<input type="checkbox"/>	<input type="checkbox"/>	<input type="checkbox"/>	<input type="checkbox"/>
14	You feel tired	<input type="checkbox"/>	<input type="checkbox"/>	<input type="checkbox"/>	<input type="checkbox"/>
15	You fear you may not manage to attain your goals	<input type="checkbox"/>	<input type="checkbox"/>	<input type="checkbox"/>	<input type="checkbox"/>
16	You have too many decisions to make	<input type="checkbox"/>	<input type="checkbox"/>	<input type="checkbox"/>	<input type="checkbox"/>
17	You feel frustrated	<input type="checkbox"/>	<input type="checkbox"/>	<input type="checkbox"/>	<input type="checkbox"/>
18	You feel tense	<input type="checkbox"/>	<input type="checkbox"/>	<input type="checkbox"/>	<input type="checkbox"/>
19	Your problems seem to be piling up	<input type="checkbox"/>	<input type="checkbox"/>	<input type="checkbox"/>	<input type="checkbox"/>
20	You are in a hurry	<input type="checkbox"/>	<input type="checkbox"/>	<input type="checkbox"/>	<input type="checkbox"/>
21	You have many worries	<input type="checkbox"/>	<input type="checkbox"/>	<input type="checkbox"/>	<input type="checkbox"/>
22	You are under pressure from other people	<input type="checkbox"/>	<input type="checkbox"/>	<input type="checkbox"/>	<input type="checkbox"/>
23	You feel discouraged	<input type="checkbox"/>	<input type="checkbox"/>	<input type="checkbox"/>	<input type="checkbox"/>
24	You are afraid for the future	<input type="checkbox"/>	<input type="checkbox"/>	<input type="checkbox"/>	<input type="checkbox"/>
25	You are doing things because you have to not because you want to	<input type="checkbox"/>	<input type="checkbox"/>	<input type="checkbox"/>	<input type="checkbox"/>
26	You feel criticized or judged	<input type="checkbox"/>	<input type="checkbox"/>	<input type="checkbox"/>	<input type="checkbox"/>
27	You feel mentally exhausted	<input type="checkbox"/>	<input type="checkbox"/>	<input type="checkbox"/>	<input type="checkbox"/>
28	You have trouble relaxing	<input type="checkbox"/>	<input type="checkbox"/>	<input type="checkbox"/>	<input type="checkbox"/>
29	You feel loaded down with responsibilities	<input type="checkbox"/>	<input type="checkbox"/>	<input type="checkbox"/>	<input type="checkbox"/>
30	You feel under pressure from deadlines	<input type="checkbox"/>	<input type="checkbox"/>	<input type="checkbox"/>	<input type="checkbox"/>

**Table D.1:** Perceived Stress Questionnaire (Likert Scale 1-4)

# Appendix E

## Individual Subject Plots

This appendix offers a more transparent visualization of the plots for all subjects, facilitating the interpretation of individual data. Legends are explained in the thesis.

Individual Subject Plots

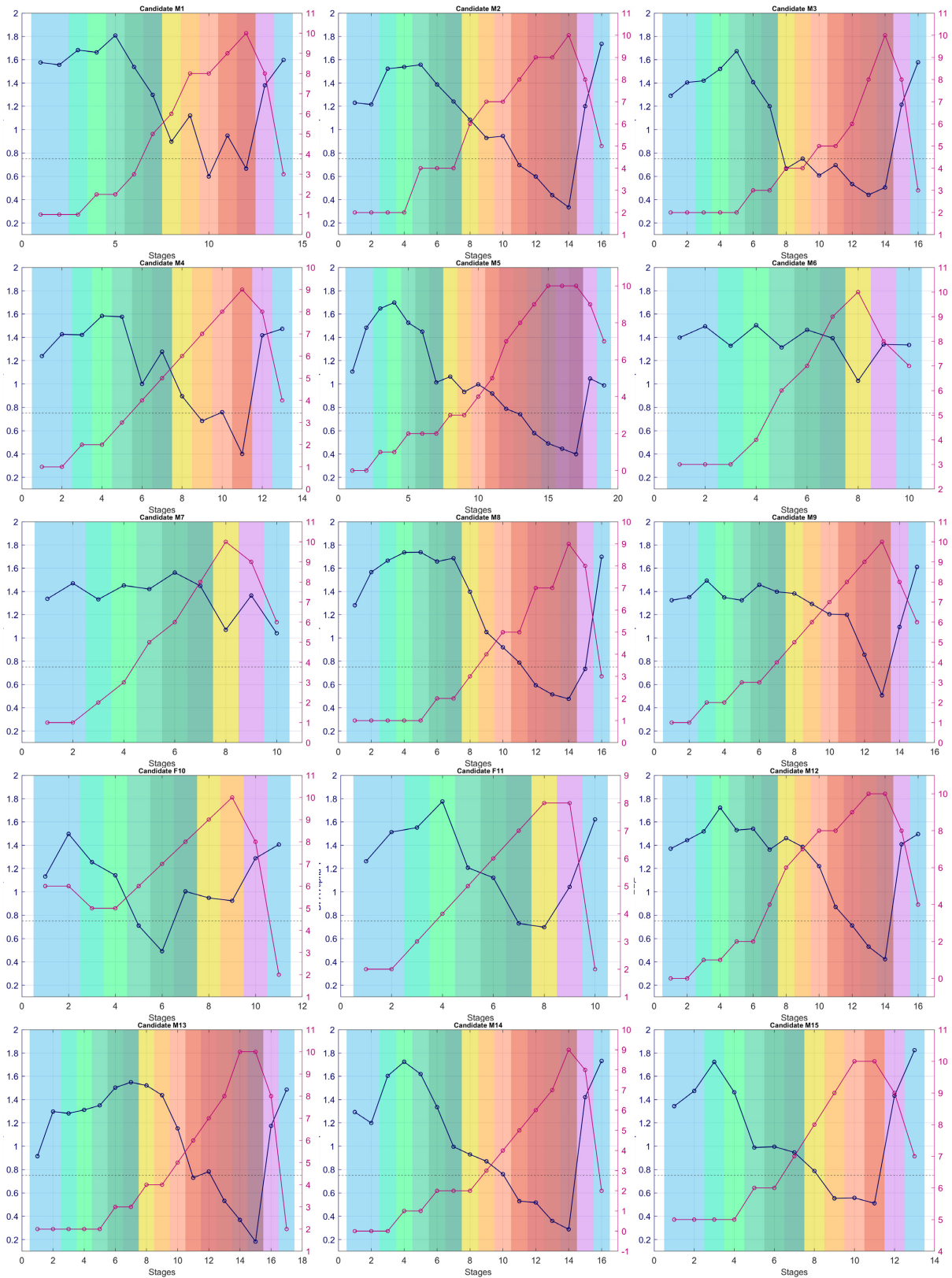


Figure E.1: DFA-alpha1 vs RPE and Power Stages: 1-15

Individual Subject Plots

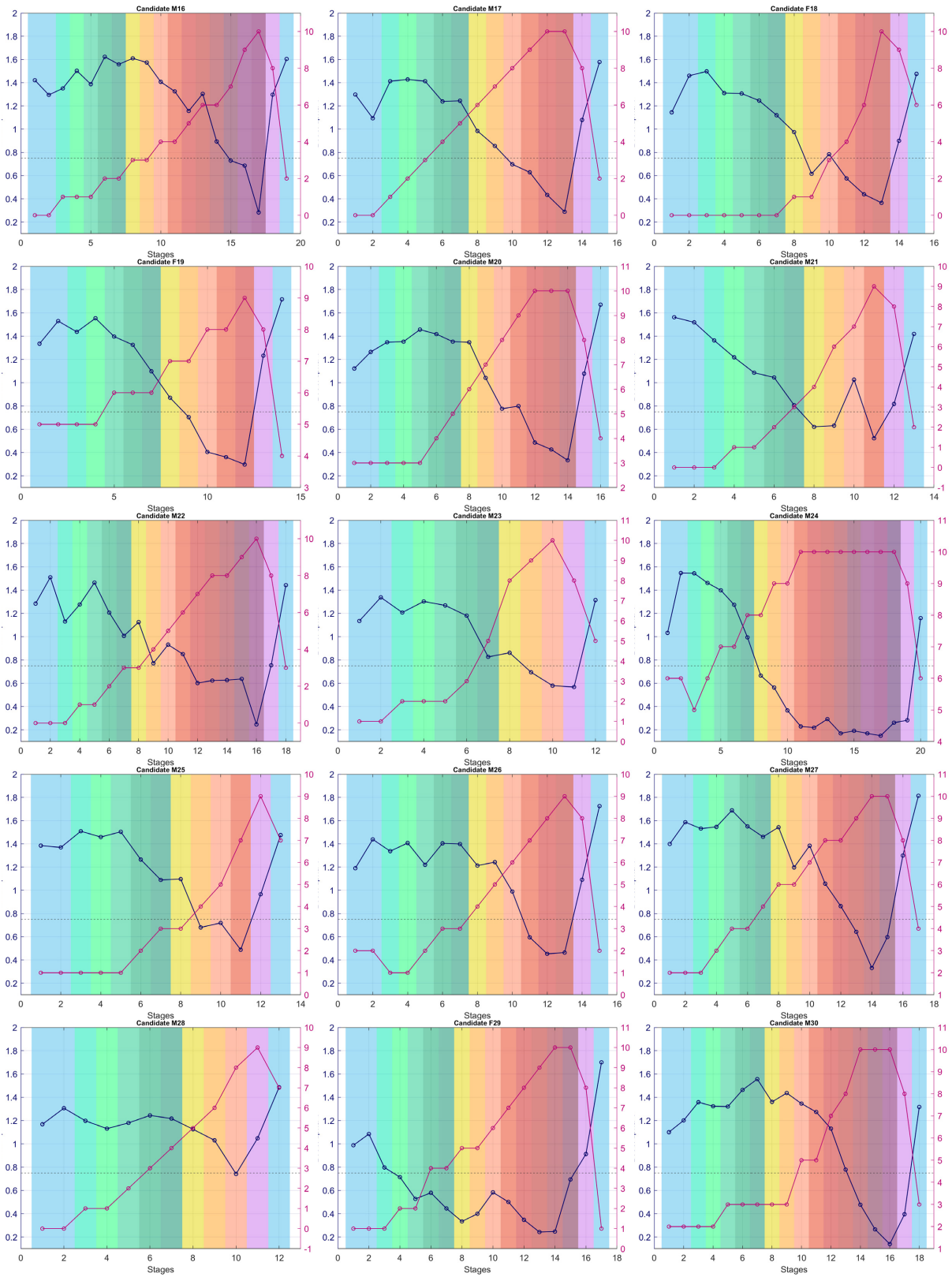


Figure E.2: DFA-alpha1 vs RPE and Power Stages: 16-30

Individual Subject Plots

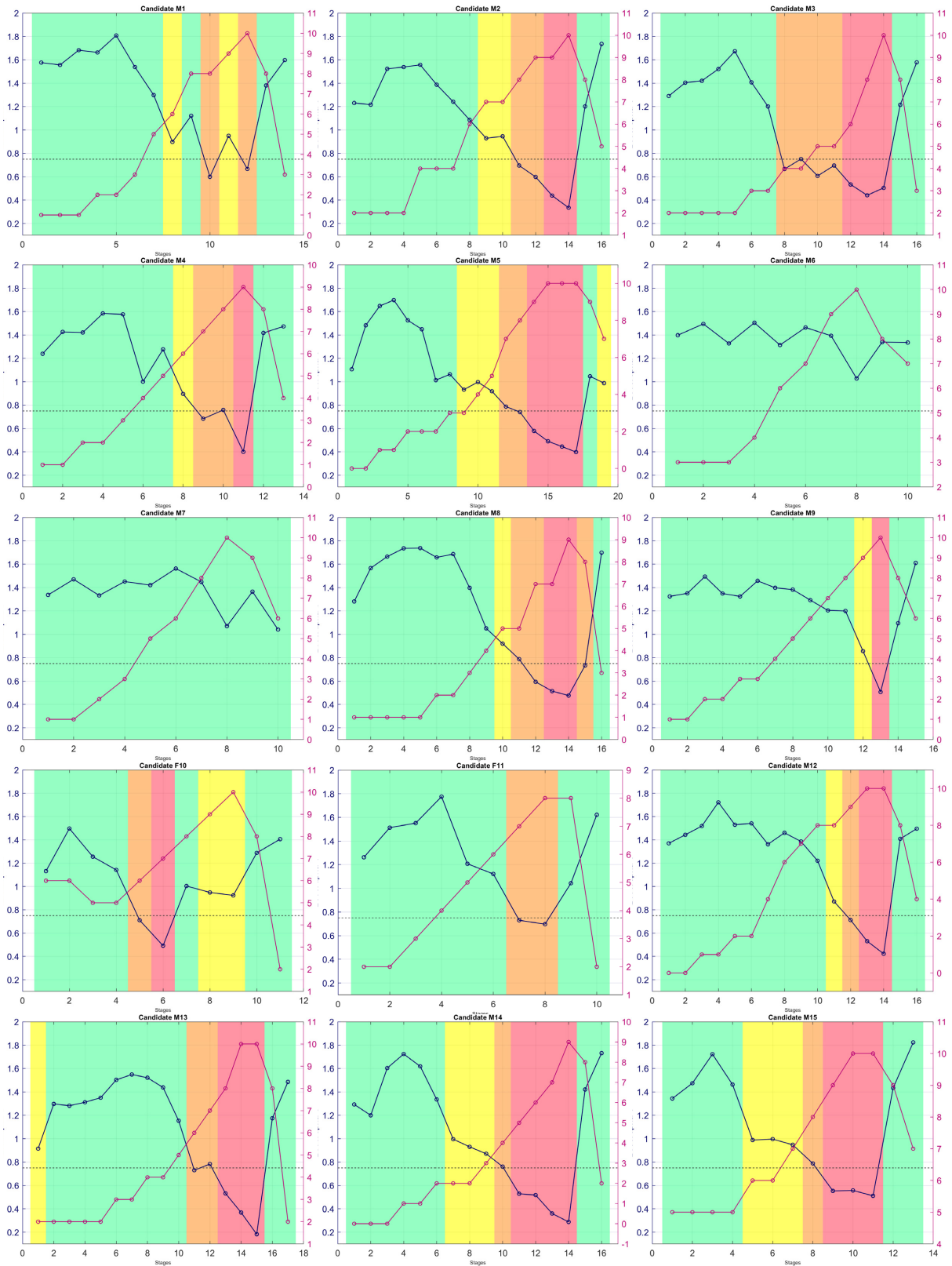


Figure E.3: DFA-alpha1 vs RPE and Fatigue Classification: 1-15

Individual Subject Plots

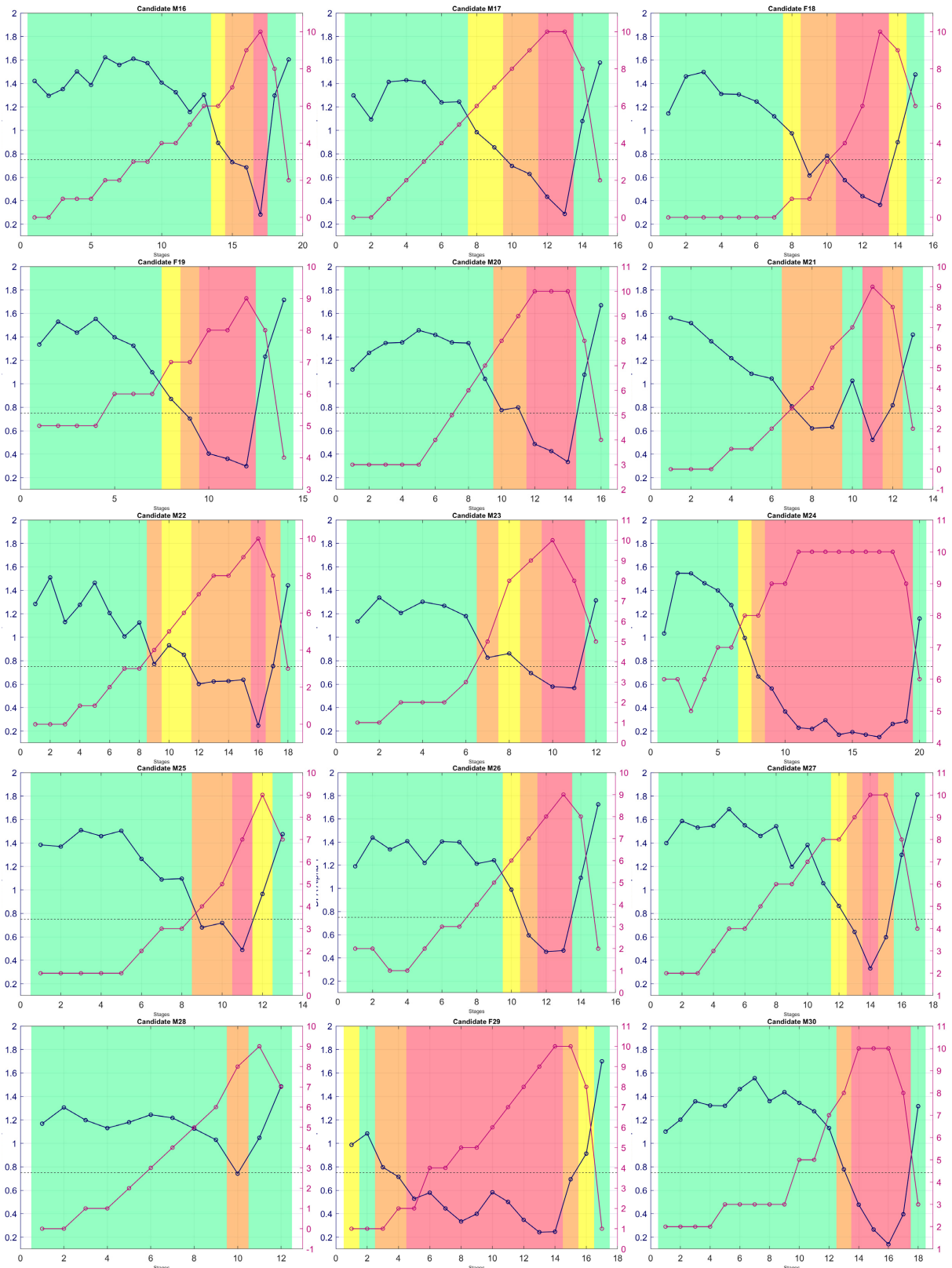


Figure E.4: DFA-alpha1 vs RPE and Fatigue Classification: 16-30



# Bibliography

- [1] M. H. Rahman, N. B. Alam, F. Dai, and J. Ryu. «A Critical Review of Methods for Physical Fatigue Assessment for Construction Workers». In: *Proc. 2024 ASCE Int. Conf. on Computing in Civil Engineering*. Pittsburgh, PA, USA, July 2024 (cit. on pp. 1, 19).
- [2] Bojan Makivić, Marina Djordjević Nikić, and Monte S. Willis. «Heart Rate Variability (HRV) as a Tool for Diagnostic and Monitoring Performance in Sport and Physical Activities». In: *Journal of Exercise Physiology Online* 16.3 (June 2013), pp. 103–131. URL: [https://www.researchgate.net/publication/285968540\\_Heart\\_Rate\\_Variability\\_HRV\\_as\\_a\\_Tool\\_for\\_Diagnostic\\_and\\_Monitoring\\_Performance\\_in\\_Sport\\_and\\_Physical\\_Activities](https://www.researchgate.net/publication/285968540_Heart_Rate_Variability_HRV_as_a_Tool_for_Diagnostic_and_Monitoring_Performance_in_Sport_and_Physical_Activities) (cit. on pp. 4, 6).
- [3] Labfront. *Sinoatrial Node and Autonomic Nervous System*. Online. Accessed: Feb. 19, 2025. 2024. URL: <https://www.labfront.com/course-video/sinoatrial-node-and-ans> (cit. on pp. 5, 6).
- [4] M. P. Tulppo, T. H. Mäkikallio, T. Seppänen, R. T. Laukkanen, and H. V. Huikuri. «Vagal modulation of heart rate during exercise: effects of age and physical fitness». In: *American Journal of Physiology* 274.2 (Feb. 1998), H424–H429. DOI: 10.1152/ajpheart.1998.274.2.H424. URL: <https://pubmed.ncbi.nlm.nih.gov/9486244/> (cit. on p. 6).
- [5] Bernhard Grässler, Beatrice Thielmann, Irina Böckelmann, and Anita Hökelmann. «Effects of Different Training Interventions on Heart Rate Variability and Cardiovascular Health and Risk Factors in Young and Middle-Aged Adults: A Systematic Review». In: *Frontiers in Physiology* 12 (Apr. 2021), p. 657274. DOI: 10.3389/fphys.2021.657274. URL: <https://www.frontiersin.org/articles/10.3389/fphys.2021.657274/full> (cit. on p. 6).

- 
- [6] Fred Shaffer and J. P. Ginsberg. «An overview of heart rate variability metrics and norms». In: *Frontiers in Public Health* 2 (Sept. 2014), pp. 1–17. DOI: 10.3389/fpubh.2014.00258. URL: <https://www.frontiersin.org/articles/10.3389/fpubh.2014.00258/full> (cit. on pp. 6, 7).
- [7] Gernot Ernst. «Hidden Signals—The History and Methods of Heart Rate Variability». In: *Frontiers in Public Health* 5 (Oct. 2017), p. 265. DOI: 10.3389/fpubh.2017.00265. URL: <https://www.frontiersin.org/articles/10.3389/fpubh.2017.00265/full> (cit. on pp. 7, 8).
- [8] Task Force of the European Society of Cardiology, the North American Society of Pacing, and Electrophysiology. «Heart Rate Variability: Standards of Measurement, Physiological Interpretation, and Clinical Use». In: *European Heart Journal* 17.3 (Mar. 1996), pp. 354–381. URL: <https://www.escardio.org/static-file/Escardio/Guidelines/Scientific-Statements/guidelines-Heart-Rate-Variability-FT-1996.pdf> (cit. on p. 7).
- [9] Sylvain Laborde, Emma Mosley, and Julian F. Thayer. «Heart Rate Variability and Cardiac Vagal Tone in Psychophysiological Research – Recommendations for Experiment Planning, Data Analysis, and Data Reporting». In: *Frontiers in Psychology* 8 (Feb. 2017), p. 213. DOI: 10.3389/fpsyg.2017.00213. URL: <https://www.frontiersin.org/articles/10.3389/fpsyg.2017.00213/full> (cit. on pp. 7, 8).
- [10] Brian W. Johnston, Richard Barrett-Jolley, Anton Krige, and Ingeborg D. Welters. «Heart rate variability: Measurement and emerging use in critical care medicine». In: *Journal of the Intensive Care Society* 21.2 (May 2020), pp. 148–157. DOI: 10.1177/1751143719853744. URL: <https://pubmed.ncbi.nlm.nih.gov/32489411/> (cit. on p. 8).
- [11] Dinesh Kumar, Sridhar P. Arjunan, and Behzad Aliahmad. *Fractals: Applications in Biological Signalling and Image Processing*. Boca Raton, FL: CRC Press, 2017. ISBN: 9780367782764. URL: <https://www.routledge.com/Fractals-Applications-in-Biological-Signalling-and-Image-Processing/Kumar-Arjunan-Aliahmad/p/book/9780367782764> (cit. on pp. 9–13).
- [12] Ernesto Estrada. «What is a Complex System, After All?» In: *Foundations of Science* 29 (2023), pp. 1143–1170. DOI: 10.1007/s10699-023-09917-w. URL: <https://link.springer.com/article/10.1007/s10699-023-09917-w> (cit. on p. 9).

- [13] Jianbo Gao, Yinhe Cao, Wen-wen Tung, and Jing Hu. *Multiscale Analysis of Complex Time Series: Integration of Chaos and Random Fractal Theory, and Beyond*. John Wiley & Sons, 2007. ISBN: 978-0-471-65470-4. DOI: 10.1002/9780470191651. URL: <https://onlinelibrary.wiley.com/doi/book/10.1002/9780470191651> (cit. on p. 10).
- [14] Dierk Schleicher. «Hausdorff Dimension, Its Properties, and Its Surprises». In: *The American Mathematical Monthly* 114.6 (2007), pp. 509–528. DOI: 10.1080/00029890.2007.11920440. URL: <https://doi.org/10.1080/00029890.2007.11920440> (cit. on p. 10).
- [15] Wikipedia contributors. *Triangolo di Sierpiński*. Accessed: 25 Feb. 2025. 2024. URL: [https://it.wikipedia.org/wiki/Triangolo\\_di\\_Sierpi%C5%84ski](https://it.wikipedia.org/wiki/Triangolo_di_Sierpi%C5%84ski) (cit. on p. 11).
- [16] Benoit B. Mandelbrot. *Gaussian Self-Affinity and Fractals: Globality, The Earth, 1/f Noise, and R/S*. Selected Works of Benoit B. Mandelbrot. New York: Springer, 2002. ISBN: 978-0-387-98993-8. URL: <https://link.springer.com/book/9780387989938> (cit. on p. 11).
- [17] Ladislav Kristoufek and Miloslav Vosvrda. «Measuring capital market efficiency: Long-term memory, fractal dimension and approximate entropy». In: *The European Physical Journal B* 87.7 (2014), p. 162. DOI: 10.1140/epjb/e2014-50113-6. URL: <https://link.springer.com/article/10.1140/epjb/e2014-50113-6> (cit. on pp. 11, 12).
- [18] Muzirah Musa and Abdul Aziz Jemain. «Existence of Long Memory in Ozone Time Series». In: *Sains Malaysiana* 41.11 (2012), pp. 1375–1384. URL: [https://www.researchgate.net/publication/289314792\\_Existence\\_of\\_Long\\_Memory\\_in\\_Ozone\\_Time\\_Series](https://www.researchgate.net/publication/289314792_Existence_of_Long_Memory_in_Ozone_Time_Series) (cit. on p. 11).
- [19] Tatjana Stadnitski. «Measuring fractality». In: *Frontiers in Physiology* 3 (2012), p. 127. DOI: 10.3389/fphys.2012.00127. URL: <https://www.frontiersin.org/articles/10.3389/fphys.2012.00127/full> (cit. on pp. 11, 14).
- [20] Benoit B. Mandelbrot and John W. Van Ness. «Fractional Brownian Motions, Fractional Noises and Applications». In: *SIAM Review* 10.4 (1968), pp. 422–437. DOI: 10.1137/1010093. URL: <https://doi.org/10.1137/1010093> (cit. on pp. 11, 14).

- [21] Richard Hardstone, Simon-Shlomo Poil, Giuseppina Schiavone, Rick Jansen, Vadim V. Nikulin, Huibert D. Mansvelder, and Klaus Linkenkaer-Hansen. «Detrended fluctuation analysis: a scale-free view on neuronal oscillations». In: *Frontiers in Physiology* 3 (2012), p. 450. DOI: 10.3389/fphys.2012.00450. URL: <https://www.frontiersin.org/articles/10.3389/fphys.2012.00450/full> (cit. on pp. 12, 14).
- [22] B. Dubuc, J. F. Quiniou, C. Roques-Carmes, C. Tricot, and S. W. Zucker. «Evaluating the fractal dimension of profiles». In: *Physical Review A* 39.3 (1989), pp. 1500–1512. DOI: 10.1103/PhysRevA.39.1500. URL: <https://doi.org/10.1103/PhysRevA.39.1500> (cit. on p. 12).
- [23] Espen A. F. Ihlen. «Introduction to multifractal detrended fluctuation analysis in Matlab». In: *Frontiers in Physiology* 3 (2012), p. 141. DOI: 10.3389/fphys.2012.00141. URL: <https://www.frontiersin.org/articles/10.3389/fphys.2012.00141/full> (cit. on p. 13).
- [24] Yuliia Mishura and Mounir Zili. «Fractional and Sub-fractional Brownian Motions». In: *Stochastic Analysis of Mixed Fractional Gaussian Processes*. ISTE Press - Elsevier, 2018, pp. 31–73. DOI: 10.1016/B978-1-78548-245-8.50002-1. URL: <https://doi.org/10.1016/B978-1-78548-245-8.50002-1> (cit. on p. 13).
- [25] Andras Eke, Péter Hermán, James B. Bassingthwaite, Gerald M. Raymond, Donald B. Percival, Marcia Cannon, István Balla, and Csaba Ikrényi. «Physiological time series: distinguishing fractal noises from motions». In: *Pflügers Archiv - European Journal of Physiology* 439.4 (2000), pp. 403–415. DOI: 10.1007/s004249900135. URL: <https://doi.org/10.1007/s004249900135> (cit. on p. 14).
- [26] Bruce J. West and Michael F. Shlesinger. «1/f noise». In: *Scholarpedia* 4.1 (2009), p. 3693. DOI: 10.4249/scholarpedia.3693. URL: [http://www.scholarpedia.org/article/1/f\\_noise](http://www.scholarpedia.org/article/1/f_noise) (cit. on p. 14).
- [27] Goran Krstacic, Antonija Krstacic, Anton Smalcelj, Davor Milicic, and Mirjana Jembrek-Gostovic. «The "Chaos Theory" and nonlinear dynamics in heart rate variability analysis: does it work in short-time series in patients with coronary heart disease?» In: *Annals of Noninvasive Electrocardiology* 12.2 (2007), pp. 130–136. DOI: 10.1111/j.1542-474X.2007.00151.x. URL: <https://doi.org/10.1111/j.1542-474X.2007.00151.x> (cit. on pp. 15, 16).

- [28] Ary L. Goldberger. «Non-linear dynamics for clinicians: chaos theory, fractals, and complexity at the bedside». In: *The Lancet* 347.9011 (1996), pp. 1312–1314. DOI: 10.1016/S0140-6736(96)90948-4. URL: [https://doi.org/10.1016/S0140-6736\(96\)90948-4](https://doi.org/10.1016/S0140-6736(96)90948-4) (cit. on p. 15).
- [29] M. Nakao, T. Takizawa, K. Nakamura, N. Katayama, and M. Yamamoto. «An optimal control model of 1/f fluctuations in heart rate variability». In: *IEEE Engineering in Medicine and Biology Magazine* 20.2 (2001), pp. 77–87. DOI: 10.1109/51.917727. URL: <https://pubmed.ncbi.nlm.nih.gov/11321723/> (cit. on p. 15).
- [30] Jianbo Gao, Jing Hu, Wen-wen Tung, and Erik Blasch. «Multiscale analysis of biological data by scale-dependent Lyapunov exponent». In: *Frontiers in Physiology* 2 (2012), p. 110. DOI: 10.3389/fphys.2011.00110. URL: <https://www.frontiersin.org/articles/10.3389/fphys.2011.00110/full> (cit. on p. 16).
- [31] Aftab Alam, Nanping Wang, Ermioni Petraki, Luciano Telesca, Chuan-Jian Lin, Chien-Hung Chen, and Chien-Hsiung Wang. «Fluctuation Dynamics of Radon in Groundwater Prior to the Gansu Earthquake, China, July 22, 2013 (M s 6.6): Investigation with DFA and MF DFA Methods». In: *Pure and Applied Geophysics* 178 (2021), pp. 2377–2392. DOI: 10.1007/s00024-021-02818-8. URL: <https://link.springer.com/article/10.1007/s00024-021-02818-8> (cit. on p. 16).
- [32] Richard M. Bryce and Kevin B. Sprague. «Revisiting detrended fluctuation analysis». In: *Scientific Reports* 2 (2012), p. 315. DOI: 10.1038/srep00315. URL: <https://www.nature.com/articles/srep00315> (cit. on p. 16).
- [33] Lillian M. Rigoli, Tamara Lorenz, Charles A. Coey, Rachel W. Kallen, Scott Jordan, and Michael J. Richardson. «Co-actors Exhibit Similarity in Their Structure of Behavioural Variation That Remains Stable Across Range of Naturalistic Activities». In: *Scientific Reports* 10.1 (2020), p. 6308. DOI: 10.1038/s41598-020-63056-x. URL: <https://www.nature.com/articles/s41598-020-63056-x> (cit. on p. 17).
- [34] C.-K. Peng, S. Havlin, H. E. Stanley, and A. L. Goldberger. «Quantification of scaling exponents and crossover phenomena in nonstationary heartbeat time series». In: *Chaos: An Interdisciplinary Journal of Nonlinear Science* 5.1 (1995), pp. 82–87. DOI: 10.1063/1.166141. URL: <https://doi.org/10.1063/1.166141> (cit. on p. 18).

- [35] Thomas Gronwald and Olaf Hoos. «Correlation properties of heart rate variability during endurance exercise: A systematic review». In: *Annals of Noninvasive Electrocardiology* 25.1 (2019), e12697. DOI: 10.1111/anec.12697. URL: <https://doi.org/10.1111/anec.12697> (cit. on pp. 18, 61, 65, 67).
- [36] Keith Willson, Darrel P. Francis, Roland Wensel, Andrew J. S. Coats, and Kim H. Parker. «Relationship between detrended fluctuation analysis and spectral analysis of heart-rate variability». In: *Physiological Measurement* 23.2 (2002), pp. 385–401. DOI: 10.1088/0967-3334/23/2/314. URL: <https://doi.org/10.1088/0967-3334/23/2/314> (cit. on p. 18).
- [37] Ross O. Phillips. «A review of definitions of fatigue – And a step towards a whole definition». In: *Transportation Research Part F: Traffic Psychology and Behaviour* 29 (2015), pp. 48–56. DOI: 10.1016/j.trf.2015.01.003 (cit. on pp. 19, 20).
- [38] Oxford University Press. *Fatigue - Definition*. <https://www.oxfordlearnersdictionaries.com/definition/english/fatigue>. Accessed: 2025-03-24. 2013 (cit. on p. 20).
- [39] Ivan D. Brown. «Methodological Issues in Driver Fatigue Research». In: *Fatigue and Driving: Driver Impairment, Driver Fatigue, and Driving Simulation*. Ed. by Lynn T. T. and Kalow H. CRC Press, 1997, pp. 321–335. DOI: 10.1201/9780203756140-17. URL: <https://www.taylorfrancis.com/chapters/edit/10.1201/9780203756140-17/methodological-issues-driver-fatigue-research-ivan-brown> (cit. on p. 20).
- [40] R. S. Job and J. Dalziel. «Defining Fatigue as a Condition of the Organism and Distinguishing It From Habituation, Adaptation, and Boredom». In: *Stress, Workload, and Fatigue*. Ed. by P. A. Hancock and P. A. Desmond. CRC Press, 2001, pp. 466–475. DOI: 10.1201/9781420041107.ch28. URL: [https://www.researchgate.net/publication/347778763\\_Defining\\_Fatigue\\_as\\_a\\_Condition\\_of\\_the\\_Organism\\_and\\_Distinguishing\\_It\\_From\\_Habituation\\_Adaptation\\_and\\_Boredom](https://www.researchgate.net/publication/347778763_Defining_Fatigue_as_a_Condition_of_the_Organism_and_Distinguishing_It_From_Habituation_Adaptation_and_Boredom) (cit. on p. 20).
- [41] P.A. Hancock and W.B. Verwey. «Fatigue, workload and adaptive driver systems». In: *Accident Analysis & Prevention* 29.4 (1997), pp. 495–506. DOI: 10.1016/S0001-4575(97)00029-8 (cit. on p. 20).
- [42] J. F. Tornero-Aguilera, J. Jimenez-Morcillo, A. Rubio-Zarapuz, and V. J. Clemente-Suárez. «Central and Peripheral Fatigue in Physical Exercise Explained: A Narrative Review». In: *Int. J. Environ. Res. Public Health* 19.7 (Mar. 2022), p. 3909. DOI: 10.3390/ijerph19073909 (cit. on p. 20).

- [43] S. C. Gandevia. «Spinal and Supraspinal Factors in Human Muscle Fatigue». In: *Physiol. Rev.* 81.4 (Oct. 2001), pp. 1725–1789. DOI: 10.1152/physrev.2001.81.4.1725 (cit. on p. 20).
- [44] B. Bigland-Ritchie and J. J. Woods. «Changes in muscle contractile properties and neural control during human muscular fatigue». In: *Muscle & Nerve* 7.9 (1984), pp. 691–699. DOI: 10.1002/mus.880070902 (cit. on p. 20).
- [45] Jerome A. Dempsey, Lee M. Romer, Joseph R. Rodman, Joshua D. Miller, and Christine A. Smith. «Consequences of exercise-induced respiratory muscle work». In: *Medicine & Science in Sports & Exercise* 40.3 (2008), pp. 608–617. DOI: 10.1249/MSS.0b013e31815c6d2d (cit. on p. 21).
- [46] Gunnar Borg. *Borg's Perceived Exertion and Pain Scales*. Champaign, IL: Human Kinetics, 1998. ISBN: 9780880116237 (cit. on p. 21).
- [47] Markus D. Jakobsen, Emil Sundstrup, Roger Persson, and Lars L. Andersen. «Is Borg's perceived exertion scale a useful indicator of muscular and cardiovascular load in blue-collar workers with lifting tasks? A cross-sectional workplace study». In: *European Journal of Applied Physiology* 114.2 (2014), pp. 425–434. DOI: 10.1007/s00421-013-2782-9. URL: <https://doi.org/10.1007/s00421-013-2782-9> (cit. on pp. 22, 63, 64).
- [48] R. Gao, Y. Wang, X. Zhang, Y. Zhang, and Y. Liu. «Study on the nonfatigue and fatigue states of orchard workers based on electrocardiogram signal analysis». In: *Scientific Reports* 12.1 (2022), p. 4915. DOI: 10.1038/s41598-022-08705-z. URL: <https://www.nature.com/articles/s41598-022-08705-z> (cit. on pp. 22, 25, 26).
- [49] Paolo Castiglioni, Gianfranco Parati, Carolina Lombardi, Luc Quintin, and Marco Di Rienzo. «Assessing the fractal structure of heart rate by the temporal spectrum of scale exponents: a new approach for detrended fluctuation analysis of heart rate variability». In: *Biomedizinische Technik/Biomedical Engineering* 56.4 (2011), pp. 175–183. DOI: 10.1515/bmt.2011.010. URL: <https://doi.org/10.1515/bmt.2011.010> (cit. on p. 22).
- [50] Hye-Geum Kim, Eun-Jin Cheon, Dai-Seg Bai, Young Hwan Lee, and Bon-Hoon Koo. «Stress and Heart Rate Variability: A Meta-Analysis and Review of the Literature». In: *Psychiatry Investigation* 15.3 (2018), pp. 235–245. DOI: 10.30773/pi.2017.08.17. URL: <https://doi.org/10.30773/pi.2017.08.17> (cit. on pp. 23, 26).

- [51] Bruce Rogers, Laurent Mourot, Gregory Doucende, and Thomas Gronwald. «Fractal correlation properties of heart rate variability as a biomarker of endurance exercise fatigue in ultramarathon runners». In: *Physiological Reports* 9.14 (2021), e14956. DOI: 10.14814/phy2.14956. URL: <https://physoc.onlinelibrary.wiley.com/doi/full/10.14814/phy2.14956> (cit. on pp. 23, 62, 65, 67).
- [52] Thomas Gronwald, Bruce Rogers, and Olaf Hoos. «Fractal Correlation Properties of Heart Rate Variability: A New Biomarker for Intensity Distribution in Endurance Exercise and Training Prescription?» In: *Frontiers in Physiology* 11 (2020), p. 550572. DOI: 10.3389/fphys.2020.550572. URL: <https://www.frontiersin.org/articles/10.3389/fphys.2020.550572/full> (cit. on pp. 23, 27, 60, 67).
- [53] Noemí Sempere-Ruiz, José Manuel Sarabia, Sabina Baladzhaeva, and Manuel Moya-Ramón. «Reliability and validity of a non-linear index of heart rate variability to determine intensity thresholds». In: *Frontiers in Physiology* 15 (2024), p. 1329360. DOI: 10.3389/fphys.2024.1329360. URL: <https://pubmed.ncbi.nlm.nih.gov/38375458/> (cit. on pp. 23, 26, 62, 67).
- [54] Y. Zhang, Y. Liu, F. Sun, and Z. Ni. «Detection of Exercise Fatigue Using Neural Network with Grey Relational Analysis from HRV Signal». In: *Proceedings of the 2019 International Conference on Computer and Communication Engineering Technology (CCET)*. IEEE, 2019, pp. 1–5. DOI: 10.1109/ICCCE48422.2019.9010890. URL: <https://doi.org/10.1109/ICCCE48422.2019.9010890> (cit. on pp. 23, 25, 26, 67).
- [55] Laurent Schmitt, Jacques Regnard, and Grégoire P. Millet. «Monitoring fatigue status with HRV measures in elite athletes: an avenue beyond RMSSD?» In: *Frontiers in Physiology* 6 (2015), p. 343. DOI: 10.3389/fphys.2015.00343. URL: <https://www.frontiersin.org/articles/10.3389/fphys.2015.00343/full> (cit. on pp. 23, 26).
- [56] Shahnawaz Anwer, Heng Li, Waleed Umer, Maxwell Fordjour Antwi-Afari, Imran Mehmood, Yantao Yu, Carl Haas, and Arnold Yu Lok Wong. «Identification and Classification of Physical Fatigue in Construction Workers Using Linear and Nonlinear Heart Rate Variability Measurements». In: *Journal of Construction Engineering and Management* 149.7 (2023), p. 04023057. DOI: 10.1061/JCEMD4.COENG-13100. URL: <https://doi.org/10.1061/JCEMD4.COENG-13100> (cit. on pp. 24, 27).

- [57] S. Chen, K. Xu, X. Zheng, J. Li, B. Fan, and X. Yao. «Linear and nonlinear analyses of normal and fatigue heart rate variability signals for miners in high-altitude and cold areas». In: *Computer Methods and Programs in Biomedicine* 196 (2020), p. 105667. DOI: 10.1016/j.cmpb.2020.105667. URL: <https://doi.org/10.1016/j.cmpb.2020.105667> (cit. on p. 24).
- [58] Yufeng Jiang, Wei Chen, Xue Zhang, Xuejun Zhang, and Guowei Yang. «Real-Time Monitoring of Underground Miners' Status Based on Mine IoT System». In: *Sensors* 24.3 (2024), p. 739. DOI: 10.3390/s24030739. URL: <https://www.mdpi.com/1424-8220/24/3/739> (cit. on p. 24).
- [59] Zhiqiang Ni, Fangmin Sun, and Ye Li. «Heart Rate Variability-Based Subjective Physical Fatigue Assessment». In: *Sensors* 22.9 (2022), p. 3199. DOI: 10.3390/s22093199. URL: <https://www.mdpi.com/1424-8220/22/9/3199> (cit. on p. 26).
- [60] Marcelle Schaffarczyk, Bruce Rogers, Rüdiger Reer, and Thomas Gronwald. «Validation of a non-linear index of heart rate variability to determine aerobic and anaerobic thresholds during incremental cycling exercise in women». In: *European Journal of Applied Physiology* 123.2 (2023), pp. 299–309. DOI: 10.1007/s00421-022-05050-x. URL: <https://link.springer.com/article/10.1007/s00421-022-05050-x> (cit. on pp. 27, 29, 30).
- [61] Paloma Rabaey, Peter Decat, Stefan Heytens, Dirk Vogelaers, An Mariman, and Thomas Demeester. «Time-dependent complexity characterisation of activity patterns in patients with Chronic Fatigue Syndrome». In: *BioPsychoSocial Medicine* 18.10 (2024). DOI: 10.1186/s13030-024-00305-9. URL: <https://bpsmedicine.biomedcentral.com/articles/10.1186/s13030-024-00305-9> (cit. on p. 27).
- [62] S Michelsen. «Reproducibility of cumulative work, heart rate and blood pressure response during stepwise versus continuous load ergometry». In: *Scandinavian Journal of Clinical and Laboratory Investigation* 50.5 (1990), pp. 409–415. DOI: 10.3109/00365519009091599. URL: <https://www.tandfonline.com/doi/abs/10.3109/00365519009091599> (cit. on pp. 29, 30).
- [63] Thomas Gronwald, Olaf Hoos, Sebastian Ludyga, and Kuno Hottenrott. «Non-linear dynamics of heart rate variability during incremental cycling exercise». In: *Research in Sports Medicine* 27.1 (2018), pp. 88–98. DOI: 10.1080/15438627.2018.1502182. URL: <https://doi.org/10.1080/15438627.2018.1502182> (cit. on pp. 29, 67).

- [64] Cristina Blasco-Lafarga, Borja Camarena, and Manuel Mateo-March. «Cardiovascular and Autonomic Responses to a Maximal Exercise Test in Elite Youngsters». In: *International Journal of Sports Medicine* (2017). DOI: 10.1055/s-0043-110680. URL: <https://www.thieme-connect.com/products/ejournals/abstract/10.1055/s-0043-110680> (cit. on p. 29).
- [65] Wesley Quirino Alves da Silva, Zayonara Larissa Lima, Eduardo Bodnariuc Fontes, Daniel Gomes da Silva Machado, Rodrigo Menezes Forti, Andréa Camaz Deslandes, Erika Hussey, Nathan Ward, and Hassan Mohamed Elsangedy. «Affect during incremental exercise: The role of inhibitory cognition, autonomic cardiac function, and cerebral oxygenation». In: *PLOS ONE* 12.11 (2017), e0186926. DOI: 10.1371/journal.pone.0186926. URL: <https://journals.plos.org/plosone/article?id=10.1371/journal.pone.0186926> (cit. on p. 29).
- [66] Lenise Fronchetti, Fábio Y. Nakamura, Fernando R. De-Oliveira, Adriano E. Lima-Silva, and Jorge R. P. De Lima. «Effects of high-intensity interval training on heart rate variability during exercise». In: *Journal of Exercise Physiology Online* 10.4 (Aug. 2007), pp. 1–9. URL: [https://www.researchgate.net/publication/257874986\\_Effects\\_of\\_high-intensity\\_interval\\_training\\_on\\_heart\\_rate\\_variability\\_during\\_exercise](https://www.researchgate.net/publication/257874986_Effects_of_high-intensity_interval_training_on_heart_rate_variability_during_exercise) (cit. on pp. 29, 30).
- [67] Pablo R. Fleitas-Paniagua, Rafael de Almeida Azevedo, Mackenzie Trpcic, Juan M. Murias, and Bruce Rogers. «Effect of ramp slope on intensity thresholds based on correlation properties of heart rate variability during cycling». In: *Physiological Reports* 11.15 (Aug. 2023), e15782. DOI: 10.14814/phy2.15782. URL: <https://doi.org/10.14814/phy2.15782> (cit. on p. 29).
- [68] Jean Cassirame, Elodie Eustache, Luca Garbellotto, Jean-Benoît Morin, and Christophe Nicol. «Detrended fluctuation analysis to determine physiologic thresholds, investigation and evidence from incremental cycling test». In: *European Journal of Applied Physiology* 125 (2025), pp. 523–533. DOI: 10.1007/s00421-024-05614-z. URL: <https://doi.org/10.1007/s00421-024-05614-z> (cit. on p. 29).
- [69] Max J. Nelson et al. «Diagnostic sensitivity of 2-day cardiopulmonary exercise testing in Myalgic Encephalomyelitis/Chronic Fatigue Syndrome». In: *Journal of Translational Medicine* 17.1 (2019), p. 80. DOI: 10.1186/s12967-019-1836-0. URL: <https://doi.org/10.1186/s12967-019-1836-0> (cit. on p. 29).

- [70] Niels Wessel, Andreas Voss, Hagen Malberg, Christine Ziehmann, Henning U Voss, Alexander Schirdewan, Udo Meyerfeldt, and Jürgen Kurths. «Nonlinear analysis of complex phenomena in cardiological data». In: *Herzschrittmachertherapie & Elektrophysiologie* 11.3 (2000), pp. 159–173. DOI: 10.1007/s003990070035 (cit. on p. 34).
- [71] Thomas Gronwald, Olaf Hoos, and Kuno Hottenrott. «Effects of a Short-Term Cycling Interval Session and Active Recovery on Non-Linear Dynamics of Cardiac Autonomic Activity in Endurance Trained Cyclists». In: *Journal of Clinical Medicine* 8.2 (2019), p. 194. DOI: 10.3390/jcm8020194. URL: <https://www.mdpi.com/2077-0383/8/2/194> (cit. on pp. 60, 61, 66, 67).
- [72] Philip J. Millar, Mark Rakobowchuk, Neil McCartney, and Maureen J. MacDonald. «Heart rate variability and nonlinear analysis of heart rate dynamics following single and multiple Wingate bouts». In: *Applied Physiology, Nutrition, and Metabolism* 34.5 (2009), pp. 875–883. DOI: 10.1139/H09-086. URL: <https://cdnsiencepub.com/doi/abs/10.1139/h09-086> (cit. on pp. 65, 67).
- [73] Jean-François Casties, Denis Mottet, and Daniel Le Gallais. «Non-Linear Analyses of Heart Rate Variability During Heavy Exercise and Recovery in Cyclists». In: *International Journal of Sports Medicine* 27.10 (2006), pp. 780–785. DOI: 10.1055/s-2005-872968. URL: <https://www.thieme-connect.de/products/ejournals/abstract/10.1055/s-2005-872968> (cit. on pp. 65, 67).